CORA Cork Open Research Archive
Cartlann Taighde Oscailte Chorcaí

Title	Stabilisation of dehydrated nanoemulsions using sugar - protein matrices
Authors	Maher, Patrick G.
Publication date	2015
Original Citation	Maher, P.G. 2015. Stabilisation of dehydrated nanoemulsions using sugar - protein matrices. PhD Thesis, University College Cork.
Type of publication	Doctoral thesis
Rights	© 2015, Patrick G. Maher. - http://creativecommons.org/licenses/by-nc-nd/3.0/
Download date	2026-10-06 18:07:16
Item downloaded from	https://hdl.handle.net/10468/2773

UCC
University College Cork, Ireland
Coláiste na hOllscoile Corcaigh

The National University of Ireland, Cork

School of Food and Nutritional Sciences

University College Cork

Stabilisation of Dehydrated Nanoemulsions using Sugar – Protein Matrices

Thesis Presented to the National University of Ireland for the Degree of Doctor of Philosophy

By

Patrick G. Maher, B. Eng. (Hons.)

15th May 2015

Under the supervision of

Dr Mark A. Fenelon, Dip. Proc. & Chem. Eng., B.Sc., Ph.D.

Prof Yrjö H. Roos, M.Sc., Ph.D.

Table of contents

Declaration…….iii

Dedication……...…iv

Acknowledgements…….....v

Abstract……...…...vi

Abbreviations used……..viii

List of Tables……xvi

List of Figures…….xvii

Publications……..xxi

Chapter 1 – Literature Review……..1

Chapter 2 – Optimisation of β-casein stabilised nanoemulsions using experimental mixture design……...…53

Chapter 3 – Physicochemical properties of spray dried nanoemulsions with varying final water and sugar contents……81

Chapter 4 – Microstructure and lactose crystallisation properties in spray dried nanoemulsions……...97

Chapter 5 – Levels of pentanal and hexanal in spray dried nanoemulsions……118

Chapter 6 – Overall discussion……..136

References……...144

Declaration

I hereby declare that work described in this thesis is entirely my own and has not been submitted for another academic award, either in University College Cork or elsewhere.

_____

Patrick Maher

15th May 2015

Dedication

This thesis is dedicated to my parents, Pat and Helen Maher.

Acknowledgements

I would sincerely like to thank my supervisors Dr. Mark Fenelon and Prof. Yrjö Roos for their guidance and support throughout this thesis. Their hard work and valuable advice are very much appreciated.

Funding for this PhD was provided by the Irish Department of Agriculture, Fisheries & Food under the Food Institutional Research Measure (FIRM). I am very grateful for the funding that allowed me to pursue a postgraduate qualification.

I would also like to thank all the staff in Moorepark who helped me throughout my thesis, Dr. Phil Kelly, Jim Kelly, Dr. Donal O'Callaghan, Dr. Sean Hogan, Dr. Mark Auty, Dr. Kieran Kilcawley, Siobhan Ryan, Bernard Corrigan, and Joe Roche. Thanks to all the friends I made in Moorepark; Eoin, Noel, Ian, Dave, John, Tony, Grace, Vivian, Brian, Sandra, Alan, Solene, Valerie, Lisa, Clodagh, Deirdre, Kate, Ronan, Sean, and Noelle. Thanks to Noel, Eoin, and Tony for being great housemates and all the lads from Wednesday night soccer.

Thank you to Grace for her support and patience over the past few years. I thank my parents Pat and Helen for their constant support during all my years of study. Finally, I'd like to thank my brothers Niall, Aidan, Geoff, and Tom and my three sister-in-laws Valerie, Áine, and Alice for their support also.

Abstract

There are many uses of nanotechnology in food including: nanocomposites in food packaging; nanobiosensors for detection of contaminants; nanoencapsulation for delivery of nutraceuticals; and nano-sized structures/crystals for improved texture and flavour. In addition, interest in colloidal applications, inclusive of nanoemulsions, for food applications, has grown in recent years. Researchers have studied nanoemulsions, associated physical properties, and how they compare to other emulsion systems such as conventional emulsions and microemulsions, however, little research is available on dried nanoemulsions.

The objectives of this research were to (i) study the effect of varying viscosity and glass transition temperature in nanoemulsions with different carbohydrate/protein ratios on subsequent emulsion stability, (ii) compare the physicochemical properties of spray dried nanoemulsions compared to spray dried conventional emulsions having different water and sugar contents, (iii) characterise lactose crystallisation and microstructure of these spray dried powders, and (iv) compare powders in terms of their lipid oxidation.

Nanoemulsions containing sunflower oil (10% w/w), β-casein (0 – 10% w/w) and lactose or trehalose (0 – 20%) were produced following optimisation of the continuous phase by maximising and minimising viscosity and glass transition temperature (T_g') using mixture design software. Increasing levels of β-casein from 2.5% to 10% w/w caused a significant (P <0.05) increase in viscosity (5 to 156 mPa.s), particle size (186 to 199 nm) and nanoemulsion stability, while resulting in a decrease in T_g' (- 45 to - 50 ℃).

Powders were produced following heat treatment (100 ℃, 30 s), homogenisation (17 MPa) or microfluidisation (100 MPa), and spray drying at two different outlet temperatures (80 and 90 ℃) of emulsions/nanoemulsions consisting of lactose or a 70:30 mixture of lactose: sucrose (23.9%), sodium caseinate (5.1%) and sunflower oil (11.5%) in water. Nanoemulsions, produced by microfluidisation, had higher stability and lower viscosity than control emulsions with lower solvent extractable free fat in the resulting powder. Increasing dryer outlet temperature (80 to 90 ℃) reduced water content, water activity, particle size, tapped bulk density, while increasing the onset temperature of glass transition (T_g) and crystallisation (T_{cr}) of lactose in powders, measured by differential scanning calorimetry (DSC). Reducing the fat globule size by microfluidisation lowered

T_{cr} of lactose, possibly caused by the lower level of protein in the continuous phase. Partial replacement of lactose with sucrose decreased T_g and delayed crystallisation, measured by dynamic vapour sorption (DVS).

Differences in lactose crystallisation of a nanoemulsion powder and a conventional emulsion powder were studied using DVS and polarised light microscopy (PLM); crystallisation kinetics were modelled with the Avrami equation based on DVS data. Lactose crystallised in three dimensions (n ~3) and at a faster rate (k) in powders with a smaller FGS i.e. nanoemulsion powders. This was verified visually by PLM where an increase in crystal growth rate was seen at 55% relative humidity over 4 days. More evenly distributed small fat globules inside powder particles prepared from spray dried nanoemulsions were seen with confocal laser scanning microscopy (CLSM) and cryo-scanning electron microscopy (Cryo-SEM) images. After lactose crystallisation, powder surfaces were uneven and ruptured, with crystals observed thought to be a mixture (5:3 molar ratio) of α- and β-lactose.

A gas chromatographic headspace solid-phase microextraction (HS-SPME) method was validated and used to quantify volatile compounds pentanal and hexanal (indicators of lipid oxidation) in powders stored over 24 months. Pentanal and hexanal levels were significantly (P <0.05) lower in powders made from nanoemulsions compared to those from control emulsions, due to their altered structure and lower porosity (measured with a pycnometer). Partial replacement of lactose with sucrose significantly (P <0.05) reduced lipid oxidation.

This research has shown the effect of altering the continuous phase of nanoemulsions on its physical properties, and how the physical properties and microstructure of spray dried nanoemulsions affect glass transition temperature, sugar crystallisation, and lipid oxidation.

Abbreviations used

~	Approximately
°	Degree
=	Equals
>	Greater than
<	Less than
-	Minus
%	Percent
+	Plus
±	Plus or minus
3D	Three dimensional
α	Alpha
AFM	Atomic Force Microscopy
ANOVA	Analysis of Variance
a_w	Water activity
β	Beta
BP	Boiling Point
C	Celcius
C18:1	Oleic acid
C18:2	Linoleic acid
C18:3	Linolenic acid
CAR/PDMS	Carboxen™/polydimethylsiloxane

C_g'	Solute concentration at maximum freeze-concentration
CLSM	Confocal Laser Scanning Microscopy
d	Day
D	Translational diffusion coefficient
D[4,3]	De Brouckere mean diameter
Da	Dalton
DE	Dextrose Equivalence
Δ	Translational coefficient of particle
ΔC_p	Change in heat capacity
ΔH_m	Change in molar enthalpy
DHGC	Dynamic Headspace Gas Chromatography
DIC	Differential Interference Contrast
DOE	Design of Experiments
D_p	Diameter of particle
ΔP	Change in Laplace pressure
δ_s	Shell thickness
DSC	Differential Scanning Calorimetry
E_A	Activation energy
ESCA	Electron Spectroscopy for Chemical Analysis
exp	Exponential
ϕ	Disperse phase volume fraction
ϕ_C	Critical disperse phase volume fraction

$\phi_{effective}$	Effective disperse phase volume fraction
FCF	For Colouring Food
Fe	Iron
FF	Free fat
FGS	Fat Globule Size
FID	Flame Ionisation Detector
g	Gram
g	Acceleration due to gravity
γ	Interfacial tension
GC	Gas Chromatography
η	Emulsion viscosity
η_0	Continuous phase viscosity
h	Hour
H•	Hydrogen radical
HS	Headspace
HS-SPME	Headspace Solid-phase Microextraction
IDF	International Dairy Federation
IS	Internal Standard
J	Joule
κ	Kappa
k	Avrami rate constant
kg	Kilogram

K_{OW}	Oil-water partition coefficient
kV	Kilovolt
L	Litre
μ	Viscosity
m	Metre
mg	Milligram
μg	Microgram
min	Minute
mL	Millilitre
μL	Microlitre
mm	Millimetre
μm	Micron
m_0	Mass at onset
MPa	Mega Pascal
mPa.s	Milli Pascal seconds
m_t	Mass at time t
m_∞	Mass at endpoint
n-6	Omega-6 fatty acid
n	Avrami integer
ng	Nanogram
nm	Nanometre
O/W	Oil-in-water

O/W/O	Oil-in-water-in-oil
Pa.s	Pascal seconds
PLM	Polarised Light Microscopy
PLV	Polarised Light Videomicroscopy
psi	Pounds per square inch
PV	Peroxide value
R	Universal gas constant
r	Urbanovici-Segal equation parameter
r	Radius
ρ	Density
ρ_f	Density of fluid
ρ_p	Density of particle
R^2	Coefficient of determination
R•	Alkyl free radical
RH	Relative Humidity
RH_c	Critical Relative Humidity
RO•	Diradical
ROO•	Peroxyl radical
ROOH	Hydroperoxide
rpm	Revolutions per minute
RSD	Relative Standard Deviation
s	Second

S(r)	Water solubility of oil droplet
S_∞	Water solubility of oil droplet of infinite curvature
SEM	Scanning Electron Microscopy
SCF	Self-consistent Field
SHGC	Static Headspace Gas Chromatography
SMP	Skimmed Milk Powder
SNF	Solids-Non-Fat
t	Time
T	Temperature
$t_{1/2}$	Half time of encapsulated compound release/crystallisation
θ_t	Fraction crystallised
TAG	Triacylglycerol
TBA	Thiobarbituric Acid
TBARS	Thiobarbituric Acid Reacting Substances
T_{cr}	Crystallisation temperature
T_g	Glass transition temperature
T_g'	Glass transition temperature at maximum freeze-concentration
T_{gm}	Glass transition temperature of mixture
T_m	Freezing/melting temperature
T_m'	Melting temperature at maximum freeze-concentration
UK	United Kingdom
USA	United States of America

$V_{effective}$	Overall particle volume
V_{OA}	Volume of occluded air
V_{IA}	Volume of interstitial air
V_m	Molar volume
V_s	Particle shell volume
v_{Stokes}	Stokes' creaming/sedimentation velocity
w	Mole fraction
W/O	Water-in-oil
W/O/W	Water-in-oil-in-water
w/w	Weight per weight
w(h)	Total colloidal interactions
w_E	Electrostatic interaction
w_H	Hydrophobic interaction
w_S	Steric interaction
w_{VDW}	van der Waals interaction
WLF	Williams-Landel-Ferry
WMP	Whole Milk Powder
WPC	Whey Protein Concentrate
WPC50	Whey Protein Concentrate (50% protein)
WPC75	Whey Protein Concentrate (75% protein)
WPI	Whey Protein Isolate
XRD	X-ray Diffraction

y	Year

List of Tables

Table 1.1 Comparison of the properties of different emulsion types that can be prepared from oil, water and emulsifier (McClements, 2011).

Table 1.2 Factors capable of inhibiting lipid oxidation in oil-in-water emulsions (Waraho et al., 2011).

Table 2.1 Mixture design formulations of carbohydrate-protein mixtures with experimental results of viscosity (μ at 400 s^{-1}) and glass transition (T_g', T_m', T_g) values.

Table 2.2 Optimised formulations for minimum and maximum viscosity (μ at 400 s^{-1}) and glass transition temperature (T_g') for nanoemulsions at fixed β-casein contents (2.5, 5, 7.5, 10 % w/w).

Table 2.3 Statistical significance of models, both transformed and untransformed, for carbohydrate-protein mixtures and nanoemulsions.

Table 2.4 Coefficients for each term in the coded polynomial equation, both transformed and untransformed, for carbohydrate-protein mixtures and nanoemulsions.

Table 3.1 2^3 factorial experimental design and coding system of powders.

Table 3.2 Comparison of mean fat globule size (FGS), D[4,3], and pre- and post-homogenisation/microfluidisation apparent viscositity (for control emulsion and nanoemulsions) pre-spray drying.

Table 3.3 Mean fat globule size (FGS), D[4,3], apparent viscosity and creaming rate measurements for reconstituted powders at 12.5% w/w solids.

Table 3.4 Comparison of properties of control to nanoemulsion powders.

Table 3.5 Onset temperature of glass transition (T_g) and onset temperature of lactose crystallisation (T_{cr}) for control and nanoemulsion powders.

Table 4.1 Summary of kinetic parameters obtained by fitting the crystallisation isotherms to the Avrami model and Yang model.

Table 5.1 Experimental design and coding system of powders.

Table 5.2 Analytical parameters for pentanal and hexanal.

Table 5.3 Mean pentanal and hexanal contents (ng/g) of powders after 24 months storage (12 months each at 10 and 20 °C), and mean particle density, occluded air, and interstitial air in powders from triplicate spray drying trials.

List of Figures

Figure 1.1 Application matrix of nanotechnology in food science (Weiss et al., 2006).

Figure 1.2 Picture of nanoemulsion (left) and conventional emulsion (right) with droplet diameters of 35 nm and 1 μm, respectively (Solans et al., 2005).

Figure 1.3 Schematic diagram of the free energy of microemulsion and nanoemulsion systems compared to the phase separated state. Microemulsions have a lower free energy than the phase separated state, whereas nanoemulsions have higher free energy. The two states are separated by an activation energy ΔG* (McClements, 2012).

Figure 1.4 Schematic diagram of microemulsions and nanoemulsions fabricated from oil, water and surfactant. The structure of the particles in both types of colloidal dispersion is fairly similar – a hydrophobic core of oil and surfactant tails and a hydrophilic shell of surfactant head groups (McClements, 2012).

Figure 1.5 Schematic representations of three mechanical devices that can be used to continuously produce food-grade nanoemulsions using the high-energy approach: high pressure valve homogeniser, microfluidisers, and ultrasonic jet homogeniser (McClements, 2011).

Figure 1.6 Predicted velocity of upward movement for oil-in-water emulsions with different size droplets due to gravitational forces and Brownian motion (McClements, 2011).

Figure 1.7 Schematic diagram of most common instability mechanism that occur in food emulsions: creaming, sedimentation, flocculation, coalescence, Ostwald ripening and phase inversion (McClements, 2011).

Figure 1.8 Morphology of different types of microcapsules (Gibbs et al., 1999).

Figure 1.9 Schematic representation of physical changes on droplets during spray drying process (Dehydration I, II, III represent only the arbitrary stages of dehydration, μ – viscosity, T_g – glass transition temperature, $T_{surface}$ – surface temperature of drying particle) (Bhandari et al., 1997).

Figure 1.10 Surface oil content of fish oil (20% w/w) encapsulated powders containing two different surface-active biopolymers (WPC and Hi-Cap) and from emulsions of three different emulsification techniques (Jafari et al., 2008).

Figure 1.11 Micrographs of infant formula powders P1 and P5 before (stored at 0% RH) and after lactose crystallisation (stored at 55% RH). Row 1: Confocal images of P1 (A,

pre- crystallisation; B, post- crystallisation) and P5 (C, pre- crystallisation; D, post-crystallisation), scale bars represent 10 μm; Row 2; scanning electron microscope (SEM) images of P1 (E, pre-crystallisation; F, post- crystallisation) and P5 (G, pre-crystallisation; H, post- crystallisation), scale bars represent 10 μm; Row 3: Light micrographs of P1 (I, pre- crystallisation; J, post- crystallisation) and P5 (K, pre-crystallisation; L, post- crystallisation), scale bars represent 100 μm. FF indicates free fat; arrows indicate lactose crystal (McCarthy et al, 2013).

Figure 2.1 Contour and response surface plots of viscosity (at 400 s^{-1}) in carbohydrate-protein mixtures comprising of lactose, trehalose, and β-casein (0 to 20 % w/w).

Figure 2.2 Contour and response surface plots of onset glass transition temperature of maximally freeze-concentrated solids (T_g') in carbohydrate-protein mixtures comprising of lactose, trehalose, and β-casein (0 to 20 % w/w).

Figure 2.3 Contour and response surface plots of onset temperature of ice melting (T_m') in carbohydrate-protein mixtures comprising of lactose, trehalose, and β-casein (0 to 20 % w/w).

Figure 2.4 Contour and response surface plots of glass transition temperature of freeze dried powder (T_g) in carbohydrate-protein mixtures comprising of lactose, trehalose, and β-casein (0 to 20 % w/w).

Figure 2.5 Contour and response surface plots of mean particle size in nanoemulsions comprising of lactose, trehalose, and β-casein contents.

Figure 2.6 Contour and response surface plots of viscosity (at 400 s^{-1}) in nanoemulsions comprising of lactose, trehalose, and β-casein contents.

Figure 2.7 Contour and response surface plots of glass transition temperature of maximally freeze-concentrated solids in nanoemulsions (T_g') comprising of lactose, trehalose, and β-casein.

Figure 2.8 Contour and response surface plots of separation rate in nanoemulsions comprising of lactose, trehalose, and β-casein.

Figure 3.1 Moisture sorption kinetics comparison (0–90–0 % RH for 2 cycles) of high moisture powders with lactose (LC80 and LN80) measured on a Solids-Non-Fat (SNF) basis.

Figure 3.2 Moisture sorption kinetics comparison (0–90–0 % RH for 2 cycles) of high moisture powders with lactose: sucrose (SC80 and SN80) measured on a Solids-Non-Fat (SNF) basis.

Figure 4.1 a) Dynamic vapour sorption graph of control (C) and nanoemulsion (N) powders held at 55% RH for 48 h showing lactose crystallisation. b) Crystallisation isotherms for C and N at 25 °C for experimental data and those calculated using the Avrami equation.

Figure 4.2 Polarised light (crossed polars) micrographs of control (a,c,e,g,i) and nanoemulsion (b,d,f,h,j) powders. after storage for 0 (a,b), 1 (c,d), 2 (e,f), 3 (g,h) and 4 (i,j) days at 55% relative humidity. Arrows indicate small crystals, scale bar =100 μm.

Figure 4.3 Confocal laser scanning micrographs of showing internal microstructures of control (a,c,e) and nanoemulsion (b,d,f) powders after storage for 0 (a,b) and 4.3 (c,d,e,f) days at 55% relative humidity. Figure 4.3 a – d are fluorescently labelled with Nile Red/Fast Green to show fat (green) and protein (red); Figure 4.3 e & f are labelled with Nile Red to show fat phase. Arrows indicate air vacuoles (a, b), discrete fat droplets (c) and solid lactose crystals (d). Fig 4.3e inset shows irregularly shaped coalesced fat regions. Scale bars =100 μm.

Figure 4.4 Cryo-scanning electron micrographs of control (a,c,e,g) and nanoemulsion (b,d,f,h) powders prior to crystallisation. Images show powder particle surface morphology (a,b) and interior features of fractured particles (c – h). Arrows indicate air vacuoles (c,d) and fat droplets (e,g,h). Scale bars =20 μm (a,b), 10 μm (c,d), 2 μm (e,f) and 500 nm (g,h).

Figure 4.5 Cryo-scanning electron micrographs of control (a,c,e) and nanoemulsion (b,d,f) powders after storage for 4 days at 55% relative humidity showing crystals (arrowed) on the powder surfaces (a,b,c,d) and also interior of fractured particles. Scale bars =20 μm (a,b), 5 μm (c,d) and 2 μm (e,f).

Figure 5.1 Pentanal content of powders (LC ■, LN □, SC ⧫, SN ◊) stored at (a) 20 °C and (b) 50 °C for 8 weeks after prior storage at 10 °C for 12 months. Values presented are the mean ± standard deviation of three replicates from one spray drying experiment.

Figure 5.2 Hexanal content of powders (LC ■, LN □, SC ⧫, SN ◊) stored at (a) 20 ℃ and (b) 50 ℃ for 8 weeks after prior storage at 10 ℃ for 12 months. Values presented are the mean ± standard deviation of three replicates from one spray drying experiment.

Figure 5.3 Cryo-scanning electron micrograph showing distribution of oil droplets and air vacuoles in powders LC (a) and LN (b & c).

Publications

Peer reviewed publications

Maher, P.G., Fenelon, M.A., Zhou, Y., Haque, Md. K., and Roos, Y.H. 2011. Optimisation of β-casein stabilised nanoemulsions using experimental mixture design. *Journal of Food Science* 76(8): 1108–1117.

Maher, P.G., Roos, Y.H., and Fenelon, M.A. 2014. Physicochemical properties of spray dried nanoemulsions with varying final water and sugar contents. *Journal of Food Engineering* 126: 113–119.

Maher, P.G., Auty, M.A.E., Roos, Y.H., Zychowski, L.M., and Fenelon, M.A. 2015. Microstructure and lactose crystallisation properties in spray dried nanoemulsions. *Food Structure* 3: 1-11.

Maher, P.G., Roos, Y.H., Kilcawley, K.N., Auty, M.A.E., and Fenelon, M.A. 2015. Levels of pentanal and hexanal in spray dried nanoemulsions. *LWT – Food Science and Technology* In Press.

Co-author on other published work

McCarthy, N.A., Kelly, P.M., Maher, P.G., and Fenelon, M.A. 2014. Dissolution of milk protein concentrate (MPC) powders by ultrasonication. *Journal of Food Engineering* 126: 142–148.

Murphy, E.G., Roos, Y.H., Hogan, S.A., Maher, P.G., Flynn, C.G., and Fenelon, M.A. 2014. Physical stability of infant milk formula made with selectively hydrolysed whey proteins. *International Dairy Journal* 40: 39–46.

Conference and poster presentations

P.G. Maher, Y. Zhou, K.Haque, Y.H.Roos and M.A. Fenelon. Optimisation of glass transition and rheological properties in nanoemulsions using a statistical mixture design. 39th UCC Annual Conference, Cork, Ireland. 3-4 September 2009.

P. G. Maher, Y. Zhou, M. K. Haque, Y. H. Roos, M. A. Fenelon. 2010. Physicochemical properties of β-casein stabilised nanoemulsions. Institute of Food Technologists (IFT) Annual Meeting, Chicago, IL, USA. 17-20 July 2010.

P.G. Maher, J.T. Tobin, V. Chaurin Y.H. Roos, and M.A. Fenelon. 2011. Stability of β-carotene in sodium caseinate stabilised nanoemulsions in simulated retort sterilisation. European Federation of Food Science and Technology (EFFoST) Annual Meeting, Berlin, Germany. 9-11 November 2011.

P.G. Maher, Y.H. Roos and M.A. Fenelon. 2012. Physicochemical properties of dairy powders prepared from nanoemulsions. 5th IDF/INRA International Symposium of Spray Dried Dairy Products, St. Malo, France. 19-21 June 2012.

P.G. Maher, Y.H. Roos and M.A. Fenelon. 2012. Comparison of spray dried emulsion and nanoemulsion dairy powders. Society of Dairy Technology Autumn Conference, UCC, Cork, Ireland. 5-7 September 2012.

P.G. Maher. 2013. Spray dried nanoemulsions for biosensitives stabilisation. Workshop on Biosensitives Advanced Stabilisation, University College Cork, Cork, Ireland. 7 March 2013.

Chapter 1 - Literature review: Stabilisation of dehydrated nanoemulsions using sugar – protein matrices

1.1 Introduction

The use of nanotechnology could potentially create improved characteristics of food in terms of taste, texture, stability during shelf life, colouring strength, and processability. It can also improve the water solubility, thermal stability, and oral bioavailability of bioactive compounds (McClements et al., 2009; Huang et al., 2010). At the moment, applications of nanotechnology in the food industry include nanocomposites in food packing material for controlling diffusion and microbial protection, nanoencapsulation for controlled delivery of nutraceuticals, and nanobiosensors for detection of contaminants and quality deterioration (Figure 1.1) (Chen et al., 2006; Sanguansri and Augustin, 2006; Weiss et al., 2006; Sozer and Kokini, 2009). A number of works focusing on nanoencapsulation of food ingredients exist (Mozafari et al., 2006; Augustin and Hemar, 2009; Quintanilla-Carvajal et al., 2010; Fathi et al., 2012).

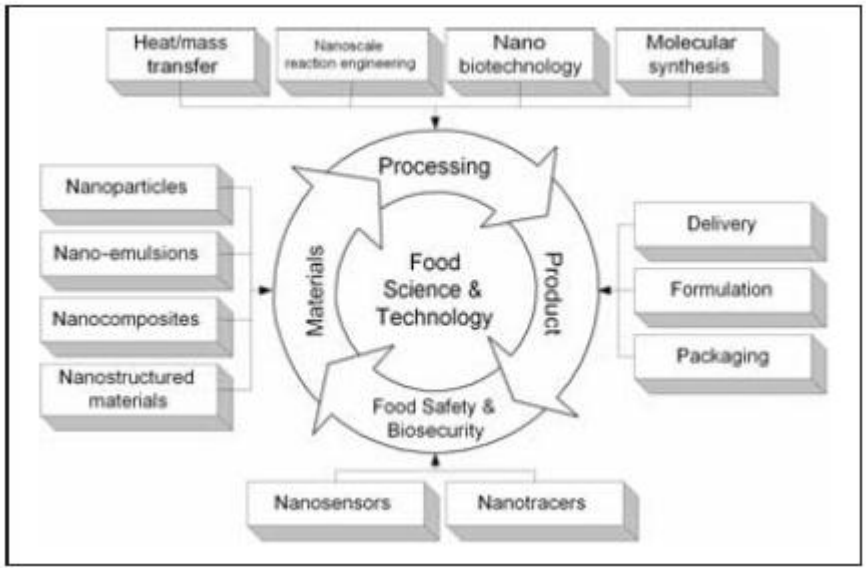

Figure 1.1 Application matrix of nanotechnology in food science (Weiss et al., 2006).

Little to no research has been done on the physical properties of powders produced from nanoemulsions compared to powders produced from conventional emulsions. It is not known whether there are microstructural differences between these both systems, and if these differences affect their long term storage stability in terms of glass transition temperature, sugar crystallisation and lipid oxidation. The objective of this work was to look at the importance of the continuous phase of nanoemulsions in terms of viscosity and

glass transition properties, and also examine how the continuous phase of emulsion systems (conventional emulsions and nanoemulsions) impact upon the microstructure, physical properties, and storage stability after spray drying.

1.2 Nanoemulsions

The use of nanoemulsions in the food, beverage, and pharmaceutical industries has grown in recent years. This is due to their advantages of increased bioavailability of lipophilic substances (Acosta, 2009) and high stability to particle aggregation and gravitational separation, leading to increased shelf life (Tadros et al., 2004), compared to conventional emulsions. They are also optically transparent which is suitable for certain applications where their inclusion does not have a negative visual effect (Mason et al., 2006; Velikov and Pelan, 2008; Wooster et al., 2008). They can have high viscosity and gel-like characteristics at low droplet concentrations, and, therefore, be used to create products of low fat content with novel textures (Tadros et al., 2004; Mason et al., 2006; Ciron et al., 2012).

1.2.1 Nanoemulsion characteristics

Emulsions typically consist of two different immiscible liquid phases (oil and water) where one liquid is dispersed as small spherical droplets (dispersed phase) in a liquid continuous phase (Dickinson and Stainsby, 1982; McClements, 2005). Emulsions can, therefore, be either oil-in-water (O/W) or water-in-oil (W/O). Double emulsions can also be created in the form of O/W/O or W/O/W emulsions. Various different terms are used to describe emulsions based on their oil droplet size, as reviewed by McClements (2011) and McClements and Rao (2011), while other authors highlight the key differences between conventional emulsions, nanoemulsions, and microemulsions (Mason et al., 2006; Anton and Vandamme, 2011; McClements, 2012). There has been confusion over the terminology in recent years so the key differences between the various emulsion types will be discussed. Distinguishing between these different emulsion types is necessary when formulating foods to help optimise product stability, physicochemical properties, and functional performance (Table 1.1).

Table 1.1 Comparison of the properties of different emulsion types that can be prepared from oil, water and emulsifier (McClements, 2011).

Emulsion type	Diameter (nm)	Stability	Surface-to-mass ratio (m^2/g)	Appearance
Emulsion	200-200,000	Metastable	0.07-70	Turbid/opaque
Nanoemulsion	20-200	Metastable	70-330	Clear/turbid
Microemulsion	4-100	Stable	130-1300	Clear

Conventional emulsions have a mean particle size of between 200 nm and 200 μm. Due to positive free energy (interfacial tension) between water and oil phases, they are thermodynamically unstable. They are optically opaque due to the particles having a size comparable to the wavelength of light, so strong scattering of light occurs, providing there is a difference in refractive index between the dispersed and continuous phase and that droplet concentration is sufficiently high (Figure 1.2). They are prone to gravitational separation due to their relatively large particle size.

Figure 1.2 Picture of nanoemulsion (left) and conventional emulsion (right) with droplet diameters of 35 nm and 1 μm, respectively (Solans et al., 2005).

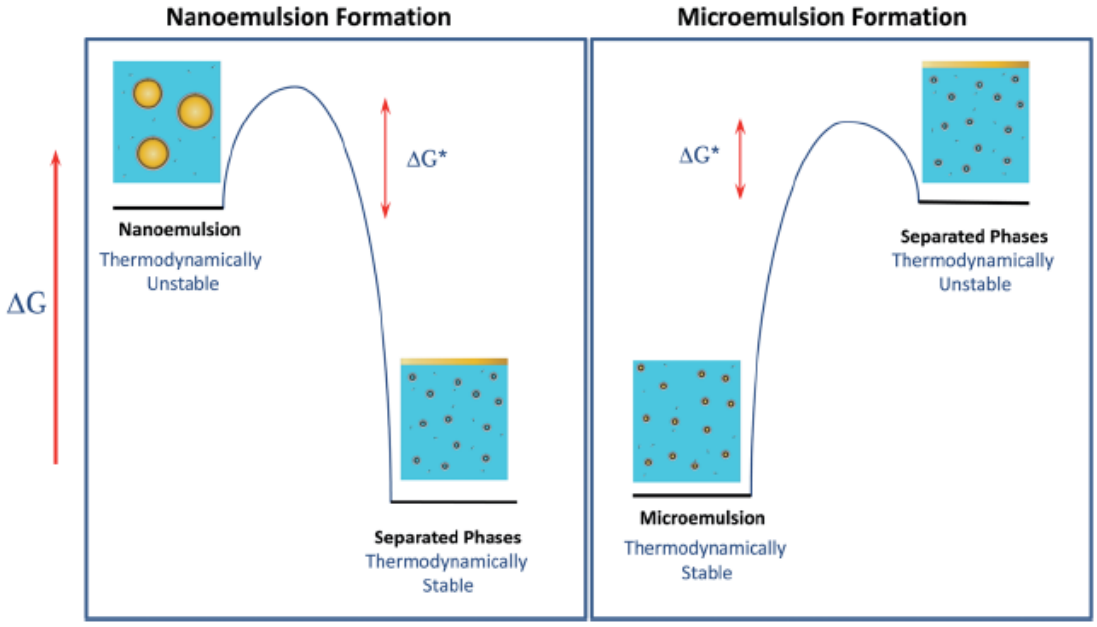

Figure 1.3 Schematic diagram of the free energy of microemulsion and nanoemulsion systems compared to the phase separated state. Microemulsions have a lower free energy than the phase separated state, whereas nanoemulsions have higher free energy. The two states are separated by an activation energy ΔG* (McClements, 2012).

Nanoemulsions are conventional emulsions of smaller droplet size, typically between 20 and 200 nm (Tadros et al., 2004; Mason et al., 2006). High pressure homogenisers and microfluidisers are typically used, at pressures up to 200 MPa, to provide sufficient high shear to produce a small droplet size. Like conventional emulsions, nanoemulsions are thermodynamically unstable (Figure 1.3). As particle size is significantly lower than the wavelength of light, nanoemulsions can be transparent or slightly turbid. Due to their smaller particle size than conventional emulsions, they are much less prone to particle aggregation and gravitational separation (Tadros et al., 2004; Wooster et al., 2008). They also have a much greater surface area for emulsifiers or surfactants to adsorb to, due to their smaller size.

Contrary to what the name suggests, microemulsions are not simply sub-micron emulsions. They are in fact smaller in size (4 - 100 nm) than nanoemulsions (Figure 1.4), and are thermodynamically stable emulsion systems due to their free energy being lower than that of separate oil and water phases; therefore, they can form spontaneously. They are optically transparent due to their size being much lower than the wavelength of light.

They require a certain set of conditions of temperature and composition, and if these change, they may no longer have thermodynamic stability. They can change into nanoemulsions, conventional emulsions, or separate phases but will change back to microemulsions if the original environmental conditions are returned to. The particle shape can be much different for microemulsions compared to nanoemulsions due to the interfacial tension being much lower, which leads to possible ellipsoid or worm-like shaped particles rather than simply spherical particles.

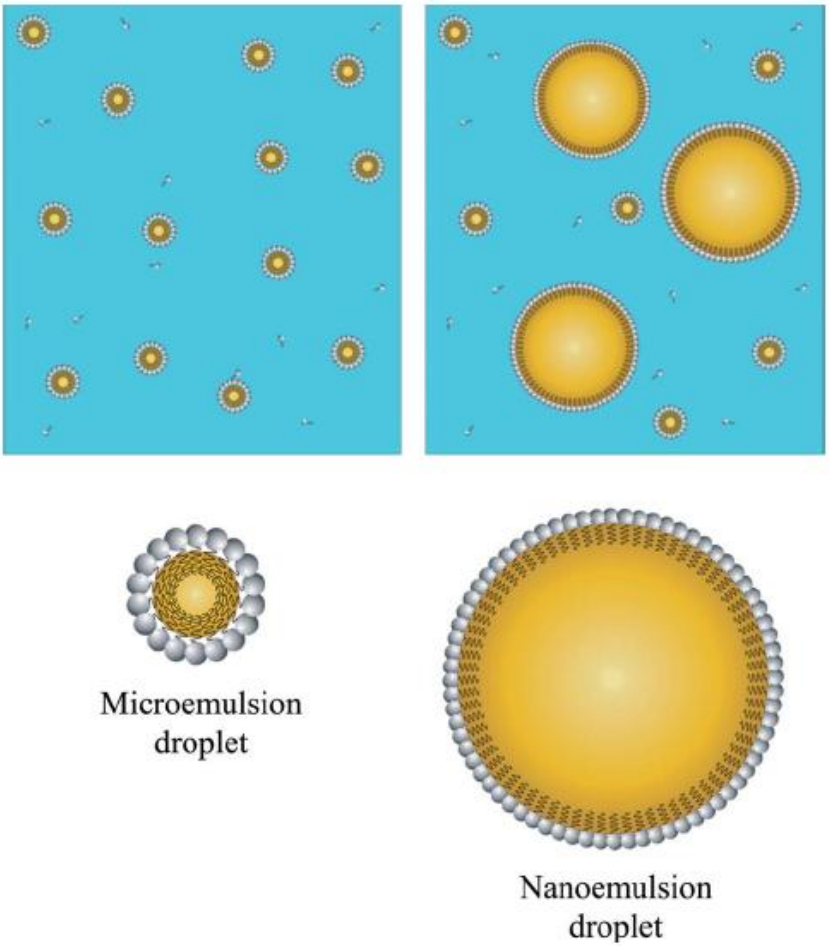

Figure 1.4 Schematic diagram of microemulsions and nanoemulsions fabricated from oil, water and surfactant. The structure of the particles in both types of colloidal dispersion is fairly similar – a hydrophobic core of oil and surfactant tails and a hydrophilic shell of surfactant head groups (McClements, 2012).

This thesis focuses primarily on nanoemulsions and how they differ from conventional emulsions. As stated previously, nanoemulsions are simply conventional emulsions of

smaller particle size. This means that while both emulsions are thermodynamically unstable they have differences in kinetic stability due to the large difference in mean particle size. Nanoemulsions can be unstable to Ostwald ripening, but have increased stability to gravitational separation, flocculation, and coalescence. The selection of appropriate stabilisers and oil phase are vitally important to produce stable nanoemulsions. Nanoemulsions can be produced by either high or low energy methods.

1.2.2 Nanoemulsion properties

McClements (2011) gives a detailed overview of how nanoemulsion particle properties are maintained by carefully selecting of ingredients such as lipids, surfactants, proteins, and polysaccharides. In terms of emulsifiers, surfactants can be used to prepare nanoemulsions using low energy methods, whereas high energy emulsification methods are required for proteins or polysaccharides.

Nanoemulsions can be different to conventional emulsions with the same composition. Consider a droplet to have a lipophilic core (containing oil-soluble vitamins, nutraceuticals etc.) surrounded by a shell comprised of surfactants, proteins, phospholipids, polysaccharides or minerals. Physicochemical properties and biological fate of these ingredients are dependent on their concentration, type, and location. The size of the lipophilic core and adsorbed shell of emulsifier on the outside of the droplet have a large effect. Equation 1.1 describes Φ_S, the particles shell volume (V_S) to the overall particle volume ($V_{effective}$) ratio, where δ_S is the shell thickness and r is the particle radius:

$$\Phi_S = \frac{V_S}{V_{effective}} = \frac{(r+\delta_S)^3 - r^3}{(r+\delta_S)^3} \quad (1.1)$$

Shell thickness varies for small molecule surfactants (1-2 nm), protein monolayers (2-10 nm), and biopolymer multilayers (10-50 nm). This small shell size is negligible in comparison to the size of conventional emulsions, but has a significant effect on the much smaller nanoemulsions. This is important as it impacts the physicochemical properties (refractive index and density) of nanoemulsion particles, which can alter separation rate and optical properties.

The effective concentration of particles in a nanoemulsion is different to a conventional emulsion of the same composition (Tadros et al., 2004; Mason et al., 2006). The effective oil volume fraction ($\phi_{effective}$) relates to the volume fraction of uncoated oil droplets (ϕ) in the following equation:

$$\phi_{effective} = \phi\left(1+\frac{\delta_S}{r}\right) \quad (1.2)$$

For conventional emulsions, the shell thickness to radius ratio is negligible and so $\phi_{effective}$ equals ϕ. In nanoemulsions $\phi_{effective}$ can be appreciably larger than ϕ when the shell thickness is high or the particle radius is low. This increase in $\phi_{effective}$ may cause significant rheological and stability changes in nanoemulsions, which may allow for the creation of novel highly viscous or gelled food products with lower oil contents than conventional emulsions.

Encapsulation of lipophilic ingredients such as nutraceuticals, vitamins, and flavours in nanoemulsions is an important part of the food and pharmaceutical industries (McClements et al., 2007; Acosta, 2009). The main reasons why these ingredients are encapsulated are to increase bioavailability, facilitate incorporation into a product, and control their release rate or location. Highly polar lipophilic ingredients are located within the core, whereas more hydrophilic ingredients can be located in the amphiphilic shell. Ingredients are better protected when in the core only, where no water soluble ingredients can degrade them.

1.2.3 Formation of nanoemulsions

As previously stated, nanoemulsions are produced by either low energy methods (spontaneous emulsification or phase inversion temperature) or high energy methods. High energy methods use mechanical devices, generating intense forces that physically break down the oil droplets to a very small size. Devices used are high pressure homogenisers, microfluidisers, and ultrasonic devices (Figure 1.5) (Tadros et al., 2004; Leong et al., 2009a; McClements, 2011). High energy is required to disrupt the restorative forces (Laplace pressure) that keep the particles together (Schubert et al., 2003; Schubert

and Engel, 2004). Laplace pressure increases with decreasing particle diameter (d_p) and increasing interfacial tension (γ) according to Equation 1.3:

$$\Delta P = \frac{\gamma}{d_p} \tag{1.3}$$

Microfluidisers are very effective at producing nanoemulsions, and were the primary focus throughout this thesis. A microfluidiser uses high pressure (up to ~150 MPa) to convert coarse emulsions into nanoemulsions. The resulting nanoemulsions have smaller droplets and a narrower fat globule size distribution than those from traditional emulsification techniques (Pinnamaneni et al., 2003). The design of a microfluidisers is slightly different to that of high pressure homogenisers (Figure 1.5). The liquid flowing through the channel is divided into two streams and, thus, recombined at high speed in the interaction chamber, creating intense forces leading to droplet size reduction (McClements and Rao, 2011). Droplet size decreases with increasing homogenisation pressure, number of passes, and emulsifier concentration, and decreasing dispersed phase content (Jafari et al., 2006; Jafari et al., 2007a; Leong et al., 2009a). Protein adsorbs relatively slowly to the interface compared to surfactants and so smaller particles can be obtained with surfactants, rather than proteins, as emulsifiers.

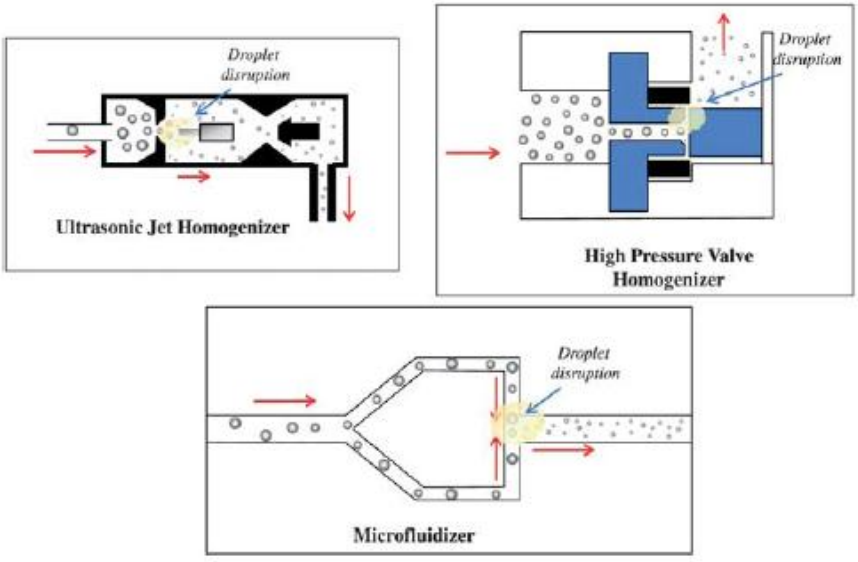

Figure 1.5 Schematic representations of three mechanical devices that can be used to continuously produce food-grade nanoemulsions using the high-energy approach: high pressure valve homogeniser, microfluidisers, and ultrasonic jet homogeniser (McClements, 2011).

1.2.4 Nanoemulsion applications

Bioavailability of lipophilic ingredients increases when encapsulated in nanoemulsions (Kesisoglou et al., 2007; Acosta, 2009). Various reasons exist for this bioavailability increase with decreasing droplet size. Firstly, smaller oil droplets have greater surface area available and so digestive enzymes can more quickly break down particles, making them more available for absorption. Secondly, their water solubility increases with decreasing droplet size, making them more readily absorbed. Thirdly, the small droplets can penetrate the mucous layer coating the epithelium cells within the small intestine, which increases their residence time, bringing them closer to absorption sites. Finally, the tiny particles can be transported directly across the epithelium cell layer by parracellular or transcellular mechanisms. Nanoemulsions have improved the bioavailability of nutraceuticals and pharmaceuticals, while the oral availability of curcumin has also been shown to increase in nanoemulsions (Wang et al., 2008b; Huang et al., 2010).

A major advantage of nanoemulsions is their potential to incorporate lipophilic ingredients (flavours, antioxidants, and nutraceuticals) into optically clear products (Given Jr, 2009), which can be achieved using either high energy (Wooster et al., 2008; Leong et al., 2009a; Leong et al., 2009b), or low energy methods (Wang et al., 2008a; Wang et al., 2009). Wooster et al. (2008) reported that nanoemulsions are optically transparent at a diameter <80 nm. Therefore, it is vital to produce emulsions with a very small particle size and narrow size distribution that will be stable over the long term, so that they remain optically clear.

Gravitational separation is a major cause of instability in conventional emulsions; emulsions will either cream or sediment depending on the density of the continuous and disperse phases. Creaming is more common in conventional O/W emulsions, due to liquid oil being less dense than the water based continuous phase, with the rate of creaming calculated from Stokes law:

$$v_{Stokes} = -\frac{2gr^2(\rho_2 - \rho_1)}{9\eta_1} \qquad (1.4)$$

Here, v_{Stokes} is the creaming velocity, r is the particle radius, g is acceleration due to gravity, ρ is the density, η is the shear viscosity, and subscripts 1 and 2 represent the

continuous and disperse phases, respectively. Brownian motion forces are also prevalent in nanoemulsions according to the equation:

$$\Delta = \sqrt{2Dt} \tag{1.5}$$

Here, Δ is the particle translational diffusion coefficient, D is the particle translational diffusion coefficient, and t represents time. Brownian motion increases with decreasing droplet size, in contrast to creaming separation. McClements (2011) has shown that below a certain particle radius (~90 nm) Brownian motion has a greater effect than creaming (Figure 1.6). The shell layer of nanoemulsions form a significant volume fraction of the overall particle volume, and the density of the shell layer is generally greater than that of either the oil or the continuous phase. Therefore, increasing shell layer volume causes an increase in particle density, which brings the density of the dispersed phase closer to that of the continuous phase, reducing the creaming rate. Sedimentation may even occur if the density of the shell layer is sufficiently high. This means that density matched particles can be produced so that creaming/sedimentation does not occur in emulsified systems.

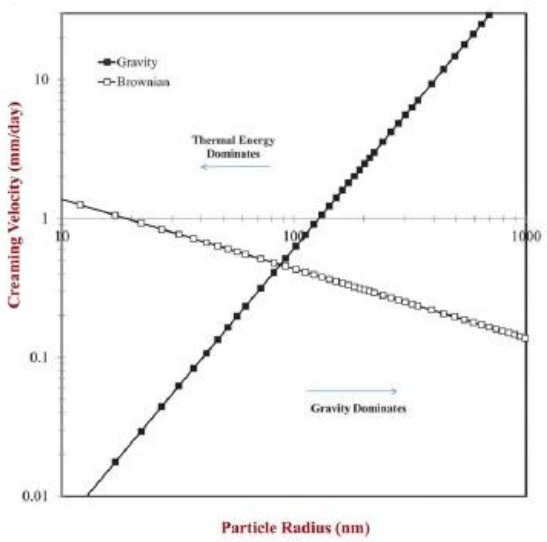

Figure 1.6 Predicted velocity of upward movement for oil-in-water emulsions with different size droplets due to gravitational forces and Brownian motion (McClements, 2011).

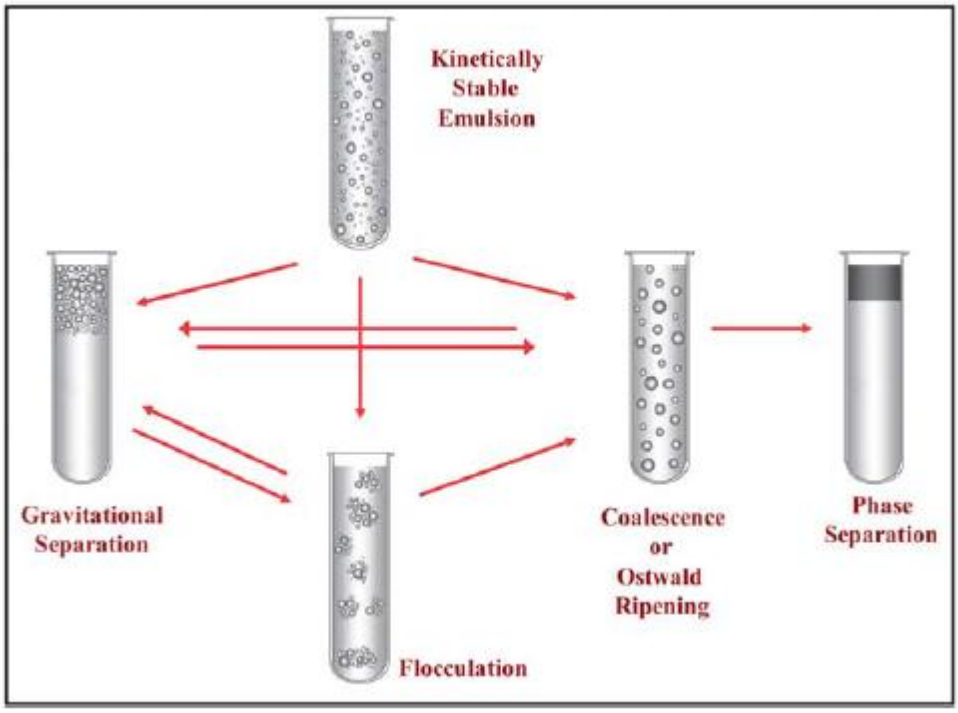

Figure 1.7 Schematic diagram of most common instability mechanism that occur in food emulsions: creaming, sedimentation, flocculation, coalescence, Ostwald ripening and phase inversion (McClements, 2011).

Nanoemulsions are less likely to aggregate (flocculation and coalescence) than conventional emulsions due to the effect of their smaller size on colloidal interactions (Tadros et al., 2004). Total colloidal interactions can be summarised with the following equation:

$$w(h) = w_{VDV}(h) + w_E(h) + w_S(h) + w_H(h) \qquad (1.6)$$

Here, the van der Waals (w_{VDW}), electrostatic (w_E), steric (w_S), and hydrophobic interactions (w_H) are summed. Generally, the magnitude of the attractive (van der Waals and hydrophobic interactions) and repulsive forces (steric and electrostatic interactions) increase with increasing particle size (McClements, 2005).

The process of Ostwald ripening occurs when small oil droplets migrate to become larger droplets in an emulsion (Solans et al., 2005). The rate of Ostwald ripening increases with decreasing droplet size, due to increased water solubility at smaller sizes (McClements, 2005). Water solubility of oil droplets is described by:

$$S(r) = S_{\infty} \exp\left(\frac{2\gamma V_m}{RTr}\right) \quad (1.7)$$

Here, S(r) is the water solubility of the oil droplet with a radius r, S_{∞} is the water solubility of the oil droplet of infinite curvature (i.e. a planar interface), V_m is the molar volume of the oil, γ is the oil-water interfacial tension, R is the universal gas constant, and T is the absolute temperature. Small droplets have a higher concentration of solubilised oil molecules, and they tend to migrate to larger droplets because of the concentration gradient. The main factor determining the influence of Ostwald ripening is S_{∞}; therefore, it is not a big factor for nanoemulsions prepared using highly non-polar oils, such as long chain triglycerides like corn, sunflower, or fish oils, but is a factor for short-chain triglycerides like flavour and essential oils (Wooster et al., 2008; Li et al., 2009). The most common instability mechanisms are summarised in Figure 1.7.

The chemical stability of nanoemulsions can be lower than conventional emulsions, due to the fact that light sensitive components can be degraded in optically clear systems (Mao et al., 2010). Also, their large surface area means that chemical degradation occurring at the oil-water interface, such as lipid oxidation, will be increased (McClements and Decker, 2000). The addition of antioxidants or chelating agents can be used to decrease oxidation of both water and oil soluble sensitive ingredients (McClements and Decker, 2000; Mao et al., 2009).

Nanoemulsions can be produced with very different rheological properties to conventional emulsions. Increased droplet concentration causes an increase in viscosity according to the equation:

$$\frac{\eta}{\eta_0} = \left(1 - \frac{\phi}{\phi_C}\right)^{-2} \quad (1.8)$$

Here, η is the concentrated emulsion viscosity, η_0 is the continuous phase viscosity, ϕ is the disperse phase volume fraction, and ϕ_C is the critical disperse phase volume fraction where droplets cannot flow past each other. This means that it may be possible to promote the gelation of nanoemulsions at lower oil contents than for conventional emulsions. This may be useful in the manufacture of low fat products where the texture and mouth feel of full fat products can be replicated. Ciron et al. (2012) have showed that the perceived

creaminess of microfluidised low fat yogurts were similar to full fat yogurts. This may also be useful for sauces, dressings, or mayonnaises that have a high fat content.

Flavours, nutraceuticals, and vitamins can be incorporated into and released from nanoemulsions, depending on the molecular characteristics of the functional components, composition, properties, and microstructure. For volatile compounds, it is expected that the size of the nanoemulsion droplets is irrelevant in terms of the release profile, as the diffusion rate of volatiles is so quick. For non-volatile compounds, targeted release of the encapsulated compound in certain areas of the body (mouth, stomach, or small intestine) is required. The release of non-volatile compounds from nanoemulsions can be quite different to those from conventional emulsions. As Equation 1.7 shows, solubility of oil droplets increase with decreasing oil droplet size which may change the oil-water partition coefficient (K_{OW}) of encapsulated compounds, which also effects their bioavailability (McClements, 2011). The time required for half of the encapsulated compounds to be released ($t_{1/2}$) are calculated from the following equation:

$$t_{1/2} = \frac{0.0585 r^2 K_{OW}}{D} \tag{1.9}$$

This equation shows that encapsulated compounds are released faster from nanoemulsions than they are from conventional emulsions. Highly lipophilic non-volatile compounds, i.e., high K_{OW}, are only released in the body after lipid digestion.

1.3 Microencapsulation

Microencapsulation is the process in which tiny particles or droplets are surrounded by a coating or embedded in a homogeneous or heterogeneous matrix to give small capsules with many useful properties (Gharsallaoui et al., 2007). It provides a physical barrier so that core ingredients are protected against other components in the matrix and surrounding atmosphere. The core can contain one or multiple ingredients and the wall can be single or double layered. Core retention depends on its solubility, polarity, chemical functionality, and volatility. Six reasons have been proposed by Shahidi and Han (1993) for applying microencapsulation to the food industry. The reasons are to (i) reduce the core reactivity with environmental factors, (ii) decrease the transfer rate of

core material to the outside environment, (iii) control the release rate of core material, (iv) mask the core taste, (v) promote easier handling, and (vi) dilute the core material when it should be used in small amounts.

A microcapsule consists of a core or dispersed phase which is surrounded by the wall or continuous phase. The size and morphology of microcapsules depend on how they are prepared; different microcapsules can be produced using different wall materials (monomers and/or polymers) and by different processes such as spray drying, freeze drying, spray chilling, air suspension coating, centrifugal extrusion, coacervation, co-crystallisation, extrusion, rotational suspension separation, liposome entrapment, interfacial polymerisation, molecular inclusion etc. (Shahidi and Han, 1993; Gibbs et al., 1999; Gouin, 2004; Desai and Park, 2005). Different shaped particles can be obtained depending on the microencapsulation technique used, the wall composition, and the physicochemical properties of the core. They can be particles with a spherical core surrounded by a uniform coating, irregularly shaped cores, multi-core particles embedded in a continuous wall matrix, several cores or several walls (Figure 1.8) (Gibbs et al., 1999).

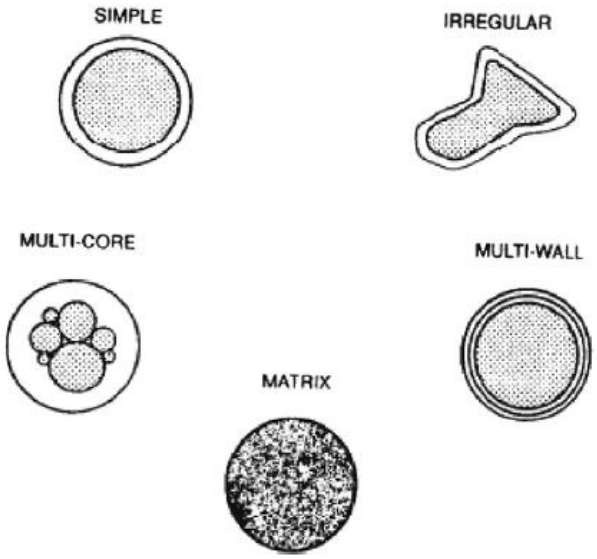

Figure 1.8 Morphology of different types of microcapsules (Gibbs et al., 1999).

1.3.1 Spray drying

Gharsallaoui et al. (2007) reviewed the microencapsulation of food ingredients by spray drying. Spray drying is a unit operation in which powder is produced following a liquid (solution, emulsion, or suspension) being atomised and passed through a current of hot air. Depending on the materials and operating conditions used, very fine powders (10 – 50 μm) or larger sized powders (2 – 3 mm) can be produced. Dehydration by spray drying decreases powder water content and water activity, leading to increased microbiological stability of dried products. In addition, it reduces the risk of chemical/biological degradation, storage costs, and transportation costs. Drying milk, for example, is a microencapsulation process where milk fat is the core, protected by a wall matrix of lactose and milk proteins. Lactose provides structure through glass formation while proteins provide good emulsification properties.

The purpose of liquid atomisation is to maximise the heat transfer surface area between the liquid droplet and the hot air. Different atomiser configurations can be used, depending on the feed viscosity, and desired characteristics of the resulting powder. Increasing feed viscosity results in powders of increasing size. Bowen (1938) and Masters (1968) have described the various types of atomisers used in spray drying such as pressure nozzle, two fluid nozzle, sonic nozzle, pneumatic atomiser, spinning disk configurations, centrifugal, steam and homogenising atomisers.

The contact between the droplet after atomisation and the hot air is the next stage in spray drying. Two different forms exist, co-current drying and counter-current drying. Co-current drying is when the liquid is sprayed in the dryer in the same direction as hot air, whereas counter-current drying the liquid is sprayed in the opposite direction to hot air. In co-current drying, powders are exposed to more moderate temperatures than in counter-current drying, making this method suitable for thermo-sensitive products. Counter-current drying is more economical, with less energy being consumed during processing.

Three steps occur during the evaporation of water from atomised droplets. Firstly, the heat is transferred from the air to the droplet until the temperature is constant. Secondly, evaporation occurs at a constant temperature and water vapour partial pressure. Finally, the droplet reaches a critical value and a dry crust is formed at the particle surface, upon which the drying rate rapidly decreases. After evaporation, the particle temperature rises

to that of the drying chamber (Papadakis and King, 1988), upon which drying is theoretically finished. Drying times of 15 – 30 s are acceptable for spray dried particles passing through the drying zone (Fogler and Kleninschmidt, 1938).

Separation of dry powder from humid air is usually done through a cyclone. The denser particles are collected at the bottom of the dryer, while the lighter particles pass through the cyclone to be separated from the humid air. Multi stage dryers are used as they increase the residence time and reduce the drying temperature, having the advantage of reducing thermal denaturation, and improving thermal effectiveness (Schuck, 2002). Also, fluidised beds placed outside dryers can help better control particle size and water content (Turchiuli et al., 2005). Alamilla-Beltran et al. (2005) described the particle morphology changes of during spray drying, which are related to moisture content and drying temperature.

1.3.1.1 Spray drying for microencapsulation

Spray drying is the most common method used for microencapsulation of food materials. This is because the equipment is readily available and production costs are lower than other methods; for example, freeze drying is 30 – 50 times more expensive than spray drying (Desobry et al., 1997). Spray drying is more economical than other methods (Quinn, 1965; Masters, 1968), even though spray drying itself is considered an energy inefficient operation, because a lot of the heat going through the dryer is unutilised. The process has been used for several decades, when in the 1930's flavours were encapsulated using gum Arabic as the wall material (Shahidi and Han, 1993; Gouin, 2004). Products including milk, cheese, coffee creamers, eggs, caseinates, and whey can be produced (Fäldt and Bergensåthl, 1995). The advantages of microencapsulation are that oxidation of fat is minimised, stickiness of powder is reduced, and particle size distribution of the original emulsion should be unchanged (Millqvist-Fureby, 2003). Drying minimises the packaging and storage requirements, thereby reducing the storage weight and costs (Landström et al., 2000).

Three steps are required before a liquid product can be spray dried (Dziezak, 1988). Firstly the emulsion is prepared, followed by homogenisation, and finally atomisation of

the emulsion in the spray dryer. Shahidi and Han (1993) have suggested a fourth step to be added; dehydration of the atomised particles. The first stage involves the formation of a stable emulsion of the core material in the wall solution. The core material (usually hydrophobic) is added to a solution containing the wall material of which it is immiscible. The solution is then heated and homogenised with or without the presence of an emulsifier, if it is required. The emulsion formed after homogenisation should be stable over time (Liu et al., 2001). After homogenisation, oil droplets should be small, and the viscosity of the emulsion should be low enough so that air is not included in the particles (Drusch, 2007). High emulsion viscosity can also interfere with the atomisation process leading to large elongated droplets that adversely affect the drying rate (Rosenberg et al., 1990). The retention of the core material is, therefore, dependant on the composition and properties of the emulsion, as well as the operating conditions in the spray dryer. Atomisation then occurs, leading to the evaporation of water and formation of microcapsules which are spherical in shape with the encapsulated oil protected inside the continuous phase (Dziezak, 1988).

The advantages of spray drying are, (i) the powder specifications remain constant throughout the dryer, (ii) it is a continuous and easy drying operation that is fully adaptable to full automatic control, and (iii) a wide range of designs are available depending on the application (such as heat sensitive materials) (Vega-Mercado et al., 2001).

1.3.1.2 Optimal drying conditions

Optimal spray drying conditions must be chosen to maximise the encapsulation efficiency of the desired material. The main factors to be optimised are the feed temperature, inlet air temperature, and outlet air temperature (Liu et al., 2004). Increasing the feed temperature reduces the viscosity of the feed which aids atomisation, however, increasing feed temperature is not recommended if heat-sensitive ingredients are present. Air inlet temperature is directly proportional to drying rate and water content. Low inlet temperatures cause powders with high water contents, poor fluidity, and easiness of agglomeration to be produced. However, high inlet temperatures can cause excessive evaporation leading to cracks in the powder leading to premature release of the

encapsulated material (Zakarian and King, 1982). Therefore, moderate air inlet temperatures must be found that do not damage the product and can safely be used without causing operational hazards (Fogler and Kleninschmidt, 1938). Air outlet temperature is used to control the dryer, and is difficult to predict. It is not controlled directly as it depends on the air inlet temperature. Ideally, it should be between 50 – 80 °C for the microencapsulation of flavours. The optimal spray drying conditions are a balance between high air temperature, high solids concentration of the feed, and easy drying without expansion or cracks (Bimbenet et al., 2002). Microencapsulation efficiency can be improved by increasing the solids concentration of the wall material (Young et al., 1993a). Rosenberg and Sheu (1996) found that the addition of lactose to a whey protein based system improved crust formation, limiting the loss of volatiles, which mainly occurs in the early stages of drying, prior to crust formation (Reineccius, 1988). The addition of lactose increases the hydrophilicity of the powder particle, which limits volatile diffusion (Moreau and Rosenberg, 1996). Disadvantages of spray drying for microencapsulation are that (i) only a limited number of water soluble wall materials are available, and (ii) in some cases, further processing (agglomeration) may be required for very fine powder particles.

1.3.2 Wall materials for microencapsulation

The core should be completely surrounded and protected by the wall material. An ideal wall material should have bland flavour, high solubility, and have the necessary emulsification, film-forming and drying properties, as reviewed by Vega and Roos (2006), with a low viscosity at high solids concentration (Rosenberg and Young, 1993b). The perfect encapsulant should be a combination of a protein and a carbohydrate. Wall materials improve product stability by being transformed into amorphous materials (or glasses) during spray drying (Bhandari and Howes, 1999). Amorphous materials are thermodynamically unstable, compared to their crystalline form. They will convert to their crystalline form with a rate depending on temperature and water content, which are both important factors to control for powder storage. The glass transition temperature (T_g) is a critical property of an amorphous material, with knowledge of it used to help control shelf life stability of powders (Roos, 1995).

1.3.2.1 Carbohydrates

Lactose is a disaccharide only found in milk, and is the most commonly used wall material in encapsulation by spray drying. It is also used widely for pharmaceutical applications as fillers in tablets and capsules, and as a carrier for dry powder inhalation. Lactose has many of the necessary properties of an ideal wall material such as sufficient solubility, low viscosity in concentrated solutions, and its relatively bland flavour. During the spray drying of milk or other dairy emulsions, evaporation of water occurs so quickly that lactose cannot crystallise and remains in the powder in the amorphous state. Therefore, this lactose glass acts as the wall material in whole milk powder and spray dried dairy emulsions made with whey protein concentrates (WPC) and whey protein isolate (WPI) (Buma, 1971; Young et al., 1993a, b).

Amorphous materials are only stable below their T_g, which is 105 °C for pure lactose (Potes et al., 2012). Small quantities of water have a plasticising effect and reduce the T_g, which accelerates the rate of deteriorative processes in food such as sugar crystallisation, fat oxidation, and the Maillard reaction (Roos and Karel, 1991d; Roos, 1993; Jouppila and Roos, 1994b; Roos et al., 1996b; Vega et al., 2005a). This also impacts on stickiness and fouling during drying. As products are dried they become thermoplastic and hygroscopic, so they stick to the walls of the dryer during processing (Bhandari et al., 1997; Bhandari and Howes, 1999; Schuck et al., 2005). Stickiness is related to the low T_g of sugars (Roos and Karel, 1991d; Vega et al., 2005a). If the temperature of the particles is 10-20 °C or greater than the T_g of the powder, stickiness will occur (Figure 1.9). Post-spray drying, powder stability is affected by the relationship between humidity and temperature and its influence on product caking, lumping, flowability and wettability (Jouppila and Roos, 1994b). Lactose cannot be used as an encapsulant on its own, as it has no emulsification properties and so, therefore, must be combined with emulsifiers such as proteins. Lactose is often combined with milk proteins in emulsion systems to mimic the composition of milk.

Sucrose is another disaccharide and has a T_g of 67 °C, which is lower than that of lactose (Liu et al., 2007). The lower T_g make it unsuitable for spray drying as the outlet temperatures of dryers are often above the T_g, meaning that powder stickiness becomes a problem. Where sucrose is used, it is mostly in the presence of other carbohydrates such

as lactose (Vega et al., 2005a), maltodextrins, or native or modified starches (Onwulata et al., 1994; Onwulata et al., 1996; Christensen et al., 2002), which increase the overall T_g of the system, making stickiness less likely upon drying.

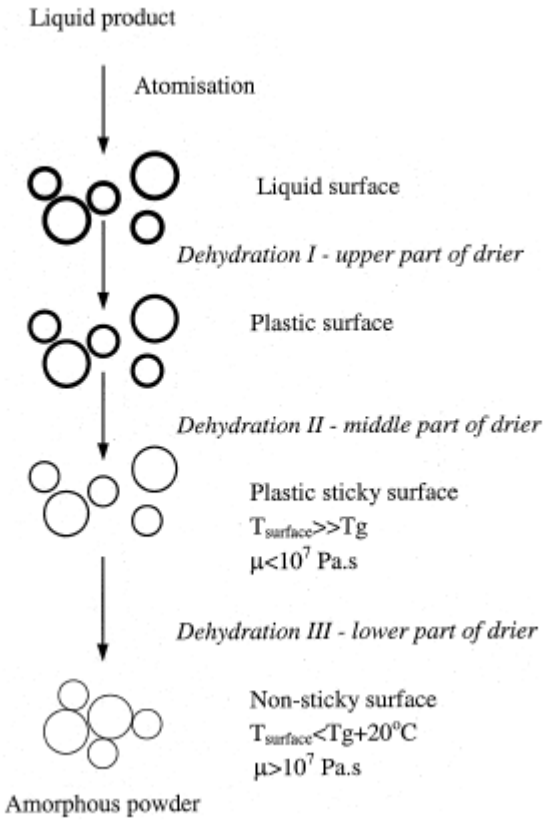

Figure 1.9 Schematic representation of physical changes on droplets during spray drying process (Dehydration I, II, III represent only the arbitrary stages of dehydration, μ – viscosity, T_g – glass transition temperature, $T_{surface}$ – surface temperature of drying particle) (Bhandari et al., 1997).

Maltodextrins are the hydrolysis products from starch with a dextrose equivalence (DE) <20. They are readily soluble in water, and are used as fat replacers in ice creams and low calorie spreads due to their functional properties such as bulking, gelling, crystallisation prevention, cryo-protectants, dispersing, and binding agents (Chronakis, 1998). They are commonly used as wall materials for microencapsulation (McNamee et al., 1998; Pedersen et al., 1998; Hogan et al., 2001a; Sliwinski et al., 2003). Hogan et al. (2001a) showed the effect of changing the DE of maltodextrins on emulsion stability, drying, and reconstitution of soybean oil emulsions stabilised by sodium caseinate. The authors

showed that as the DE increases, viscosity of emulsions decreases, reflecting the decrease in average molecular weight and improved solubility of the higher DE maltodextrins. Lowering the viscosity is beneficial for spray drying as it allows higher total solids content in the feed emulsion (Kenyon, 1995). Microencapsulation efficiency was also found to increase from 0 to 88.4% with increasing DE (0 to 28). This was due to the smaller oligosaccharides in high DE powders forming less porous, more uniform matrices upon drying which were impervious to the solvent used to extract surface oil. The authors recommended using maltodextrins with an average molecular weight of <1000 Da (DE >18.5). Scanning electron micrograph images of powders showed that above a DE of 5.5, smooth non-agglomerated powders were obtained while at a DE of 5.5, powders appeared agglomerated due to surface fat.

Gum Arabic is a very versatile material for microencapsulation due to its solubility and low viscosity in water. It is composed of molecules with a highly branched arrangement of sugars galactose, arabinose, rhamnose and glucuronic acid units (Anderson and Stoddart, 1966), while also containing 2% w/w protein (Anderson et al., 1985). As protein is present, gum Arabic can act as an emulsifier. McNamee et al. (1998) looked at the emulsification and encapsulation properties of gum Arabic with soybean oil. Oil-to-gum ratios of <2 were sufficient to produce stable emulsions with the D[4,3] being <1 μm. Similar results were found by Thevenet (1995) with microencapsulation efficiency decreasing from 100 to 48% when the oil-to-gum ratio was increased from 0.25 to 5.0, respectively. In terms of redispersion, powders with an oil-to-gum ratio of 0.25 had a similar particle size distribution to the original emulsion; whereas when the oil-to-gum ratio was 3.0 a bimodal particle size distribution was obtained due to the presence of undissolved particles. Kim and Morr (1996a) found that gum Arabic was the least effective encapsulating material for the protection of orange oil, compared to emulsions stabilised with sodium caseinate, WPI, or soy protein isolate.

1.3.2.2 Proteins

Proteins, particularly dairy proteins, are often chosen for microencapsulation. One disadvantage of proteins compared to carbohydrates is their higher cost. Mixtures of low-cost carbohydrates with dairy proteins offer the best solution to form an effective wall

material for microencapsulation. Milk proteins are widely used as food ingredients in either soluble or dispersed forms due to their good surface-active and colloid-stabilising characteristics (Dickinson, 1997a). Protein molecules and aggregates rapidly adsorb to the oil surface during homogenisation. The resulting steric-stabilising layer prevents the oil droplets from coalescing, providing stability to the emulsion during processing and storage.

Caseins and whey proteins are the two main classes of milk proteins. There are four types of bovine casein: α_{s1}-, α_{s2}-, β-, and κ-casein, representing approximately 38, 10, 36, and 12% of the whole casein, respectively (Robson and Dalgleish, 1987; Fox, 2001). Caseins, particularly β-casein, contain high levels of proline, which prevent the formation of secondary structures and makes caseins stable to denaturing agents (heat or urea) or processing conditions (homogenisation and pasteurisation), and contribute to their high surface activity, giving them good foaming and emulsifying properties (Fox, 2001). The whey protein fraction of bovine milk contains four main proteins: β-lactoglubulin (50%), α-lactalbumin (20%), Bovine Serum Albumin (10%), and Immunoglobulin (10%) (Morr and Ha, 1993; Fox, 2001). Whey proteins remain soluble after the caseins coagulate at pH 4.6 at 20 ℃. Due to the compact, globular conformation of native whey protein, it remains soluble at, or around, its isoelectric point (4.2 – 5.0) and is completely denatured by heating at 90 °C for 10 min (Fox, 2001).

1.3.2.2.1 Caseins and caseinates

There has been a large amount of research done on using sodium caseinate as an encapsulant, with and without the presence of carbohydrates. For microencapsulation, caseins and caseinates have better surface active properties compared to whey proteins, and are more heat stable. Their excellent surfactant properties make them a useful emulsifier for a variety of applications, including spray drying (Pedersen et al., 1998; Hogan et al., 2001a; Dollo et al., 2003; Sliwinski et al., 2003). The efficiency of whey protein, sodium caseinate, mixtures of sodium caseinate/lactose at different mass ratios, on fat microencapsulation has been reported (Fäldt and Bergensåthl, 1996a, b). The highest encapsulation efficiency (>90%) was obtained by sodium caseinate with lactose, followed by sodium caseinate alone (>70%), followed by whey protein with lactose

(<45%), followed by whey protein alone (<45%). Similar results were reported by other authors (Rosenberg and Young, 1993b; Young et al., 1993a, b).

Hogan et al. (2001a) studied the microencapsulating properties of sodium caseinate with soybean oil at different oil-to-protein ratios (0.25 – 3.0), and homogenisation pressure ranging from 10 to 50 MPa, with 4 passes. Volume average diameter decreased with increasing homogenisation pressure up to 20 MPa, with higher pressure not significantly reducing the mean particle size, even at the highest oil-to-protein ratios. This indicated that there was a limiting amount of sodium caseinate required to stabilise the liquid emulsion. Fat globule protein coverage decreased from 3.1 to 2.04 mg/m^2 with increasing oil-to-protein ratio. Microencapsulation efficiency also decreased from 89 to 19% with increasing oil-to-protein ratio. The emulsion droplet size increased after reconstitution, compared to the fresh emulsion showing that fat coalescence occurred during drying, particularly for high oil-to-protein ratios.

Millqvist-Fureby et al. (1999) compared the encapsulation properties of calcium caseinate and sodium caseinate in terms of powder surface composition and liquid surface tension. At a rapeseed oil content of 30% w/w, surface fat coverage for sodium caseinate powders was 35% at pH 3 and <10% at pH 7. For calcium caseinate, maximum fat coverage occurred at pH 3 (45%) with the minimum fat coverage occurring at pH 5.5 (<5%). Surface fat content at pH 7 was ~25%. This shows the pH-dependant aggregation of calcium caseinate, where at pH 5.5, calcium caseinate aggregates and precipitates leading to larger structures that are more efficient at fat encapsulation.

Very few studies have compared the encapsulating properties of micellar to nonmicellar casein. Keogh et al. (2001) studied the stability to oxidation of fish oil encapsulated in sodium caseinate, calcium caseinate, and skimmed milk powder (SMP). Their hypothesis was that as the level of protein aggregation increases, then the vacuole volume in the powder decreases which would impact on lipid oxidation. Powders with SMP had the best shelf life, due to the lower vacuole volume. The authors also found that there was a significant interaction between the effects of homogenisation pressure and number of passes, and vacuole volume on free fat. For SMP (low vacuole powder), free fat decreased from 24.5 to 2 g fat/100 g fat as homogenisation pressure and recirculation passes increased. For sodium caseinate (high vacuole powder), free fat remained

relatively unchanged with increased homogenisation pressure and recirculation passes (7.6 and 4.8 g fat/100 g fat). Homogenisation pressure or number of recirculation passes had no effect on surface fat (~60%) for SMP. Powders with sodium caseinate had the lowest surface fat content. Similar results were reported by Vega et al. (2005b).

1.3.2.2.2 Whey

Whey proteins were proposed as potential encapsulants in the early 1990's (Rosenberg and Young, 1993a; Young et al., 1993a, b). The main disadvantage of using whey proteins as encapsulants is their susceptibility to heat denaturation, and subsequent effects on emulsion particle size before spray drying and after reconstitution (Sliwinski et al., 2003). Aggregation of particles and reduced kinetic stability are the result of heating whey protein stabilised emulsions to 80 °C (Damodaran, 1997). Denaturation and aggregation of unadsorbed protein is the main reason for instability; therefore, increasing whey protein concentration accelerates the rate and degree of aggregation (Euston et al., 2000).

Young et al. (1993a) found that WPC50 gave the best encapsulation efficiency of anhydrous milk fat, compared to WPC75 and WPI. WPC50 had the best microencapsulation efficiency, because it had the highest lactose content (37%). The low encapsulation efficiency of WPI was improved to 95% when lactose was added to WPI in a 1:1 ratio. Other studies have found whey proteins on their own are poor encapsulating agents; the encapsulation of soybean oil was found to be much lower using whey protein compared to sodium caseinate (Fäldt and Bergensåthl, 1996b, a). They found that fat coverage varied from 45 to 60% with increasing whey protein concentration. Poor encapsulation of fat was attributed to less flexible proteins that diffuse at slower rates after denaturation, creating a less stable emulsion that allowed leakage of fat to the surface. Poor encapsulation was likely to be caused by protein aggregation and subsequent fat coalescence.

Different ratios of whey proteins in combination with sodium caseinate have been used for encapsulation (Sliwinski et al., 2003). At a 1:1 ratio of sodium caseinate: whey protein for the encapsulation of soybean oil, little effect on the physicochemical properties of

powders was found. Sodium caseinate adsorbed preferentially at the oil-water interface with nearly 90% of the adsorbed layer being sodium caseinate. However, after spray drying and reconstitution, some whey protein replaced sodium caseinate on the interface. The authors concluded that, during drying, whey proteins must be capable of displacing adsorbed caseins from the surface. The change in protein composition was probably due to the heat denaturation and aggregation of whey protein by disulphide bond formation.

1.3.3 Encapsulated food ingredients

Ingredients that are generally encapsulated are flavours, lipids, and carotenoids. As previously mentioned, one single wall material does not possess all the necessary requirements for encapsulation, therefore, mixtures of carbohydrates, proteins, and gums are typically used. Microencapsulation of flavours is very difficult due to their high volatility compared to water, making them easily lost during the spray drying process. Thijsen and Rulkens (1968) described the selective diffusion concept in which the diffusion coefficient of flavour decreases more quickly than the diffusion coefficient of water during drying. Spray drying is the most common method of microencapsulation of flavours, although various encapsulation methods have been proposed (Dziezak, 1988; Shahidi and Han, 1993).

Various studies have demonstrated that flavours can be encapsulated using spray drying. The effect of capsule wall material (Sheu and Rosenberg, 1995; McNamee et al., 1998; Buffo and Reineccius, 2000; McNamee et al., 2001), emulsion type (Risch and Reineccius, 1988; Liu et al., 2000; Mongenot et al., 2000; Liu et al., 2001), the properties of volatile compounds (Rulkens and Thijssen, 1972; Reineccius, 1988), drying process conditions (Rulkens and Thijssen, 1972; Zakarian and King, 1982; Rosenberg et al., 1990; Bhandari et al., 1992), and powder morphology during and after spray drying (El-Sayed et al., 1990; Rosenberg and Young, 1993a; Hecht and King, 2000) have been reported.

Different studies have shown the effect of reducing the mean FGS of emulsions on encapsulated volatile retention and stability prior to spray drying. Risch and Reineccius (1988) found that the retention of orange oil was improved with lower levels of surface

oil, when stabilised by gum Arabic or Amiogum 23, by reducing the mean FGS prior to spray drying. However, the shelf life of powders did not improve. Sheu and Rosenberg (1995) showed that retention of ethyl caprylate, in combination with whey and maltodextrin carriers, was improved when the mean FGS of the dispersed core was reduced. Also, Soottitantawat et al. (2003) showed that reducing the FGS of emulsions created powders with higher retention of *d*-limonene, ethyl butyrate, and ethyl propionate with less surface oil when stabilised by gum Arabic, soybean water-soluble polysaccharides or modified starch blended with maltodextrin.

Microencapsulation is an important technology used in the food industry for increasing the chemical stability of ingredients. Madene et al. (2006) have reviewed the effect of different wall materials and processing conditions on the retention of volatiles. Soottitantawat et al. (2005b) showed that highly volatile compounds, such as *L*-menthol, can be encapsulated with high retention using a matrix of maltodextrin and gum Arabic. They found that the optimal concentration of *L*-menthol in the feed emulsion was *L*-menthol: wall material 1: 4. Oregano, citronella and marjoram were successfully encapsulated in wall matrices of skimmed milk powder and whey protein concentrate (Baranauskienė et al., 2006). The oxidative stability of encapsulated *d*-limonene in a matrix of spray dried gum Arabic, soybean water-soluble polysaccharides and modified starch with maltodextrin was studied by Soottitantawat et al. (2004) and Soottitantawat et al. (2005a). Kaushik and Roos (2007) looked at the effect of ultra-high homogenisation (50 – 250 MPa) on flavour retention, and found that the retention of *d*-limonene in freeze dried gum Arabic-sucrose-gelatin systems was greatest when the emulsion was homogenised at 100 MPa. The biggest problem reported for microencapsulation of these flavours is that their molecular composition can be modified during drying.

Lipids are generally difficult to disperse in food products. Microencapsulation is one method of preservation of lipids. It is particularly useful for lipids highly susceptible to oxidation (e.g. polyunsaturated fatty acids), which result in off-flavours and undesirable compounds. Lipids can be used as solvents in which hydrophobic substances, such as aromatic compounds, can be solubilised. There are five main advantages of lipid encapsulation, (i) enhancing stability, (ii) retarding auto-oxidation, (iii) controlling lipid-soluble flavour release, (iv) masking bitter taste of lipid-soluble substances, and (v) protecting dissolved substances against enzyme hydrolysis (Matsuno and Adachi, 1993).

Spray drying is a suitable microencapsulation technique for oils. Hogan et al. (2001a) improved the microencapsulation efficiency of soybean oil in sodium caseinate/carbohydrate blends by increasing the dextrose equivalence of the carbohydrates. Spray dried butter oil was encapsulated in sucrose and double encapsulated in a matrix of vegetable waxes, making the powder more resistant to moisture sorption, but less flowable (Onwulata et al., 1998). The oxidative and thermal stability of crude squid oil was improved significantly by microencapsulation *via* spray drying using wall materials gelatin, sodium caseinate and maltodextrin (Lin et al., 1995).

Microencapsulation is used for carotenoids as they need to be protected against isomerisation or oxidation; degradation lowers the quality of the final product in terms of colour and nutritional properties. β-carotene in the *trans*-form is more bioavailable than in the *cis*-form (Deming et al., 2002), so preventing isomerisation from *trans*- to *cis*- is critical. Carotenoids in paprika oleoresin were protected by maltodextrins in a study by Beatus et al. (1985). Encapsulation and preservation of β-carotene in maltodextrin using different drying techniques was studied by Desobry et al. (1997). Spray drying of vitamins is an excellent method to preserve their nutritional value (Hartman et al., 1967). Wilson and Shah (2007) published a review paper on microencapsulation of vitamins, particularly focusing on vitamin C and vitamin A.

1.3.4 How to improve encapsulation efficiency

In recent years, the main emphasis has been on improving microencapsulation efficiency during spray drying, i.e., preventing volatile losses and extending the shelf life of products by minimising the quantity of unencapsulated oil at powder surfaces (Reineccius, 2001; Desai and Park, 2005; Madene et al., 2006). The purpose is to maximise the amount of encapsulated compound that is recovered. The properties of wall and core materials, as well as emulsion characteristics and spray drying parameters, have a significant impact on encapsulation efficiency.

Emulsification is one of the most important steps in the encapsulation of food oils and flavours through spray drying. Emulsion properties such as fat globule size (FGS) and stability are critical in optimising the encapsulation efficiency during processing (Risch

and Reineccius, 1988; Liu et al., 2001; Danviriyakul et al., 2002). Stable emulsions with minimum FGS can increase the retention of volatiles and shelf life of encapsulated oil products through reducing the amount of unencapsulated oil at the powder surface (Minemoto et al., 2002; Soottitantawat et al., 2003; Soottitantawat et al., 2005a). Surface oil on powder particles is one of the most undesirable properties of encapsulated powders, as it deteriorates the wettability and dispersability of the powder (Millqvist-Fureby et al., 2001), and surface oil is more likely to oxidise, causing the powder to become rancid more quickly.

Most of the work in the area of encapsulation has been done using conventional emulsions. Little research has been done on spray drying of nanoemulsions. With modern emulsification systems and their potential application of food ingredients, understanding the effect of reducing the FGS pre-spray drying has on surface oil content is essential (Jafari et al., 2008b).

1.4 Nanoencapsulation

Nanoencapsulation techniques are used to produce suspensions of nanoparticles either encapsulated within wall materials or coated with an active compound. They can be in liquid or dried form. Some of the main problems of nanocapsules are irreversible aggregation and chemical instability, caused by the hydrolysis of polymeric substances resulting in the leakage of encapsulated components (Chacon et al., 1999). Therefore, converting nanocapsule suspensions from liquid to dried form maintains their stability (Nakagawa et al., 2011). Being in dried form also makes them easier to handle and store prior to later rehydration.

Spray drying and freeze drying are commonly used techniques for nanoencapsulation (Choi et al., 2004; Abdelwahed et al., 2006). The operating conditions during spray drying and freeze drying have a significant effect on nanocapsule stabilisation (Nakagawa et al., 2011). Other than their improved stability compared to liquid nanosuspensions, dried powders can control and sustain bioactive compound release (Guterres et al., 2009). However, the process of drying brings additional stresses for nanocapsules, therefore, it is

necessary to investigate the effect varying process parameters has on nanocapsule stability (Nakagawa et al., 2011). In this review only spray drying will be considered.

1.4.1 Spray drying of nanocapsules

Spray drying is a well-established technique for encapsulation of a range of food ingredients such as vitamins, minerals, flavours, colours, fats, and oils to increase their shelf life by protecting them from environmental factors (Pillai et al., 2012). Spray drying is also considered to be a suitable technique for encapsulation of nanoparticles (Okuyama and Wuled Lenggoro, 2003).

Catechin was encapsulated in a carbohydrate matrix by homogenisation followed by spray drying (Ferreira et al., 2007). Spherical-shaped particles (80 nm in size) with a smooth surface were produced, and the encapsulated catechin had reduced oxidation and perhaps improved bioavailability. The zeta potential of these capsules was highly negative, contributing to their high stability. De Paz et al. (2012) produced nanosuspensions by encapsulating β-carotene using modified *n*-octenyl succinate starch using an emulsification-evaporation technique with spray drying. Different operational conditions were used with the best encapsulation efficiency (65 – 90%) occurring for particles of 300 – 600 nm in size. Recently, β-carotene was encapsulated through production of nanoemulsions stabilised by modified starch (Hi-Cap) (Liang et al., 2013). The mean droplet size of nanoemulsions was 114 – 160 nm prior to spray drying, and after drying, the powders were micron-sized. Powders had good rehydration properties and had very similar mean droplet sizes, suggesting that spray drying had no adverse effect on the droplets. Storage stability of β-carotene at 25 °C was monitored at varying relative humidity for 30 days. Degradation of β-carotene was linked to powder glass transition temperature and moisture sorption properties.

A comparison was made between different emulsification techniques, microfluidisation, ultrasonication, and Silverson mixing, for stabilisation of *d*-limonene (Jafari et al., 2007a, b) and fish oil (Jafari et al., 2008a) in spray dried emulsions. Jafari et al. (2007b) used maltodextrin combined with modified starch (Hi-cap), WPC, and Tween 20 to stabilise *d*-limonene. Microfluidisation of emulsions resulted in the highest encapsulation efficiency

of stabilise *d*-limonene in powders. Jafari et al. (2008a) encapsulated fish oil in maltodextrin combined with either WPC or Hi-Cap in a 3: 1 ratio. Microfluidisation resulted in the smallest FGS (210 – 280 nm) and highest encapsulation efficiency (170 – 690 mg surface oil/100 g powder), with Hi-cap having better encapsulation efficiency compared to WPC (Figure 1.10). Encapsulation efficiency is influenced by emulsion droplet size, with finer emulsions having better encapsulation than coarse emulsions. For all studies, microfluidisation was found to be the best method, due to its highest encapsulation efficiency and smallest fat globule size with good stability during processing, followed by ultrasound and Silverson rotor-stator mixing. The authors suggest that there is no clear-cut evidence on how sub-micron emulsions or nanoemulsions improve the encapsulation efficiency of food flavours and oils.

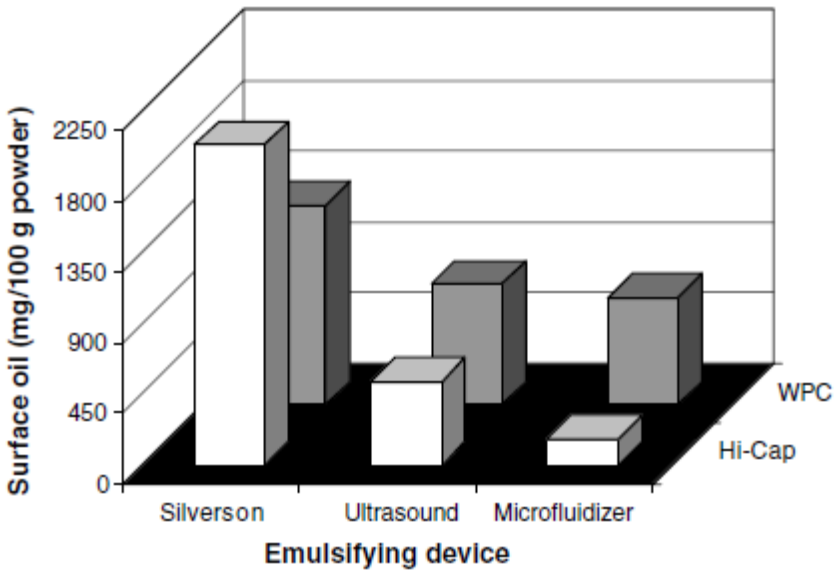

Figure 1.10 Surface oil content of fish oil (20% w/w) encapsulated powders containing two different surface-active biopolymers (WPC and Hi-Cap) and from emulsions of three different emulsification techniques (Jafari et al., 2008).

1.5 Physicochemical properties of powders

The composition of the powder surface formed during drying dictates the behaviour of the bulk powder in terms of wettability, flowability, and stability to caking and oxidative

rancidity. The free fat content of powders can be associated with how well powders flow. Free fat is defined as the amount of fat that can be extracted after contact with an organic solvent (usually petroleum ether or hexane) (Jafari et al., 2008). Solvent extraction can also reach fat through pores or cracks in powders, particularly in agglomerated powders. A technique called electron spectroscopy for chemical analysis (ESCA) was used by Faldt et al. (1993) to determine the quantities of fat, as well as protein and carbohydrate on powder surfaces.

Another important property of powders is their ease of reconstitution. Powders should reconstitute easily, but more importantly, they should reconstitute to their original fat globule size. Reconstitution involves four steps: wetting, submersion, dispersion, and dissolving (Freudig et al., 1999). Wetting is often the reconstitution rate-controlling step. It is defined as the ability of a bulk powder to imbibe a liquid under the influence of capillary forces. It depends on powder particle size, porosity, density, surface charge, surface area, presence of amphipathic substances, and the surface activity of the particles. The surface composition of powders has a big impact on wetting. Good wetting is achieved when hygroscopic materials (such as lactose) are at the powder surface due to the small contact angle (Fäldt et al., 1993; Kim et al., 2002). Wettability is also improved by agglomeration to larger particles and by the addition of natural surfactants such as soy lecithin (Schubert, 1993). Skimmed milk powder that is wetted in less than 15 s is termed "instant". Whole milk powders with significant quantities of fat on the surface are not wettable in a significant time frame (15 min). Kim et al. (2002) showed that when surface fat is removed with petroleum ether, that wetting time was reduced to 35 s.

1.5.1 Glass transition

Spray drying produces powders in an amorphous state. This makes powders thermoplastic and hygroscopic meaning that the powder can stick to the dryer walls, and they show great sensitivity to moisture and temperature-induced fluctuations during storage. This is particularly the case when high quantities of low molecular weight carbohydrates are used (Bhandari and Howes, 1999). The susceptibility of powders to deterioration during storage at high temperature and humidity for sugar containing products is related to their glass transition temperature (T_g) (Aguilera et al., 1995; Christensen et al., 2002; Vega et

al., 2005a). Glass transition is a state transition of amorphous materials occurring between the solid, glassy, and supercooled liquid states. The amorphous material is not as thermodynamically stable as its crystalline form (Flink, 1983; Slade et al., 1993). In the amorphous state, the material is highly viscous with typical viscosity above 10^{12} Pa.s (Downton et al., 1982). Molecular movement, which is necessary for an orderly alignment of molecules to crystallise, is very restricted, and over time the amorphous material will eventually crystallise at a rate dependent upon the temperature and moisture content (Flink, 1983).

Molecular weight has a significant impact upon glass transition temperature. Low molecular weight polymers (e.g. sucrose) and monomers (e.g. glucose) have lower T_g than longer chain molecules (e.g. maltodextrins). T_g of high molecular weight food polymers (e.g. proteins and starches) cannot be determined experimentally because they decompose at temperatures below their glass transition (Bhandari and Howes, 2009).

1.5.1.1 Glass transition in multicomponent systems

Carbohydrate, protein, and fat are the main solid components of food materials, with carbohydrates having the biggest influence on T_g. Common sugars (sucrose, glucose, and fructose) have very low glass transition temperatures, so their presence supresses T_g in sugar-rich food. In milk powders, fat is not a significant factor for glass transition (Jouppila and Roos, 1994b) and protein may have an increasing effect. Water is extremely effective at reducing the T_g of a food material due to its very low T_g (-135 °C), making it a strong plasticiser in food systems. Haque and Roos (2004) demonstrated the plasticising effect of water in lactose and lactose/protein mixtures measuring the T_g of these powders at varying water activity (0 – 0.44).

The glass transition temperature of a mixture of food components (including water) is a non-linear function of glass transition temperature of individual components (Bhandari and Howes, 2009). Two main mathematical relationships have been developed by Gordon and Taylor (1952) and Couchman and Karasz (1978) to determine the T_g of a mixture. The Couchman-Karasz equation (Equation 1.11) is an extension of the Gordon-Taylor equation (Equation 1.10):

$$T_{gm} = \frac{w_1 T_{g1} + k w_2 T_{g2}}{w_1 + k w_2} \tag{1.10}$$

$$T_{gm} = \frac{w_1 T_{g1} + \left(\frac{\Delta C_{p2}}{\Delta C_{p1}}\right) w_2 T_{g2}}{w_1 + \left(\frac{\Delta C_{p2}}{\Delta C_{p1}}\right) w_2} \tag{1.11}$$

Here, T_{gm} is the glass transition temperature of the mixture, w_i is the mole fraction of component I, ΔC_{pi} is the change in heat capacity of component *i* between glassy and rubbery states, and T_{gi} is the glass transition temperature of component *i*. The Gordon-Taylor model is suitable for binary mixture, but the Couchman-Karasz model can be expanded for an *n* component system:

$$T_{gm} = \frac{\sum_{i=1}^{n} w_i \Delta C_{pi} T_{gi}}{\sum_{i=1}^{n} wi \Delta C_{pi}} \tag{1.12}$$

1.5.1.2 Glass transition in spray drying

Stickiness during spray drying of sugar containing products has been related to low T_g (Roos et al., 1996a; Bhandari snd Howes. 1999). The surface of droplets during spray drying may remain plastic, resulting in sticking inside the dryer wall, dependening on product characteristics, composition, and drying conditions. The resulting amorphous product post- spray drying can be syrup, a sticky powder or a relatively free flowing powder. Roos and Karel (1991b) found that the critical viscosity of 10^7 Pa.s (Bellows and King, 1973; Downton et al., 1982) is reached at temperatures of 10 – 20 °C above T_g. Therefore, the temperature of the powder surface during spray drying should be 10 – 20 °C above T_g to prevent stickiness.

If amorphous powders are not stored at the correct conditions relative to their glass transition temperature, then they are susceptible to crystallisation, agglomeration and caking. For example, the rate of crystallisation relates to $T - T_g$ with increasing temperatures causing increased crystallisation rates (Roos and Karel, 1991b; Bhandari and Howes, 2009).

1.5.2 Crystallisation

The degree of lactose crystallisation in dairy products has a significant effect on ingredient and food properties, such as texture and flavour. In milk powders, crystallisation of lactose causes lumping and caking, which negatively impact upon powder reconstitution (Lai and Schmidt, 1990). Component crystallisation causes internal lipids in powders to be released (Shimada et al., 1991; Fäldt and Bergenståhl, 1996), making them more susceptible to oxidation.

Sugars such as lactose and sucrose readily crystallise when exposed to high temperature and humidity (Yu et al., 2007). There is a critical relative humidity at a given temperature at which sugars crystallise, therefore, it is important to know this so that powders can be stored in appropriate conditions conducive to a long shelf life.

1.5.2.1 Measurement of crystallisation

Different methods are used to quantify crystallisation of amorphous sugars. Isothermal differential scanning calorimetry (DSC) was used to study crystallisation of freeze dried lactose and sucrose (Roos and Karel, 1990; Kedward et al., 1998). X-ray diffraction (XRD) has also been used to monitor crystallisation kinetics of lactose, trehalose and lactose/trehalose mixtures (Jouppila et al., 1997; Miao and Roos, 2005). Atomic force microscopy (AFM) has been used to quantify lactose crystallisation on powder surfaces by measuring the surface roughness for lactose powder (Mahlin et al., 2004) and skimmed and whole milk powders (Murrieta-Pazos et al., 2011). Dynamic mechanical analysis (DMA) was used by Soutari et al. (2012) to quantify crystallisation rates of amorphous pharmaceuticals.

Gravimetric methods can be used to measure sugar crystallisation by monitoring changes in powder mass upon humidification (Iglesias and Chirife, 1978; Lai and Schmidt, 1990; Jouppila and Roos, 1994b). Crystallisation causes sorbed water to be released, which is measured as a mass decrease in a humidified powder (Burnett et al., 2004; Burnett et al., 2006). This method is best used at ambient temperatures where crystallisation rates are quite slow and can be easily monitored (Kedward et al., 2000).

1.5.2.2 Crystallisation kinetics

Various relationships can be used to monitor crystallisation kinetics of sugars, the most common of which is the Avrami equation (Equation 1.13) (Avrami, 1939, 1940), which has been used by several researchers (Arvanitoyannis and Blanshard, 1994; Kedward et al., 2000; Mazzobre et al., 2003; Haque and Roos, 2005). The Avrami model is obtained from the following equation:

$$\theta_t = 1 - \exp(-kt^n) \tag{1.13}$$

Here, k is the rate constant (min^{-1}) and n is the Avrami exponent. The rate constant (k) measures the rate of crystal growth indicating the stability of the system (Gaisford et al., 2009), and the Avrami exponent (n) defines the mechanism of crystallisation. The Avrami rate constant is dependent on the crystallisation temperature (Kawamura, 1979), and generally follows an Arrhenius-type temperature dependency. An Avrami exponent value of 1 represents nucleation and crystal growth from surfaces, a value of 2 represents crystal growth from edges, and a value of 3 represents crystal growth in three dimensions. Non-integer n values can be obtained representing mixed crystallisation mechanisms (Cahn, 1956; Soutari et al., 2012). Powders stored at increasing temperature and humidity crystallise at faster rates (Soutari et al., 2012).

Derivative models from the Avrami equation include the Yang equation (Yang et al., 2010) and Urbanovici-Segal equation (Urbanovici and Segal, 1990). The Yang equation is represented by Equation 1.14 and is similar to that derived by Tobin et al. (1974):

$$\theta_t = 1 - \frac{1}{1 + kt^n} \tag{1.14}$$

The Urbanovici-Segal equation is:

$$\theta_t = 1 - [1 + (r+1)(k_{us}t)^{n_{us}}]^{1/(1-r)} \tag{1.15}$$

The Urbanovici-Segal equation includes a parameter *r* ($r > 0$) that determines how far the model deviates from the Avrami equation (Soutari et al., 2012). Other kinetic models used to determine lactose crystallisation are the Williams-Landel-Ferry (WLF) equation (Roos and Karel, 1991b), and the Hoffman equation (Arvanitoyannis and Blanshard,

1994). The Arrhenius equation can be used to determine the activation energy (E_A) required for crystallisation (Schmidt et al., 1999).

Half-times of lactose crystallisation ($t_{1/2}$) can be used to predict the storage stability of lactose containing products. The crystallisation half-time is calculated using the rate constant (k) and exponent (n) in the following equation:

$$t_{1/2} = \left(\frac{\ln 2}{k}\right)^{1/n} \quad (1.16)$$

Protein has been shown to have an effect on lactose crystallisation kinetics. Schmidt et al. (1999) measured lactose crystallisation kinetics at 25 °C in the range 52.5 – 57.5% RH and obtained a rate constant of 5.6 – 15.5 x 10^{-3} min^{-1}. A lower rate constant of 1.1 x 10^{-10} min^{-1} was obtained by Jouppila et al. (1997) for lactose in SMP. Therefore, the presence of protein delayed lactose crystallisation. Thomas et al. (2004b) found that increasing the β-lactoglobulin content of lactose/β-lactoglobulin mixtures resulted in lactose crystallisation at a higher water activity compared to pure lactose. The authors reasoned that this was due to the increased presence of protein on the powder surface which was competing with lactose for water vapour.

1.5.3 Cohesion

Cohesion, defined as inter-particle stickiness, is linked to powder composition and storage conditions. Sugars (i.e. lactose), proteins, and fat all contribute to cohesion. The fat component of WMP has been found to cause double the cohesion of SMP when the temperature is increased from 30 to 65 °C. Water content has a significant effect on cohesion, particularly when >6% w/w. This can result in liquid bridges forming (amorphous lactose and water) or the plasticisation of the powder (Rennie et al., 1999). Cohesion has a big effect on powder flowability. Powder particle size also influences flowability, with particles <200 μm causing reduced flowability due to smaller particles having increased surface area per unit mass of powder. More surface area is available for cohesive forces, such as frictional forces, to resist flow (Fitzpatrick et al., 2004; Vega et al., 2005b).

1.5.4 Caking

Caking is another phenomenon negatively affecting dairy powder stability. It causes low moisture, free-flowing powders to change into lumps, then into an agglomerated solid, and then into a sticky material due to exposure to high temperatures and humidity. Free fat on the powder surface can contribute to caking (Foster et al., 2005; Vega et al., 2005b). Therefore, systems with low fat encapsulation will have an increased chance of caking.

1.6. Microscopy

1.6.1 Polarised light microscopy (PLM)

The optical or light microscope is used extensively in the food and pharmaceutical industries. It can be used to illustrate particle size and shape. The range of utility of the microscope is extended by using polarised light, which allows crystallographic data on small individual crystals to be obtained. Polarised light microscopy (PLM) provides a unique way of viewing the internal structure of crystals. It has been used for more than 200 years for examining crystal properties of minerals, inorganic chemicals and organics. PLM is similar to, yet different from, x-ray crystallography. Both techniques provide useful information on crystal structure, and they can be used together to give detailed information on crystals.

PLM has been used by few studies to observe crystallisation of sugars. Bhugra et al. (2007) used PLM in conjunction with x-ray powder diffraction to observe any crystals found in sucrose powders post- spray drying and post- freeze drying. It was also used to measure the onset time of crystallisation for powder samples stored below the glass transition temperature by detecting the presence of birefringence of samples immersed in silicone oil. No images were shown in this study. Mazzobre at al. (2003) used polarised light videomicroscopy (PLV) and differential scanning calorimetry (DSC) as two comparative methods for determining the isothermal lactose crystallisation kinetics in powders of lactose and lactose: trehalose (80: 20). A major advantage of PLV was that real-time observations of crystallisation could be taken and it showed that lactose crystallisation occurred at different rates in different areas of the samples. Differential

interference contrast (DIC) is another light microscope technique that can be used. McCarthy et al. (2013) used DIC on the light microscope to observe lactose crystals in infant formula powders before and after storage at 55% RH. Tomahawk-shaped lactose crystals in powders were observed but the crystals are less clear than they would be if PLM was used.

1.6.2 Confocal laser scanning microscopy (CLSM)

CLSM uses a focused scanning laser to illuminate a sub-surface layer of specimens in such a way that information from this focal plane passes back through the specimen and is projected onto a pinhole (confocal aperture) in front of a detector. Only light from a defined focal plane in the specimen can pass through the confocal aperture and reach the detector, producing an image which is effectively an optical slice.

CLSM has been used to study a wide variety of food products such as chocolate, emulsions, cereal products and dairy products. Auty et al. (2001) observed the distribution of fat and protein in cheese, milk powder, and chocolate using CLSM. Very few studies have looked at dairy powders with CLSM. Kelly et al. (2014) used CLSM to analyse the distribution of fat droplets in powder samples where different fat blends were stabilised by sodium caseinate. Samples were dual labelled with Nile Red/Fast Green FCF to show the distribution of fat and protein, respectively, throughout the powder particles. Air vacuoles were also visible in powders using this technique. Auty et al. (2001) found for WMP that free fat was not restricted to the powder surface, but was also occluded within the particle and on the inner lining of occluded air bubbles. McKenna (1997) examined whole milk powder using CLSM and found that when stained for fat only, that lactose crystals could be observed by negative contrast. The crystals were tomahawk-shaped α-crystals due to the lactose crystallising in the milk prior to spray drying. Caric and Kaleb (1987) found that β-anhydride crystals were formed upon storage of milk powder. McCarthy et al. (2013) showed increased levels of free fat (FF) in infant formula post-lactose crystallisation (Figure 1.11).

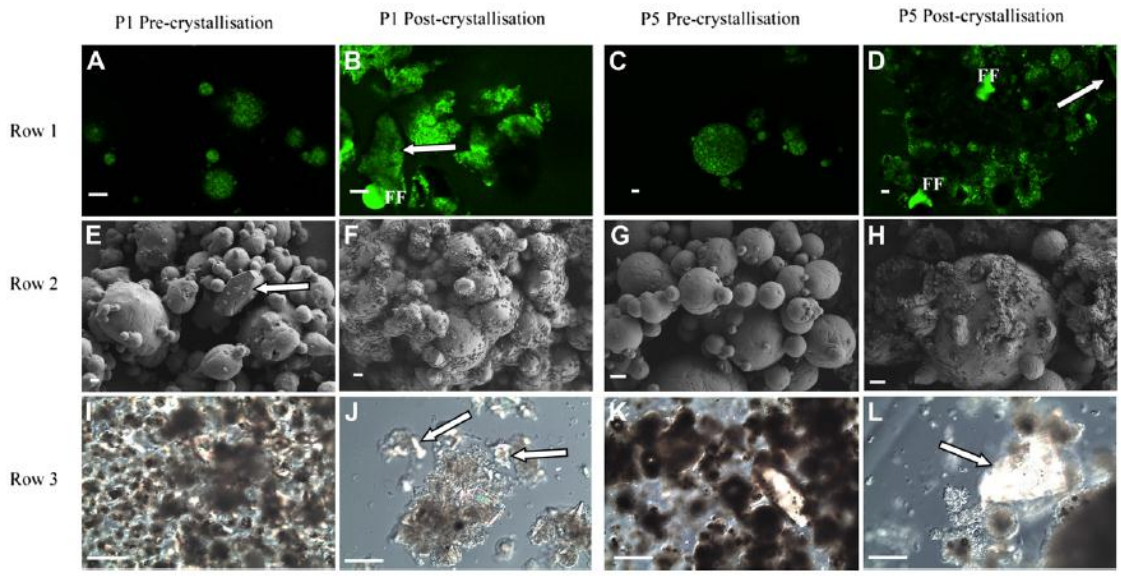

Figure 1.11 Micrographs of infant formula powders P1 and P5 before (stored at 0% RH) and after lactose crystallisation (stored at 55% RH). Row 1: Confocal images of P1 (A, pre-crystallisation; B, post- crystallisation) and P5 (C, pre-crystallisation; D, post-crystallisation), scale bars represent 10 μm; Row 2; scanning electron microscope (SEM) images of P1 (E, pre- crystallisation; F, post- crystallisation) and P5 (G, pre-crystallisation; H, post- crystallisation), scale bars represent 10 μm; Row 3: Light micrographs of P1 (I, pre- crystallisation; J, post- crystallisation) and P5 (K, pre-crystallisation; L, post- crystallisation), scale bars represent 100 μm. FF indicates free fat; arrows indicate lactose crystal (McCarthy et al., 2013).

1.6.3 Cryo-scanning electron microscopy (Cryo-SEM)

Scanning electron microscopy (SEM) was first introduced into food science in the late 1960's. It plays an important role in image analysis as it gives high resolution information, much greater than that from light microscopy. Observation of bulk specimens is possible because use is made of secondary electrons emerging from the specimen surface. The surface and internal structure can be analysed by applying appropriate fracturing techniques. Cryo-SEM investigates the microstructure of bulk samples, and is a useful technique in analysing nanosized objects embedded in food matrices (Dudkiewicz et al., 2011).

SEM is extensively used for detailed analysis of food powders. It is important to characterise the outer topography of particles as it can give information on powder flow properties of spray dried powders. Various studies have used SEM to analyse powders

prepared with sodium caseinate as the emulsifier. There are various papers on the topic of surface composition of spray dried emulsions (Fäldt et al., 1993; Fäldt and Bergensåthl, 1994, 1995, 1996a, b; Fäldt and Bergenståhl, 1996). Hogan et al. (2001b) used sodium caseinate as an emulsifier to stabilise soybean oil at varying oil: protein ratios (0.25 – 3). They found that all powders had a smooth surface, and that at the low oil: protein ratio (0.25) powders had higher surface indentation than high oil: protein ratio (3). At the high oil: protein ratio, powders appeared to be agglomerated, indicating high degrees of surface fat.

Murrieta-Pazos et al. (2011) observed the surface of milk powders (SMP and WMP) by SEM, before and after lactose crystallisation, after storage at varying water activity (0.11 – 0.77). They found that the surface of powders was rougher after storage at increasing water activity, and that the surface of SMP was rougher than WMP. The irregular surface, as a result of lactose crystallisation, was also observed by Faldt and Bergenståhl (1996) who postulated that fat globules reduced the size of lactose crystals formed after humidification. McCarthy et al. (2013) found using SEM that prism-shaped lactose crystals were present on the powder surface of fresh infant formula powders and that powder surfaces were rough post- lactose crystallisation after storage at 55% RH (Figure 1.11).

1.7 Lipid oxidation

1.7.1 Lipid oxidation introduction

Lipid oxidation is the main cause of quality deterioration and reduced shelf life in foods (Sun et al., 2011). The nutritional value and quality of fat-containing foods is lowered from lipid oxidation, resulting in the formation of off-flavours, off-odours, and causing a colour change (van Ruth et al., 2001). Primary oxidation is a free radical process, resulting in the formation of hydroperoxides/peroxides (Osborn and Akoh, 2004). These intermediates are odourless, tasteless and unstable, and so readily decompose to form secondary oxidation products which are small, volatile molecules that give off-aromas associated with lipid rancidity (Chaiyasit et al., 2007). Examples of secondary oxidation compounds are aldehydes, ketones, hydrocarbons, carbonyl compounds, alcohols and

others (Akoh and Min, 2008). The greater the degree of oil polyunsaturation, the greater free radical formation and oxygen uptake that arises. For example, O'Brien et al. (2000) reported that the relative rates of autoxidation of purified esters of oleic acid (C18:1), linoleic acid (C18:2), and linolenic acid (C18:3) were 1:12:25 on the basis of peroxide or conjugated diene development in systems containing only the individual ester. The two main factors determining the susceptibility of oils to oxidation are; their fatty acid composition, and the presence of antioxidant compounds (Abramovič et al., 2007). Rancidity in oils is a growing problem in the food industry, due to consumers increasing demand for increased use of polyunsaturated oils and decreased use of synthetic antioxidants (Frankel, 1996).

1.7.2 Mechanism of lipid oxidation

Lipid oxidation, the complex free radical chain reaction between unsaturated fats and oxygen, can occur in an autocatalytic manner and be separated into three separate stages, (i) initiation, (ii) propagation, and (iii) termination (Frankel, 1998; Chaiyasit et al., 2007). During initiation, the presence of inhibitors (I) (photosensitive compounds, light, heat, or metal ions), unsaturated lipids lose a hydrogen radical (H●) at the α-methylene group adjacent to the double bond to form an alkyl free radical (R●) (Frankel, 1998; Jacobsen, 2008). A diradical (RO●) is formed when oxygen adds at the double bond. Slight off-flavours occur at this stage. During propagation, the alkyl free radical (R●) containing a labile hydrogen, quickly reacts with oxygen to form a peroxyl radical (ROO●). This peroxyl radical can react with the α-methylene group of unsaturated acids (RH). A hydrogen transfer reaction occurs to form a hydroperoxide (ROOH) and a new free radical (R●) (Frankel, 1998). The new free radical adds to the chain reaction by reacting with another oxygen molecule to produce another hydroperoxide. Propagation causes increased flavour deterioration. In the presence of heat or metal ions, peroxides may be decomposed into secondary volatile oxidation products. The rate of oxidation decreases after reaching a maximum level near the end of oxidation. During termination, non-radical products are formed from combining peroxyl radicals causing major oxidation (Coultate et al., 2002).

1.7.3 Factors affecting lipid oxidation in emulsions

Factors affecting lipid oxidation in oil-in-water emulsions are summarised in Table 1.2 (Waraho et al., 2011).

1.7.3.1 Proteins

Significant quantities of non-adsorbed protein exist in the continuous phase of food emulsions such as milk, infant formula, and nutritional beverages. The amount of non-adsorbed protein in an oil-in-water emulsion has an impact upon lipid oxidation. Oxidation can either increase or decrease through enzymatic or non-enzymatic mechanisms. Reasons for pro-oxidant or antioxidant activity of proteins are free radical scavenging, chelation of transition metals or other reactive species, catalysis of specific reactions, and preferential oxidation (Decker, 1998).

Proteins inhibit or promote lipid oxidation through non-enzymatic means. Dairy proteins such as whey, casein and lactoferrin were shown to have antioxidant properties in oil-in-water emulsion systems (Allen and Wrieden, 1982a, 1982b). For casein and lactoferrin, this was due to their ability to chelate iron. Whey proteins antioxidant capacity was probably due to scavenging of free radicals by sulfhydryl and non-sulfhydryl amino acids, and some transition metal chelation (Allen and Wrieden, 1982a; Tong et al., 2000a). Free radical scavenging and metal chelation of globular proteins can be increased by thermal processing or enzymatic hydrolysis, exposing antioxidant amino acid residues in the protein interior (Taylor and Richardson, 1980; Tong et al., 2000b; Peña-Ramos et al., 2004; Elias et al., 2005; Elias et al., 2006; Elias et al., 2007; Peng et al., 2009; Waraho et al., 2011).

Table 1.2 Factors capable of inhibiting lipid oxidation in oil-in-water emulsions (Waraho et al., 2011).

Characteristic	Property	Factors
Liquid Phase	Composition	• Degree of unsaturation. • Prooxidant impurities, e.g., free fatty acids, hydroperoxides. • Inherent antioxidants, e.g., free radical scavengers and chelators. • Added antioxidants, e.g., free radical scavengers and chelators.
	Physical state – solid fat content and crystal properties	• Solubility, partitioning and diffusion of antioxidants and prooxidants.
	Physical properties	• Rheology determines diffusion of antioxidants and prooxidants. • Polarity determines partition coefficients.
Aqueous phase	Composition – pH, ionic strength, solutes	• Prooxidant impurities, e.g., transition metals, photosensitisers, enzymes. • Inherent antioxidants, e.g., free radical scavengers and chelators. • Added antioxidants, e.g., free radical scavengers and chelators. • Micelles may alter location of antioxidants and prooxidants. • Reducing agents that can redox cycle prooxidant metals.
	Physical state – ice crystal structure and location	• Solubility, partitioning and diffusion of reactants and products.
	Physical properties	• Rheology determines diffusion of antioxidants and prooxidants. • Polarity determines partition coefficients
Interfacial phase	Composition	• Anti-/prooxidant activity. • Impurities (hydroperoxides).
	Thickness	• Steric hindrance of interactions between water- and oil-soluble components.
	Charge	• Electrostatic attraction/repulsion of antioxidants and prooxidants.
	Permeability	• Diffusion of antioxidants and prooxidants in lipid and aqueous phase.
	Emulsion	• Droplet concentration. • Droplet size distribution (surface area and light scattering).
	Spray dried powder	• Porosity. • Exposed lipid levels. • Emulsion droplet characteristics upon rehydration.
	Hydrogel particles	• Hydrogel composition, structure and properties.

1.7.3.2 Oil droplet characteristics

Oil droplet concentration and fat globule size have been investigated as significant factors affecting the autoxidation of unsaturated lipids in emulsions. Increasing oil concentration has been reported to result in a decrease in total oxidation and the concentration of volatiles in the headspace of an emulsion (Jo and Ahn, 1999). This was attributed to higher resistance to mass transfer in oil than in water, due to flavours needing to be released from the lipid phase to the aqueous phase to headspace in food emulsions. Similarly, Osborn and Akoh (2004) found that a decreasing caprylic/canola oil concentration in structured lipid-based emulsions led to increasing lipid oxidation.

Coupland et al. (1996) studied the effect of droplet concentration on the rate of oxidation of emulsified ethyl lineoate. The authors found that with increasing oil concentration, the rate of initiation was slow followed by a quick propagation step, accounting for the fact that the rate of lipid oxidation was slow initially, but increased after longer times in food emulsions. They also thought that particle size would only affect lipid oxidation kinetics when the surface activity of the substrate molecules was high and would accumulate at the surface.

The effect of varying the fat globule size at fixed oil droplet concentrations in emulsions has been shown to give differing results. Fritsch (1994) and Coupland et al. (1996) have stated that the rate of lipid oxidation increases as fat globule size decreases due to increased surface area for free radicals and oxygen to interact with the unsaturated lipid. Roozen et al. (1994) wrote that if there a limited number of reactants which scatter at the droplet surface, changing the droplet size may affect the lipid oxidation rate. In contrast, Nakaya et al. (2005) showed that the oxidative stability of soybean oil triacylglycerol (TAG) in oil-in-water emulsions decreased with increasing oil droplet size. Also, Osborn and Akoh (2004) found that reducing fat globule size caused no significant difference in primary or secondary lipid oxidation. The results from current literature show that further research needs to be done in this area.

1.7.3.3 Sugar composition

Reducing sugars promote lipid oxidation, whereas non-reducing sugars inhibit lipid oxidation. Sucrose (non-reducing sugar) was shown to reduce lipid oxidation of linoleic acid in oil-in-water emulsions stabilised by Tween-20 (Ponginebbi et al., 1999), and reduce oxidation of safflower in oil-in-water emulsions stabilised by an anionic surfactant (Sims et al., 1979; Sims, 1994). Sucrose inhibits lipid oxidation in oil-in-water emulsions because it: decreases the oxygen concentration in the aqueous phase, scavenges free radicals, and increases the viscosity of the aqueous phase which decreases the movement of the reactive species to the surface (McClements and Decker, 2000). Conversely, reducing sugars have been shown to promote lipid oxidation (Yamauchi et al., 1982; Yamauchi et al., 1984; Shimada et al., 1992) due to their ability to reduce transition metals to their most active state (i.e. Fe^{3+} to Fe^{2+}).

1.7.4 Lipid oxidation in powders

Milk can be spray dried to produce milk powder. Powdered milk has the advantage of microbial stability, leading to increased shelf life. However, dried milk and other dairy powders are susceptible to lipid oxidation due to their greater surface area in which more lipids can be exposed to the surrounding environment at low water activity (Stapelfeldt et al., 1997b). Therefore, lipid oxidation is one of the primary reasons for dairy powder spoilage.

Autoxidation of unsaturated fatty acids is a major problem for maintaining the stability of dairy powders. The higher the unsaturation level, the greater the degree of lipid oxidation and the lower storage stability (Hedegaard et al., 2006), implying that WMP has a shorter shelf life than SMP.

Various factors have an effect on lipid oxidation in dairy powders; they are water activity, particle porosity, and headspace oxygen. Powders with a water activity <0.11 are found to have increased levels of lipid oxidation, whereas powders stored at 0.11 – 0.75 have much lower oxidation levels (Stapelfeldt et al., 1997b). Other authors recommend that powder be stored at a water activity of 0.11 – 0.23, as at a_w>0.31, sensory quality of powders degrade (Dóka et al., 2000; Lloyd et al., 2004a).

Oxidative stability of powders is also related to particle porosity, which determines the permeability of the wall matrix to oxygen (Moreau and Rosenberg, 1996; Moreau and Rosenberg, 1998). Permeability to oxygen is affected by parameters such as water, temperature, mechanical compaction, particle size, chemical nature of the constituents, processing conditions, moisture, and temperature during storage (Barbosa-Cánovas and Juliano, 2005). The degree of casein aggregation has an inverse effect on the amount of lipid oxidation (Keogh et al., 2001), i.e. high aggregation leads to low porosity and *vice versa*. Keogh et al. (2001) showed that porosity, and hence, lipid oxidation, were greatest for sodium caseinate (low aggregation), followed by calcium caseinate (medium aggregation), and SMP (high aggregation). Factors that affect porosity include atomisation conditions, total solids concentration, and foaming capacity of the concentrates. Sodium caseinate has a high foaming capacity (Sánchez and Patino, 2005) meaning air is easily incorporated into the feed before drying. Oil reduces the foaming of concentrates, leading reduced porosity. Porosity can be minimised by using a small orifice size in disc or pressure nozzle atomiser.

In dairy powders, lower oxygen headspace concentrations lead to lower levels of lipid oxidation. Powders should be stored in sealed containers at oxygen levels of <2% to minimise lipid oxidation. Above 2%, oxidation is not inhibited (Lloyd et al., 2004a). When stored at 3 – 6% oxygen, powders have a long shelf life, but lipid oxidation can still occur. Keeping the oxygen level to 0.5 - 1.0% reduces the development of the tallow off-flavour. Optimum quality is obtained when the oxygen content is less than 0.01 mL/g of powder.

1.7.4.1 Powder shelf life

The shelf life of a food product is defined as how long it maintains a certain desired standard of quality. It is important to identify the key chemical and biological reactions causing deterioration of food quality, and knowing how they should be controlled (Taoukis et al., 1997). Shelf life of foods is affected by four main factors: (i) formulation, (ii) processing, (iii) packaging, and (iv) storage conditions.

Environmental factors such as storage temperature and relative humidity have a direct impact on dairy powder shelf life, with temperature in particular having the greatest effect. Increasing storage temperature increases lipid oxidation, hence, decreasing shelf life. Storage of dairy powders at >30 °C has a particularly negative effect on product shelf life (Lloyd et al., 2004b). Temperature sensitivity of reactions can be determined using Q_{10} models. They measure reaction rates at 10 °C intervals to detect the temperature sensitivity of food products, and are useful shelf life predictors (Fu and Labuza, 1993; Taoukis et al., 1997).

Relative humidity (RH) is the second most important factor affecting lipid oxidation in dried dairy products, affecting both water content and water activity (a_w). Shelf life may be reduced in dairy powders when stored at >5% RH (Lloyd et al., 2004b). Control of water activity is the basis of preservation of dried foods. Deterioration reaction rates increase exponentially with increasing a_w, due to water to reacting with other food components, which can occur above the materials water monolayer value. Uniquely, lipid oxidation reactions increase again when a_w is lower than the monolayer value (Taoukis et al., 1997).

1.7.5 Oxidation products

Hydroperoxides are the primary products from lipid oxidation, and have little or no flavour. They decompose readily into low molecular weight carbonyls, typically aldehydes, and these products subsequently form off-flavours in stored milk powders (Min et al., 1990; Jacobsen, 1999). These off-flavours have been described as metallic, oily, tallow, cardboard, buttery, and hay-like (Shipe et al., 1978; Barrefors et al., 1995; Jacobsen, 1999; Van Aardt et al., 2001; Karagül-Yüceer et al., 2002).

The most common compounds that cause off-flavour are linoleic, linolenic, oleic, and arachidonic acids. The greatest off-flavours in milk give a cardboard-like off-flavour and are from the decomposition of these fatty acids into alkanals and alkenals having at least 6 carbon atoms (Shiratsuchi et al., 1994; Barrefors et al., 1995). Hexanal is a strong indicator of oxidative rancidity, typically originating from either linoleic acid. Reduced oxygen content has led to reduced hexanal content (Karagül-Yüceer et al., 2002). Fenaille

et al. (2003) found that hexanal was the preferred chemical marker in testing of milk powders due to its prevalence and its strong correlation with off-flavours. Other aldehydes, such as pentanal and heptanal, form at room temperature but they are not as common as hexanal (García-Llatas et al., 2007).

1.7.6 Methods to measure lipid oxidation

Various analytical techniques are available for lipid oxidation measurement in foods, but no standard method exists for measuring all oxidative changes (Shahidi and Wanasundra, 2002). Therefore, a proper method is required for different applications. There are five groups of lipid oxidation measurement methods: (i) the formation of free radical, (ii) the absorption of oxygen, (iii) the loss of initial substrates, and the formation of (iv) primary and (v) secondary products (Dobarganes and Velasco, 2002). Some of the main methods are summarised below for primary and secondary oxidation measurement.

1.7.6.1 Peroxide value

Quantifying the peroxide value (PV) of oil is a commonly used method in determining primary lipid oxidation (Ulberth and Roubicek, 1995; Hogan et al., 2003; O' Dwyer et al., 2013). Due to the fast decomposition of peroxides, it does not exactly represent the true amount of lipid oxidation, nonetheless it is a suitable and highly accurate method (van der Merwe et al., 2004). PV should be measured regularly because it has an initial lag phase, followed by a rapid increase where it eventually plateaus, and over time will decompose back to 0, so timely measurements can monitor the full extent of hydroperoxide production and decomposition (van der Merwe et al., 2004). One disadvantage of the technique is that it is difficult to reproduce results due to the rapid change in rate of hydroperoxide formation/decomposition (Guillén and Cabo, 2002). The main disadvantage of the technique is that, as previously mentioned, it does not indicate the true extent of lipid oxidation.

1.7.6.2 Anisidine value

The anisidine value is a fast and easy method of measuring secondary oxidation products; occurring due to a reaction of α- and β-aldehydes (mostly 2-alkenals) with a p-anisidine reagent, giving information about secondary products formed after hydroperoxide decomposition. It is determined by spectroscopic methods and is a good indicator of secondary lipid oxidation. It is the best method of measuring secondary oxidation products in dairy powders due to its reliability, simplicity, and reproducibility compared to other methods (White, 1995; Guillén and Cabo, 2002; van der Merwe et al., 2004).

1.7.6.3 Thiobarituric Acid Reacting Substances (TBARS)

Measurement of (TBARS) is also used to quantify secondary lipid oxidation (Tarladgis et al., 1964; Ohkawa et al., 1978). This method uses a spectrophotometer to measure a pink complex at 532 nm, formed from one molecule of malondialdehyde reacting with two molecules of 2-thiobarbituric acid (TBA).

1.7.6.4 Gas chromatographic headspace methods

Aldehydes, including pentanal and hexanal, are some of the most commonly produced volatiles produced during lipid oxidation (Shahidi and Pegg, 1994). Several methods exist which measure volatiles in container headspace. Static headspace gas chromatography (SHGC) is a quick and easy method in which an aliquot of gas from the headspace above the sample is directly transferred to a GC for measurement. Romeu-Nadal et al. (2004) developed a SHGC method to determine volatile compounds (propanal, pentanal, and hexanal) in infant formula as indicators of lipid oxidation. In this method, aldehydes were separated isothermally at 75 °C in a GC equipped with a flame ionisation detector (FID). Dynamic equilibrium can also be used and does not require sample equilibrium, but does involve careful quality control (Przybylski and Eskin, 1995). Dynamic headspace gas chromatography (DHGC) can give poor reproducibility, making it unfavourable.

Solid phase microextraction (SPME) is a solventless extraction technique developed in the early 1990's as a quick and accurate method of determining the volatile organic

compounds existing in various food products (Pawliszyn, 2000). SPME sampling has three basic modes, (i) direct extraction, (ii) headspace extraction, and (iii) membrane extraction. For headspace extraction, the method uses a silica fibre coated with different adsorbent or absorbent materials that are exposed to the sample headspace in a specialised headspace (HS) vial under controlled conditions (temperature, agitation, and time). Firstly, analytes from the sample are released and adsorb/absorb to a polymer-coated fibre. After equilibration, desorption of adsorbed/absorbed compounds from the fibre occurs in the GC inlet at high temperatures, and they are introduced to the column for separation and subsequent detection. SPME has been shown to be a more effective technique than DHGC for analysing light-induced lipid oxidation products from milk (Marsili, 1999). SPME gave superior precision with reduced carryover/background peaks, which are sometimes associated with DH. SPME combined with HS, i.e., HS-SPME, is a technique used to determine the quantity of saturated aldehydes, which are the main volatile produced in infant formula (Fenaille et al., 2003; Przygonski, 2003; García-Llatas et al., 2007). Pentanal and hexanal are breakdown products from *n*-6 polyunsaturated fatty acid. Hexanal, in particular, is commonly used in determining lipid oxidation in infant formula (Romeu-Nadal et al., 2004; García-Llatas et al., 2007). These aldehydes are produced from the oxidation of sunflower oil-in-water emulsions (van Ruth et al., 1999). Several researchers have found it a valuable technique to analyse low amounts of volatiles in different beverages and foods. Its main advantages are its simplicity, low cost, ease of use, and sensitivity.

Various types of fibre exist that differ in their polymer coating. The Carboxen®/PDMS type fibre is the most suitable for extraction of low molecular weight analytes (Marsili, 2000; Perkins et al., 2005). Carboxen is a porous particle which can selectively retain volatiles such as analytes containing 2 – 12 carbon atoms (Perkins et al., 2005). Overall, quantifying aldehydes, particularly hexanal, in the headspace of containers of dairy powders using SPME make it possible to determine if lipid oxidation is occurring, and gives information on the source of any perceived aromas (Jung and Ebeler, 2003).

1.8 Conclusions

The literature discussed in this chapter show that there is significant knowledge and understanding of nanoemulsions in terms their physical and thermodynamic properties, and their many potential uses in the food industry due to their unique properties. However, it is also evident that there is a lack of research on the physical properties and functionality of dried nanoemulsions. Numerous review papers compare the emulsion stability (gravitational separation, flocculation, and coalescence) of conventional emulsions and nanoemulsions, but no papers review both emulsion types after they have been dried. The research in this thesis gives a detailed account of various ways in which both emulsion types differ after spray drying, particularly in terms of microstructure, physical properties, lactose crystallisation, and lipid oxidation upon storage.

Chapter 2 - Optimisation of β-casein stabilised nanoemulsions using experimental mixture design

Published as:

Maher, P.G., Fenelon, M.A., Zhou, Y., Haque, Md. K., and Roos, Y.H. 2011. Optimization of β-casein stabilized nanoemulsions using experimental mixture design. *Journal of Food Science* 76(8): 1108–1117.

C: Food Chemistry

Optimization of β-Casein Stabilized Nanoemulsions Using Experimental Mixture Design

Patrick G. Maher, Mark A. Fenelon, Yankun Zhou, Md. Kamrul Haque, and Yrjö H. Roos

Abstract: The objective of this study was to determine the effect of changing viscosity and glass transition temperature in the continuous phase of nanoemulsion systems on subsequent stability. Formulations comprising of β-casein (2.5%, 5%, 7.5%, and 10% w/w), lactose (0% to 20% w/w), and trehalose (0% to 20% w/w) were generated from Design of Experiments (DOE) software and tested for glass transition temperature and onset of ice-melting temperature in maximally freeze-concentrated state (T_g' & T_m'), and viscosity (μ). Increasing β-casein content resulted in significant ($P < 0.0001$) increases in viscosity and T_m' ($P = 0.0003$), and significant ($P < 0.0001$) decreases in T_g'. A mixture design was used to predict the optimum levels of lactose and trehalose required to attain the minimum and maximum T_g' and viscosity in solution at fixed protein contents. These mixtures were used to form the continuous phase of β-casein stabilized nanoemulsions (10% w/w sunflower oil) prepared by microfluidization at 70 MPa. Nanoemulsions were analyzed for T_g' & T_m', as well as viscosity, mean particle size, and stability. Increasing levels of β-casein (2.5% to 10% w/w) resulted in a significant ($P < 0.0001$) increase in viscosity (5 to 156 mPa.s), significant increase in particle size ($P = 0.0115$) from 186 to 199 nm, and significant decrease ($P = 0.0001$) in T_g' (−45 to −50 °C). Increasing the protein content resulted in a significant ($P < 0.0001$) increase in nanoemulsion stability. A mixture DOE was successfully used to predict glass transition and rheological properties for development of a continuous phase for use in nanoemulsions.

Keywords: glass transition, nanoemulsion, optimization, stability, viscosity

Introduction

Food formulations are widely produced by combining carbohydrate, protein, and oil in emulsified systems. The characteristics of individual components can be used to control texture and shelf-life (Dickinson and Pawlowsky 1997). Structure through glass formation is provided by carbohydrates. Lactose is commonly used for the continuous matrix-forming material during spray drying. It is a suitable carbohydrate due to its cheap availability, bland flavor, low viscosity in concentrated solutions, and most importantly its ability to produce a good glass. Similarly, trehalose is also a suitable carbohydrate as it has a wide pH-stability range, and is nonreducing in the presence of protein during heat treatment (Higashiyama 2002). Trehalose combined with lactose has been found to delay lactose crystallization while keeping the glass transition temperature of powders (T_g) constant (Mazzobre and others 2001), due to modifications to the molecular environment by geometric, thermodynamic, or kinetic factors. Carbohydrates are often incorporated into dairy protein stabilized nutritional beverages to meet nutritional and structural requirements. Typically, these emulsions are stabilized by amphiphilic moieties, such as caseins. The caseins are the most abundant proteins (approximately 80% w/w) in bovine milk and adsorb strongly at the oil-water interface during homogenization. This layer provides stability to the emulsion during processing and storage and prevents coalescence (Dickinson and Stainsby 1982; Vega and Roos 2006). Caseins also have low heat sensitivity and better surface-active properties compared to whey proteins, which is beneficial for spray drying (Pedersen and others 1998; Hogan and others 2001; Dollo and others 2003; Sliwinski and others 2003). β-casein is the most hydrophobic casein, and steric-stabilizing properties of the protein layer around oil droplets in emulsions are provided by the phosphoserine residues of β-casein (Dickinson 1997a). β-casein is preferentially adsorbed compared to other caseins due to lower interfacial energies, and so β-casein stabilized emulsions are less susceptible to flocculation (Dickinson and others 1987, 1988; Dickinson and Matsumara 1994). Nanoemulsions are emulsions with a particle size in the range of 20 to 200 nm that ensures stability as the diffusion rate, due to Brownian motion, is higher than that for sedimentation and creaming (Solans and others 2005).

The glass transition temperature (T_g) is the temperature at which, upon heating, an amorphous material changes from a glassy, solid-like state to a rubbery, fluid-like state (Langrish and Wang 2006). Glass transition has an effect on many processes and properties encountered in food science. In powders, temperatures above the glass transition are found to increase the molecular mobility and free volume, which can result in physico-chemical deterioration, such as crystallization of sugars, stickiness, and caking of powders (White and Cakebread 1966; Slade and Levine 1991). During processing, stickiness may reduce product yields and retard flow of particles leading to operational problems for manufacturing

MS 20101303 Submitted 11/17/2010, Accepted 7/7/2011 Authors Maher and Fenelon are with Teagasc Food Research Centre, Moorepark, Cork, Ireland. Authors Zhou, Haque, and Roos are with School of Food and Nutritional Sciences, Univ. College, Cork, Ireland. Direct inquiries to Fenelon (E-mail: mark.fenelon@teagasc.ie.).

© 2011 Institute of Food Technologists®
doi: 10.1111/j.1750-3841.2011.02343.x
Further reproduction without permission is prohibited

Journal of Food Science A Publication of the Institute of Food Technologists

Abstract

The objective of this study was to determine the effect of changing viscosity and glass transition temperature in the continuous phase of nanoemulsion systems on subsequent stability. Formulations comprising of β-casein (2.5, 5.0, 7.5 and 10% w/w), lactose (0 to 20% w/w), and trehalose (0 to 20% w/w) were generated from Design of Experiments (DOE) software and tested for glass transition temperature and onset of ice-melting temperature in maximally freeze-concentrated state (T_g' & T_m'), and viscosity (μ). Increasing β-casein content resulted in significant (P <0.0001) increases in viscosity and T_m' (P =0.0003), and significant (P <0.0001) decreases in T_g'. A mixture design was used to predict the optimum levels of lactose and trehalose required to attain the minimum and maximum T_g' and viscosity in solution at fixed protein contents. These mixtures were used to form the continuous phase of β-casein stabilised nanoemulsions (10% w/w sunflower oil) prepared by microfluidisation at 70 MPa. Nanoemulsions were analysed for T_g' & T_m', as well as viscosity, mean particle size, and stability. Increasing levels of β-casein (2.5 to 10% w/w) resulted in a significant increase (P <0.0001) in viscosity (5 to 156 mPa.s), significant increase (P =0.0115) in particle size (186 to 199 nm), and significant (P =0.0001) decrease in T_g' (-45 to -50 ºC). Increasing the protein content resulted in a significant (P <0.0001) increase in nanoemulsion stability. A mixture DOE was successfully used to predict glass transition and rheological properties for development of a continuous phase for use in nanoemulsions.

2.1 Introduction

Food formulations are widely produced by combining carbohydrate, protein, and oil in emulsified systems. The characteristics of individual components can be used to control texture and shelf life (Dickinson and Pawlowsky, 1998). Structure through glass formation is provided by carbohydrates. Lactose is commonly used for the continuous matrix-forming material during spray drying. It is a suitable carbohydrate due to its cheap availability, bland flavour, low viscosity in concentrated solutions, and most importantly its ability to produce a good glass. Similarly, trehalose is also a suitable carbohydrate as it has a wide pH-stability range, and is non-reducing in the presence of protein during heat treatment (Higashiyama, 2002). Trehalose combined with lactose has been found to delay lactose crystallisation, while keeping the glass transition temperature of powders (T_g) constant (Mazzobre et al., 2001), due to modifications to the molecular environment by geometric, thermodynamic or kinetic factors. Carbohydrates are often incorporated into dairy protein stabilised nutritional beverages to meet nutritional and structural requirements. Typically these emulsions are stabilised by amphiphilic moieties such as caseins. The caseins are the most abundant proteins (~80 % w/w) in bovine milk and adsorb strongly at the oil-water interface during homogenisation. This layer provides stability to the emulsion during processing and storage and prevents coalescence (Dickinson and Stainsby, 1982; Vega and Roos, 2006). Caseins also have low heat sensitivity and better surface-active properties compared to whey proteins, which is beneficial for spray drying (Pedersen et al., 1998; Hogan et al., 2001a; Dollo et al., 2003; Sliwinski et al., 2003). β-casein is the most hydrophobic casein and steric-stabilising properties of the protein layer around oil droplets in emulsions are provided by the phosphoserine residues of β-casein (Dickinson, 1997a). β-casein is preferentially adsorbed compared to other caseins due to lower interfacial energies, and so β-casein stabilised emulsions are less susceptible to flocculation (Dickinson et al., 1987; Dickinson et al., 1988; Dickinson and Matsumara, 1994). Nanoemulsions are emulsions with a particle size in the range of 20 to 200 nm that ensure stability as the diffusion rate, due to Brownian motion, is higher than that for sedimentation or creaming (Solans et al., 2005).

The glass transition temperature (T_g) is the temperature at which, upon heating, an amorphous material changes from a glassy, solid-like state to a rubbery, fluid-like state

(Langrish and Wang, 2006). Glass transition has an effect on many processes and properties encountered in food science. In powders, temperatures above the glass transition are found to increase the molecular mobility and free volume, which can result in physico-chemical deterioration, such as crystallisation of sugars, stickiness, and caking of powders (White and Cakebread, 1966; Slade and Levine, 1991). During processing, stickiness may reduce product yields and retard flow of particles leading to operational problems for manufacturing equipment and increased down time (Bhandari and Howes, 1999). Also the storage stability and quality changes of food systems are strongly affected by the glass transition (Schenz, 1995). Crystallisation and caking are time-dependant and are both a function of fluctuation in storage temperature and T_g. The higher the temperature above the T_g, the more viscosity decreases and molecular mobility increases leading to crystallisation and caking (Bhandari and Howes, 1999; Omar and Roos, 2007). These phenomena may also cause the continuous matrix to become unstable and release entrapped components, resulting in impaired rehydration properties (Roos and Karel, 1991c). In frozen food systems, knowing the glass transition temperature at maximal freeze concentration (T_g') and onset of ice melting temperatures at the maximal freeze concentration (T_m') is important in determining the best conditions in which to freeze dry dispersions/emulsions. T_m' is the 'mobility point' above which ice melts causing any sensitive encapsulated components to be released Optimal freeze drying (maximum T_g in powder) is attained by freezing dispersions/emulsions at a temperature above T_g' and below T_m', typically 1 °C below T_m' (Zhou and Roos, 2011). It is, therefore, important that the effects of T_g on food materials, such as emulsions in various states (liquid or dehydrated systems), are taken into account in their processing and storage.

In this study, an experimental mixture design was generated using Design of Experiments (DOE) software. DOE was used to statistically optimise the formulation of nanoemulsions using viscosity and glass transition temperatures at fixed protein concentrations as response parameters to improve their stability and, hence, properties as encapsulants. The optimum nanoemulsion should have a low viscosity, making it easier to dry, and a high glass transition temperature so that it has greater shelf life stability when dried. Data were analysed statistically to show by polynomial equations, adjusted R^2 and *P*-values which variables in the formulation have the most significance on selected responses.

The objective of this study was to produce nanoemulsions with varying viscosity and glass transition temperatures at different protein levels, and observe the effect on mean particle size and stability through the application of a statistical mixture design.

2.2 Materials and Methods

2.2.1 D-optimal experimental mixture design

The experimental mixture design was set up using the software Design Expert® Software version 7.1.3 (Stat-Ease Inc., Minneapolis, MN, USA). A D-optimal design was used with the constraints Lactose + Trehalose + β-casein =2 0% w/w with β-casein ≤10% w/w. This was used to study the continuous phase of carbohydrate-protein mixtures prior to emulsification. The model gave 12 different formulations, plus 5 replicates leading to a total of 17 experimental formulations (Table 2.1). These formulations contained 20% w/w solids and were analysed for viscosity (μ), glass transition temperature of maximally freeze-concentrated liquid (T_g'), glass transition temperature of freeze dried powder (T_g), and onset of ice melting temperature of maximally freeze concentrated liquid (T_m'). The software was used to identify the formulations that both minimised and maximised T_g' and viscosity for the carbohydrate-protein mixtures at fixed protein concentrations of 2.5, 5, 7.5, and 10% w/w. These optimised formulations (Table 2.2) were input into the software (Historical Data Initial Design) with the constraints; Lactose ≤ 17.5% w/w, Trehalose ≤ 17.5% w/w, β-casein 2.5 to 10% w/w, where Lactose + Trehalose + β-casein =20% w/w. Sunflower oil (10% w/w) was added to these formulations prior to emulsification. The purpose of optimisation is to show which amounts of each ingredient correspond to the desired result in the liquid state (low viscosity, high kinetic stability, and high glass transition temperature) and which composition of ingredients correspond to the opposite (undesired result; high viscosity, low kinetic stability, and low glass transition temperature). Nanoemulsions were analysed for viscosity, T_g', T_m', particle size, and separation rate. The data was analysed graphically, and statistically using the software. The statistical significance of the models was given by the adjusted R^2 and *P*-values (Table 2.3), and the graphical representations of models (Figure 2.1 to 2.8) along

with the Scheffe model polynomial equations for 3 components (Table 2.4) predict effects of components in the formulation. Models are deemed significant at $P < 0.05$.

2.2.2 Carbohydrate-protein mixtures

The materials used in the experiments were α-lactose monohydrate (Sigma Aldrich, Ireland), trehalose (Cargill, UK), and β-casein (Kerry Group, Ireland). β-casein was dispersed in distilled water at 45 °C for 1 h using mechanical agitation, adjusted for water loss, and stored overnight (12 h) at 4 °C to ensure protein hydration.

Table 2.1 Mixture design formulations of carbohydrate-protein mixtures with experimental results of viscosity (μ at 400 s^{-1}) and glass transition (T_g', T_m', T_g) values.

Run	Lactose (% w/w)	Trehalose (% w/w)	β-casein (% w/w)	μ (mPa.s)	T_g' (ºC)	T_m' (ºC)	T_g (ºC)
1	13.75	3.75	2.50	3.3	-43.4	-32.7	108.5
2	0	20.00	0	2.1	-42.0	-32.0	111.1
3	10.00	0	10.00	41.9	-50.1	-25.4	119.7
4	0	20.00	0	2.1	-43.0	-32.0	111.0
5	6.25	6.25	7.50	20.1	-50.0	-28.6	117.2
6	3.75	13.75	2.50	3.6	-44.7	-33.7	111.1
7	20.00	0	0	2.1	-42.0	-30.0	105.7
8	7.50	7.50	5.00	6.9	-47.0	-31.9	111.9
9	10.00	10.00	0	2.0	-41.1	-30.8	109.8
10	10.00	10.00	0	2.0	-41.1	-30.5	110.0
11	0	15.00	5.00	8.3	-47.0	-30.2	117.2
12	20.00	0.00	0	2.0	-42.0	-30.0	104.6
13	0	10.00	10.00	78.7	-49.1	-26.0	124.0
14	11.25	3.75	5.00	9.4	-47.5	-27.6	109.9
15	0	10.00	10.00	71.3	-49.0	-26.1	123.7
16	15.00	0	5.00	3.5	-46.5	-29.4	108.8
17	10.00	0	10.00	39.3	-50.5	-25.3	119.1

Lactose, trehalose, and β-casein mixtures were prepared according to Table 2.1, under mechanical agitation at 55 °C for 10 min. Formulations were adjusted to pH 7.5 using 1N HCl at 25 °C.

2.2.3 Nanoemulsion preparation

Oil in water nanoemulsions (10% w/w oil) with β-casein as emulsifier (2.5 to 10% w/w) were prepared using sunflower oil (Trilby Trading, Ireland). Coarse emulsions were prepared by blending 1 L of β-casein solutions with oil at 60 °C using a high shear mixer (Silverson) at ~8000 rpm for 2 min. Coarse emulsions were microfluidised (model M-110EH, Microfluidics, Newton, MA, USA) using a ceramic interaction chamber (70 MPa at 60 °C). Specified quantities of carbohydrates (Table 2.2) were added to the nanoemulsions in a water bath at 55 °C and mixed for 10 min. Nanoemulsions were then cooled to 25 °C and adjusted to pH 7.5 using 1N HCl. The nanoemulsions containing lactose, trehalose, β-casein, and sunflower oil according to the experimental design were heated to 60 °C and microfluidised a second time (70 MPa). Approximately 500 mL of sample was collected and stored at 4 °C prior to analysis.

2.2.4 Rheology

Rheological analysis of carbohydrate-protein mixtures and nanoemulsions was carried out using an AR G2 rheometer (TA Instruments, Crawley, UK), equipped with a 60 mm aluminium parallel plate (gap 800 μm). Samples (~2 mL) were first pre-sheared at 300 s^{-1} for 1 min and equilibrated for 2 min. Samples were then sheared from 10 to 400 s^{-1} over 3 min, held at 400 s^{-1} for 1 min, and then sheared from 400 to 10 s^{-1} over 3 min. The apparent viscosity, taken at 400 s^{-1}, was used in subsequent statistical analysis. A shear rate of 400 s^{-1} was chosen to simulate the conditions of high shear processing. All measurements were carried out at 25 °C.

2.2.5 Differential scanning calorimetry

A differential scanning calorimeter (DSC) equipped with liquid N_2 cooling (Mettler-Toledo DSC 821e, Schwerzenbach, Switzerland) was used to determine the glass transition temperatures (onset glass transition temperature of maximally freeze-concentrated solids, T_g', for liquids and onset glass transition temperature, T_g for anhydrous samples) and onset temperatures of ice melting in maximally freeze-concentrated solids (T_m') in carbohydrate-protein mixtures and nanoemulsions. Samples were prepared in pre-weighed aluminium pans (40 μL; Mettler Toledo-27331) and scanned in hermetically sealed pans. An empty pan was used as a reference. The DSC was calibrated for temperature using *n*-hexane (melting point, 95.0 ºC), mercury (melting point, -38.8 ºC), water (melting point, 0.0 ºC), gallium (melting point, 29.8 ºC), and indium (melting point, 156.6 ºC), and for heat flow using *n*-hexane (ΔH_m, 151.8 J/g), mercury (ΔH_m, 11.4 J/g), water (ΔH_m, 334.5 J/g), gallium (ΔH_m, 80.0 J/g), and indium (ΔH_m, 28.45 J/g). Liquid samples were hermetically sealed in aluminium pans (40 μL; Mettler Toledo) with an empty pan as reference and scanned from -100 °C to 25 °C to determine T_g and T_m for non-annealed samples. Samples were then annealed for 15 min at ~1 ºC below the initial onset of T_m (measured during the first temperature cycle), followed by a second temperature scan (-100 – 25 ºC) to determine the onset of T_g', and T_m'. Anhydrous samples were prepared by freeze drying the carbohydrate-protein mixtures at their various concentration levels. They were firstly heated over the glass transition temperature region (60 to 140 ºC), then cooled to below glass transition temperature, and a second heating scan was run over the glass transition region and the T_g was measured. Heating and cooling rates for both liquid and anhydrous samples were 5 °C/min and 10 ºC/min, respectively. T_g, T_g', and T_m' were determined using STAR^e thermal analysis software, version 8.10 (Mettler Toledo). Measurements were carried out in triplicate.

2.2.6 Particle size analysis

Particle size of the nanoemulsions was measured using a Zetasizer Nano system (Malvern Instruments, Inc., Worcester, UK). Measurements were carried out at 22 ºC, at a

scattering angle of 173°. Samples were diluted using distilled water by a factor of 20 prior to analysis to avoid the effects of multiple scattering. The mean average (z-average) droplet size was measured using an intensity distribution.

2.2.7 Stability analysis

A Lumifuge 116 stability analyser (L.U.M. GmbH, Berlin, Germany) was used to measure the separation rate of nanoemulsions at 25 ºC. The Lumifuge is an analytical centrifuge that continually measures the light transmitted through a sample over the total length of the measurement cell. The samples (0.4 mL aliquots) were placed in polycarbonate sample cells and centrifuged (1140 x *g*) for ~7.2 h, simulating 1 y of separation under normal gravity. Separation rates were determined using the software package SepView 4.1 (L.U.M GmbH), which calculated the velocity of the separation of the individual particles from the measurement results (μm/day).

2.3 Results and Discussion

2.3.1 Viscosity of carbohydrate-protein mixtures

The effect of increasing β-casein content (0 to 10 % w/w) on viscosity is represented graphically in Figure 2.1. Viscosity increased exponentially with increasing protein content from 2 to 78 mPa.s, possibly as a result of increased interactions between hydrated protein molecules (Boye et al., 1997), and the ability of protein molecules to absorb water and swell (Damodaran, 1997). Mora-Gutierrez and Farrell Jr. (2000) suggested that sugar molecules (lactose and sucrose) do not bind to proteins (casein), or affect viscosity in protein-sugar systems. However, trehalose-β-casein mixtures had higher viscosity than lactose-β-casein mixtures at equivalent carbohydrate contents (Table 2.1).

Table 2.2 Optimised formulations for minimum and maximum viscosity (μ at 400 s^{-1}) and glass transition temperature (T_g') for nanoemulsions at fixed β-casein contents (2.5, 5, 7.5, 10 % w/w).

Run	Lactose (% w/w)	Trehalose (% w/w)	β-casein (% w/w)	Mean particle size (nm)	μ_{Emul} (mPa.s)	T_g' (ºC)	T_m' (ºC)	Separation rate (μm/day)	Stokes' creaming rate (μm/day)
1	12.50	0	7.50	194.3	48.9	-49.1	-34.2	6.8	5.2
2	15.00	0	5.00	196.2	13.8	-48.5	-35.1	24.8	18.8
3	0	12.50	7.50	199.4	56.2	-50.0	-35.2	6.9	4.8
4	4.00	13.50	2.50	190.1	5.3	-45.3	-35.2	38.3	45.9
5	4.60	7.90	7.50	193.6	52.6	-50.2	-34.6	7.2	4.8
6	7.90	9.60	2.50	186.8	5.4	-45.6	-35.2	40.9	43.5
7	10.00	0	10.00	193.5	132.3	-50.2	-36.0	4.5	1.9
8	4.75	10.25	5.00	197.0	14.8	-48.4	-35.2	23.8	17.7
9	2.00	15.50	2.50	190.5	5.4	-44.9	-35.1	40.2	45.3
10	0	15.00	5.00	196.7	14.1	-48.4	-35.3	24.6	18.5
11	0	10.00	10.00	191.9	156.0	-50.2	-36.2	4.2	1.6
12	17.50	0	2.50	188.1	5.2	-45.7	-35.1	39.5	45.8
13	4.00	6.00	10.00	194.1	121.1	-50.1	-36.2	4.5	2.1

The data for viscosity analysis was fitted with a special cubic model, which was transformed using a natural log power law, as recommended by the Box-Cox method. This minimised the residual sum of squares in the model, thus, improving the statistical analysis. The model was significant (P <0.0001) with a high adjusted R^2 (Table 2.3). The coefficients for this coded Scheffe polynomial model are shown in Table 2.4, and together with the ternary diagram and three-dimensional (3D) surface diagram in Figure 2.1, it is shown that β-casein (component C) had the greatest effect on viscosity. Low viscosity systems are the desired outcome. The results show that low viscosity systems can be produced with lower quantities of protein (≤ 5% w/w). The negative coefficients (Table 2.4) and the downward curves (Figure 2.1) for the non-linear blending terms AC and BC show that there is synergism between lactose with β-casein, and between trehalose with β-casein, meaning that these binary mixtures can result in low viscosity. The antagonism of adding a third component to the mixture causes an increase in viscosity (positive ABC).

Table 2.3 Statistical significance of models, both transformed and untransformed, for carbohydrate-protein mixtures and nanoemulsions.

	Model Significance	
Carbohydrate-protein mixtures	Adjusted R^2	*P*-value
ln (viscosity)[a, c]	0.9864	<0.0001
T_g'	0.9871	<0.0001
T_m'	0.7819	0.0003
T_g	0.9763	<0.0001
Nanoemulsions		
mean particle size	0.7174	0.0115
inv sqrt (viscosity)[b, c]	0.9982	<0.0001
T_g'	0.9760	0.0001
T_m'	0.8282	0.0631
separation rate	0.9984	<0.0001

[a]The natural log, (ln), of the viscosity results for the carbohydrate-protein mixtures was modelled and the given R^2 values reflect this transformed result.

[b]The inverse square root of the nanoemulsion viscosity results was modelled and the given R^2 values reflect this transformed result.

[c]Viscosity measurements are quoted at 400 s^{-1}.

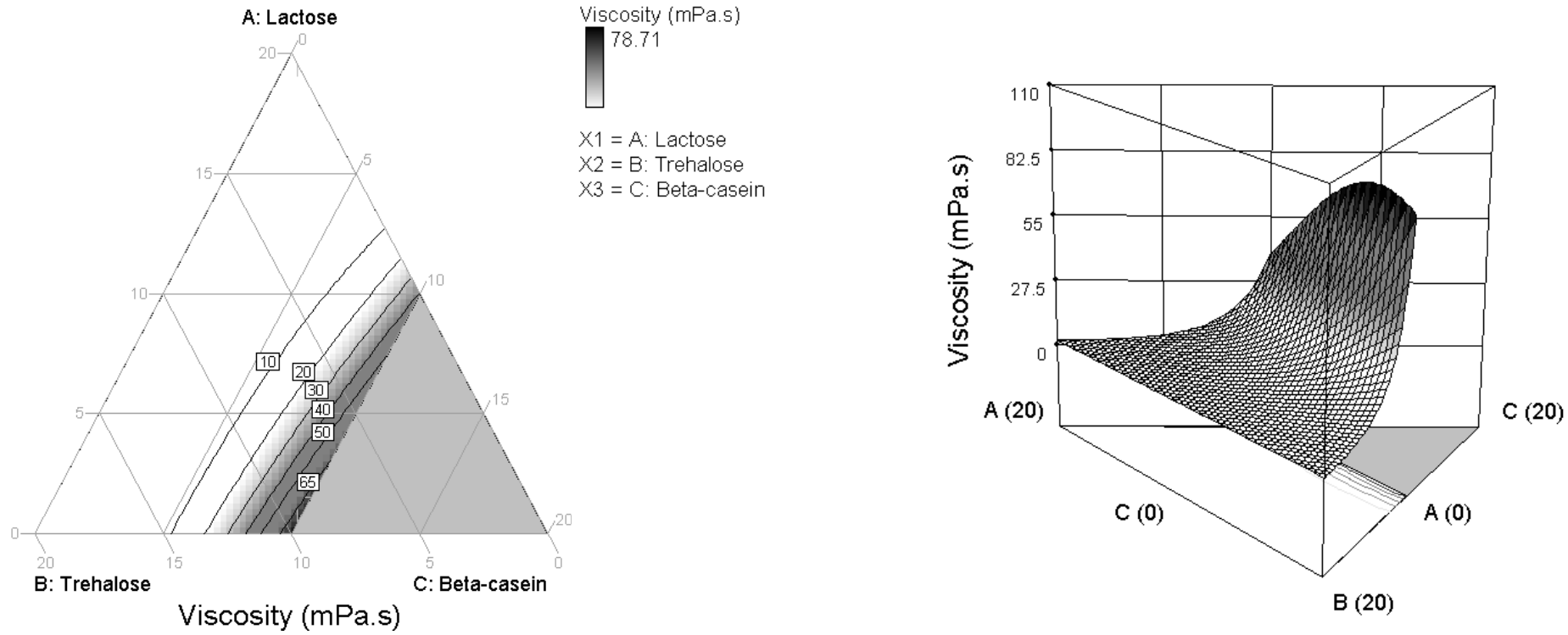

Figure 2.1 Contour and response surface plots of viscosity (at 400 s^{-1}) in carbohydrate-protein mixtures comprising of lactose, trehalose, and β-casein (0 to 20 % w/w).

2.3.2 Glass transition of carbohydrate-protein mixtures

The glass transition temperatures (T_g') of the maximally freeze-concentrated carbohydrate-protein mixtures decreased with increasing protein content (Table 2.1; Figure 2.2). It is likely that increased viscosity retarded ice formation, thus, decreasing the solute concentration at maximum freeze concentration, C_g'. This diluted the unfrozen matrix and, therefore, the T_g' decreased due to the higher plasticising effect of unfrozen water (Roos and Karel, 1991a).

A special cubic model was used to fit the data for T_g', giving significance at $P < 0.0001$ with a high adjusted R^2 value (Table 2.3). β-casein had the greatest effect on T_g', as demonstrated by the larger negative second-order non-linear blending terms involving β-casein (AC and BC) compared to the smaller positive coefficient for model term AB (Table 2.4; Figure 2.2). A high T_g' is the desired outcome for solutions. Therefore, there is antagonism between lactose with β-casein, and between trehalose with β-casein. Varying the ratio of lactose to trehalose had little effect on T_g' at fixed protein levels. The synergism of adding a 3rd component to the mixture causes an increase in T_g', as indicated by the positive coefficient for the three component non-linear blending term from Table 2.4 (ABC). It is suggested that increased viscosity is the primary reason for T_g' decrease with increasing protein content.

The onset temperature of ice melting in the maximally freeze-concentrated state, T_m', is an important property of a material as it is the 'mobility' point (Reid et al., 1994) or point at which the structure begins to collapse under its own weight during freeze drying (Kaushik and Roos, 2007). Liquids should be frozen at a temperature of 1 °C below T_m' to obtain maximal freeze concentration prior to freeze drying so that maximal sublimation occurs, resulting with a powder with maximum T_g. T_m' increased with increasing protein content (Table 2.1; Figure 2.3). As ice forms, freeze-concentration of solids occurs simultaneously; decreasing the freezing/melting temperature of the unfrozen water (Roos, 2007). Increasing β-casein contents retarded ice formation with a resultant lower T_g' and higher T_m' (ice formation ceased at a higher temperature which corresponded to the higher T_m'). Roos and Karel (1991b) found that in sucrose solutions ice formation ceased at a viscosity of 10^7 Pa.s. Although viscosity of the freeze-concentrated carbohydrate-

protein mixtures were not measured, it is likely that the viscosity increased with decreasing temperature and increasing solids content of the unfrozen phase during freeze concentration.

The data for T_m' analysis was fitted with a quadratic model and had a high adjusted R^2 with significance at P =0.0003 (Table 2.3). β-casein had a greater effect on T_m' than individual sugars (Table 2.1; Figure 2.3). Similar AC and BC values and a small coefficient for model term AB show that at fixed protein levels, the ratio of lactose to trehalose is irrelevant. It is suggested that increased viscosity is the biggest factor in increasing T_m', therefore, it is beneficial to have highly viscous systems to produce a high T_m'.

For freeze dried powders, T_g increased with increasing protein content (Table 2.1; Figure 2.4). The lowest protein content (2.5% w/w) system in the present study had a T_g of ~104 °C, whereas the highest protein content (10% w/w) system had a T_g of 124 °C. Biliaderis et al. (2002) reported that the addition of a high molecular weight carbohydrate (pullalan) to lactose increased T_g. Similarly, Shamblin et al. (1996) found that the T_g of sucrose solutions was higher in the presence of polymeric substances, such as starch and polyvinylpyrrolidone.

A quadratic model was fitted to the data for T_g with significance at P <0.0001 with a high adjusted R^2 (Table 2.3). Component C (β-casein) again had the most significant effect on T_g (Table 2.4; Figure 2.4). High T_g values are favourable in dairy powders, so high protein systems give a beneficial outcome in this respect.

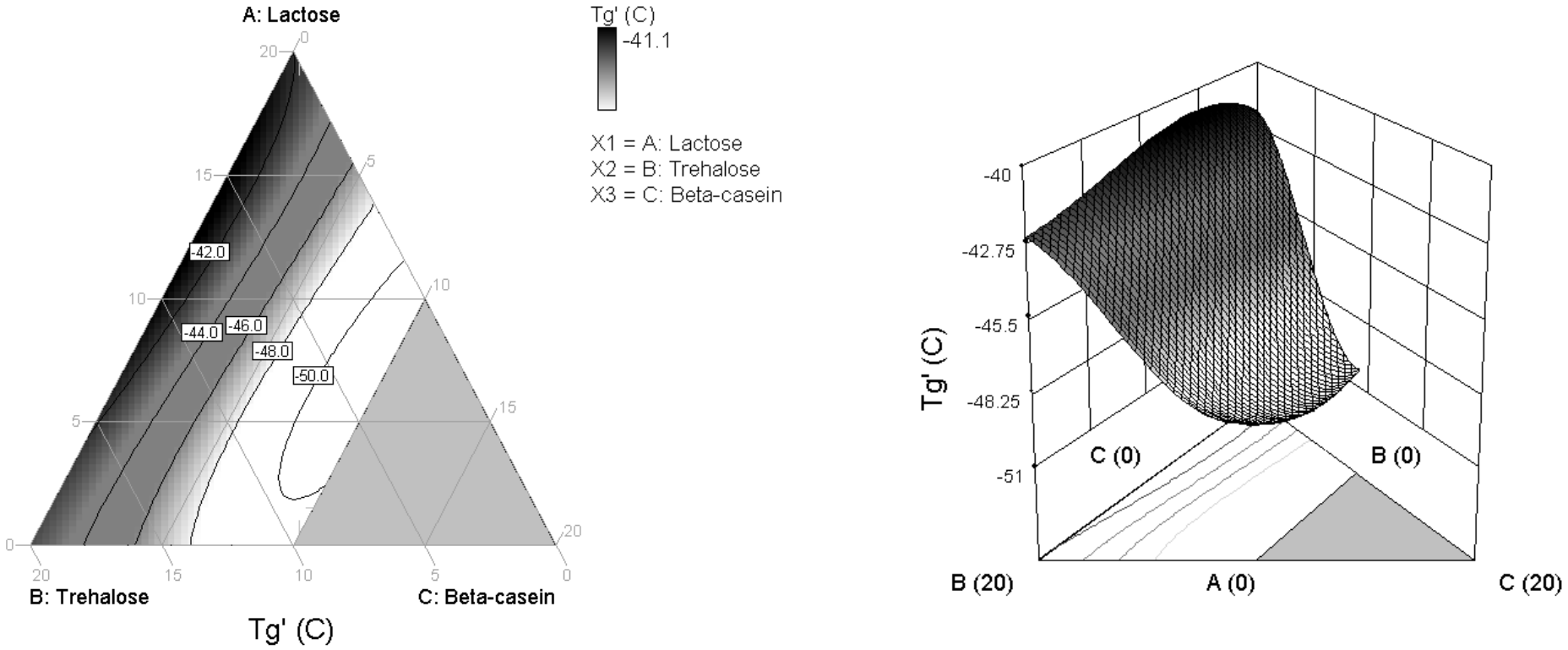

Figure 2.2 Contour and response surface plots of onset glass transition temperature of maximally freeze-concentrated solids (T_g') in carbohydrate-protein mixtures comprising of lactose, trehalose, and β-casein (0 to 20 % w/w).

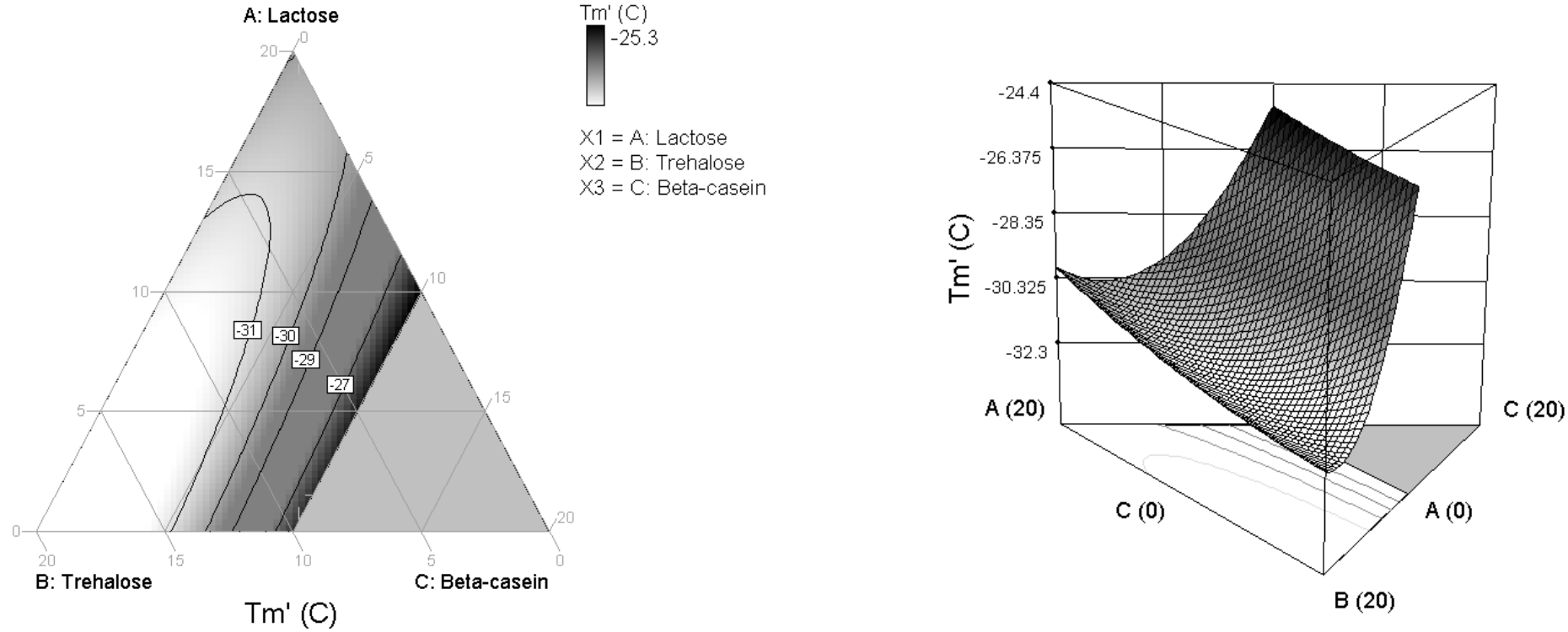

Figure 2.3 Contour and response surface plots of onset temperature of ice melting (T_m') in carbohydrate-protein mixtures comprising of lactose, trehalose, and β-casein (0 to 20 % w/w).

The presence of protein in either liquid or dehydrated systems, affects the glass transition temperature of that system. Typically a high T_g' in a liquid system should correspond to a high T_g post- dehydration. Similarly, a low T_g' should correspond to a low T_g post dehydration. In the current work, increasing protein content increased the T_g for dehydrated systems (Figure 2.4) while it decreased T_g' for liquid systems (Figure 2.2). As previously discussed, this may be due to increased solution viscosity at higher protein concentrations, which makes ice crystal formation more difficult, thus, more unfrozen water remains in the continuous phase lowering T_g'. Therefore, the glass transition temperatures in both liquid and dehydrated forms are strongly influenced by protein content.

2.3.3 Particle size of nanoemulsions

For nanoemulsions, mean particle size increased with increasing protein content (Table 2.2; Figure 2.5). Particle size increased from ~187 to 199 nm for increasing protein contents up to 7.5% w/w β-casein, however, mean particle size decreased to 193 nm for samples containing 10% w/w β-casein. The general trend toward increased mean particle size may be due to a layering effect of the protein around the small oil droplets according to self-consistent field (SCF) theory. This occurs when the bulk protein concentration goes above a certain threshold value (depending on ionic strength), causing multilayer condensation of self-associating protein onto the oil droplet surface (Dickinson, 1997a). In contrast with the current study, Qian and McClements (2011) found that mean particle size decreased with increasing protein content for sodium caseinate stabilised nanoemulsions, however, they did obtain a similar narrow size distribution.

The data for particle size was fitted with a quadratic model and was significant (P <0.0115) with a high adjusted R^2 (Table 3). Figure 5 shows that the mean particle size generally increased with increasing protein content. β-casein is the only component in the mixture that affects particle size. Lactose and trehalose are hydrophilic and remain in the continuous phase, therefore, having no direct effect on particle size. This is seen in Table 4 with the low negative coefficient value for model term AB.

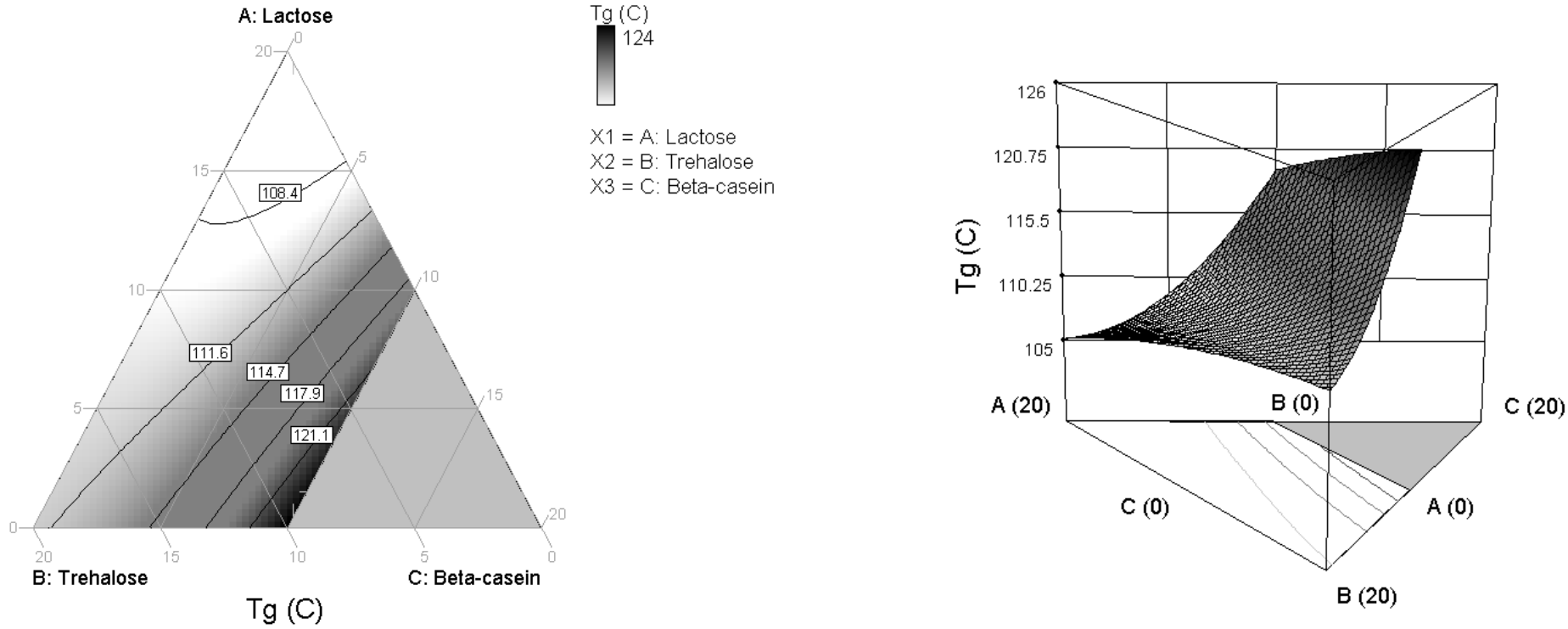

Figure 2.4 Contour and response surface plots of glass transition temperature of freeze dried powder (T_g) in carbohydrate-protein mixtures comprising of lactose, trehalose, and β-casein (0-20 % w/w).

Table 2.4 Coefficients for each term in the coded polynomial equation, both transformed and untransformed, for carbohydrate-protein mixtures and nanoemulsions.

	Coded polynomial equation coefficients for Scheffe model									
Mixtures	A[a]	B[b]	C[c]	AB	AC	BC	ABC	AB(A-B)	AC(A-C)	BC(B-C)
ln (viscosity)[d]	0.71	0.75	12.23	-0.13	-11.19	-8.63	10.67	-	-	-
T_g'	-41.99	-42.52	-6.94	4.60	-103.46	-97.26	80.48	4.11	64.11	50.66
T_m'	-29.93	-32.04	-3.04	-1.48	-34.54	-34.03	-	-	-	-
T_g	105.17	111.37	158.36	4.61	-50.90	-42.06	-	-	-	-
Nanoemulsions										
mean particle size	188.22	192.41	128.75	-10.75	122.93	115.47	-	-	-	-
inv. sqrt (viscosity)[d]	0.44	0.44	0.43	-0.02	-1.42	-1.44	-	-	-	-
T_g'	-45.67	-44.90	-37.36	-1.23	-31.38	-35.45	-	-	-	-
T_m'	-35.16	-34.91	-114.15	-0.53	145.13	143.90	-144.08	1.12	-71.45	-77.60
separation rate	39.54	43.11	468.80	1.23	-963.62	-968.70	955.75	39.01	476.76	453.40

[a]A =Lactose.

[b]B =Trehalose.

[c]C =β-casein.

[d]Viscosity measurements are quoted at 400 s^{-1}.

2.3.4 Viscosity of nanoemulsions

The viscosity of nanoemulsions increased with increasing protein content (Table 2.2, Figure 2.6). This was most likely due to increased protein-protein interaction in the continuous phase as the protein content increases. The addition of sunflower oil to the system increased the solids content by 10% (that is, 30% solids in total) and so the nanoemulsions are more viscous than carbohydrate-protein mixtures.

A quadratic model was fitted to the viscosity data, which was transformed using an inverse square-root power law recommended by the Box-Cox method. The model was significant (P <0.0001) with a high adjusted R^2 (Table 2.3). The results again show that low viscosity nanoemulsions (<15 mPa.s) can be produced at protein contents of ≤ 5% w/w. The negative coefficients (Table 2.4) and the downward curves (Figure 2.6) for the non-linear blending terms AC and BC show that there is synergism between lactose with β-casein, and between trehalose with β-casein, meaning that these emulsions can keep a low viscosity. The viscosity of the nanoemulsions in Table 2.2 shows that varying the level of lactose to trehalose, at fixed protein levels, gave similar viscosity.

2.3.5 Glass transitions of nanoemulsions

The T_g' of the nanoemulsions decreased as protein content increased (Figure 2.7), in agreement with results for carbohydrate-protein mixtures (Figure 2.2). The experimental T_g' values for nanoemulsions are similar to T_g' values predicted for mixtures by the optimisation function in the DOE software. This shows that sunflower oil did not affect T_g' most likely because the oil was in the dispersed phase, while the continuous phase is primarily responsible for changes in T_g'.

The data for T_g' was fitted with a quadratic model, and it was significant (P =0.0001) with a high adjusted R^2 (Table 2.3). The large negative coefficients for the second-order non-linear blending terms (Table 2.4) involving β-casein (AC and BC), compared to the smaller AB value, show that β-casein had the greatest effect on T_g'. High T_g' values are required for emulsions, as they are for solutions. It was found that there is antagonism between lactose with β-casein, and between trehalose with β-casein, as previously for the

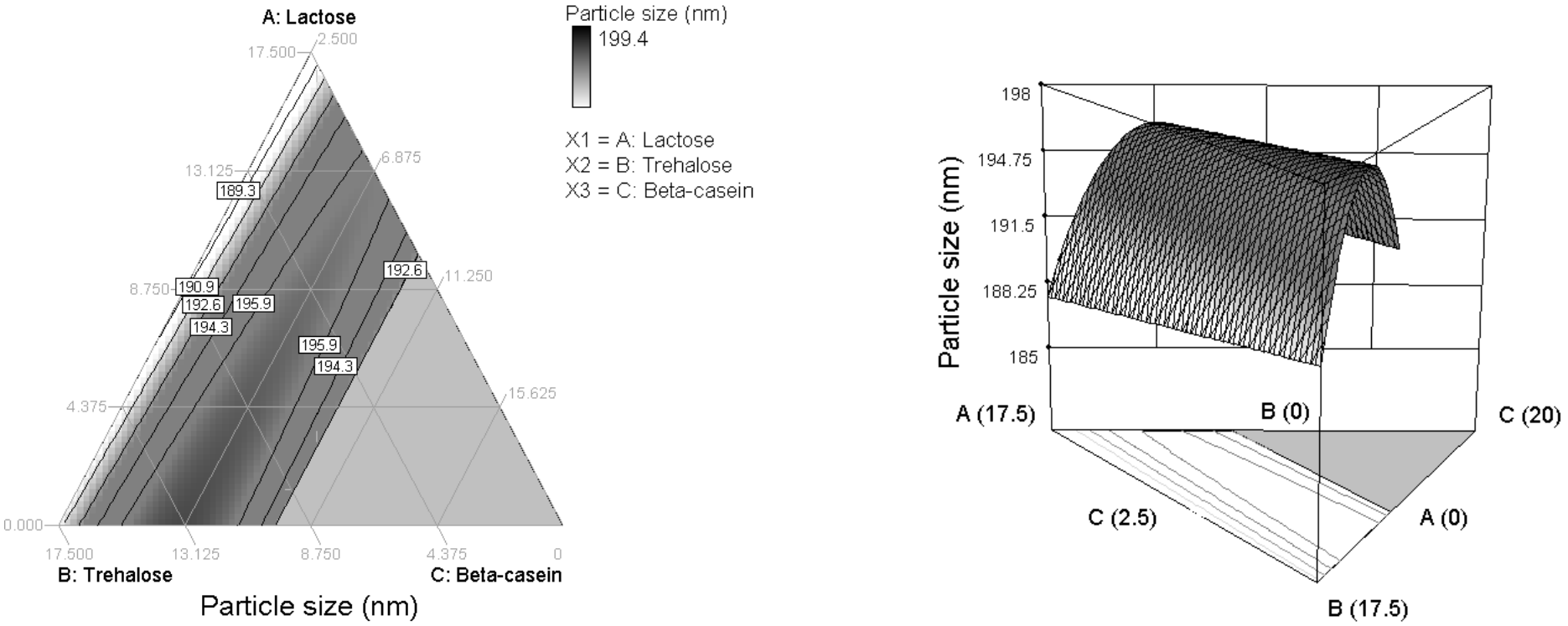

Figure 2.5 Contour and response surface plots of mean particle size in nanoemulsions comprising of lactose, trehalose, and β-casein contents.

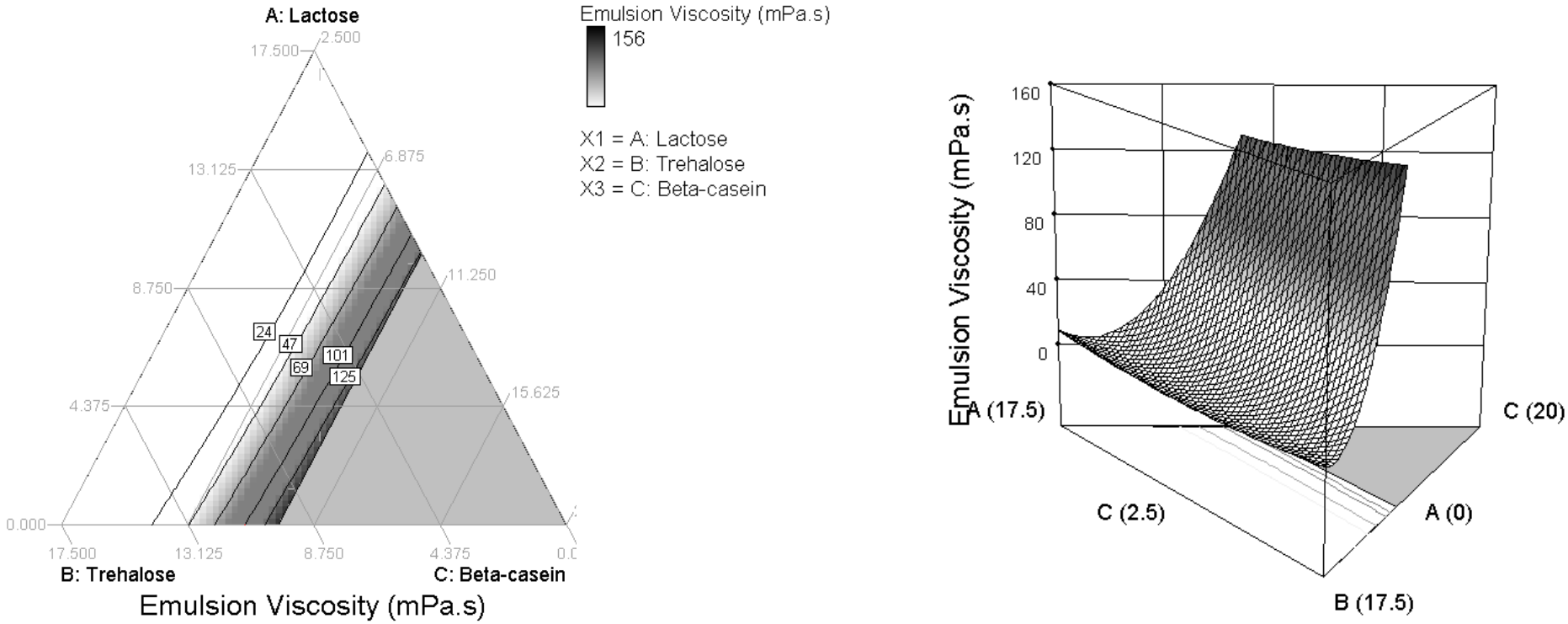

Figure 2.6 Contour and response surface plots of viscosity (at 400 s^{-1}) in nanoemulsions comprising of lactose, trehalose, and β-casein contents.

carbohydrate-protein mixtures. Therefore, low quantities of β-casein combined with lactose or trehalose give the largest T_g'. The ratio of lactose to trehalose in the emulsion, at fixed protein contents, is irrelevant as indicated the relatively low coefficient AB in Table 2.4. The decrease in T_g' with increasing protein content can be explained by a concomitant increase in viscosity.

The T_m' for nanoemulsions differed from those found for the carbohydrate-protein mixtures. In this case, T_m' decreased with increasing protein content and T_m' values were lower in each case for nanoemulsions (Table 2.2), compared to that of carbohydrate-protein mixtures (Table 2.1). The overall model generated was not significant at P =0.0631 (Table 2.3), which meant that the overall mean was a better predictor of the response than the current model.

2.3.6 Nanoemulsion stability

The nanoemulsion stability was measured by analysing the floatation/creaming rates of particles using an analytical centrifuge. The highest protein content nanoemulsions (7.5% and 10% w/w protein) were the most stable with separation rates of 7 and 4 μm/day, respectively, compared to separation rates of 41 and 24 μm/day for nanoemulsions with 2.5% and 5% w/w protein contents respectively (Table 2.2; Figure 2.8). Nanoemulsions are reported to be more stable to creaming on storage compared to conventional emulsions (d_p >200 nm) due to the effects of Brownian motion being stronger than gravitational forces. They are also more stable to flocculation and coalescence due to the lowering of interfacial tension with decreasing particle size that decreases the stress required to break up the droplets (Tadros et al., 2004; McClements, 2005). Typically, casein-coated emulsion droplets are prone to depletion flocculation at protein concentrations higher than 2% w/w (Dickinson and Golding, 1997). This could be due to the effect of unadsorbed casein in the continuous phase that passes between oil droplets causing an osmotic pressure gradient, that entropically force out aggregated casein, causing droplets to flocculate (Dickinson, 1997b, 1999). Increasing protein content increases the occurrence of depletion flocculation. In some cases it has been found that stability decreases with increasing sodium caseinate content up to a certain concentration (6% w/w). Above this concentration a more rigid structure is formed, preventing rapid creaming (Dickinson et al., 1997).

Experimental separation rates were compared to those calculated using Stokes' law equation (see Table 2.2):

$$v_{Stokes} = \frac{(\rho_f - \rho_p)}{18\mu}.g.d_p^{\ 2} \qquad (2.1)$$

Here, v_{Stokes} is the separation velocity of the particles, ($\rho_f - \rho_p$) is the difference between the density of the fluid in the continuous phase (1,060 $kg.m^{-3}$) and the particles of oil (917 $kg.m^{-3}$), *g* is gravitational acceleration (9.81 $m.s^{-2}$), d_p is the mean particle diameter (m), and μ is the viscosity of the nanoemulsion (kg/(m.s)). The units are converted to μm/day and compared with the experimental separation rates calculated from the Lumifuge in Table 2.2. It was also observed that as particle sizes of nanoemulsions were very similar overall that viscosity was the primary factor in determining the separation rate. In general, results compared well, however, Stokes' law is applicable for ideal systems and this system is not ideal due to hindrance caused by concentration effects (Robins, 2000).

A cubic model was fitted to the data for nanoemulsion stability with significance at *P* <0.0001 and a high adjusted R^2 value (Table 2.3). β-casein had the most significant effect on nanoemulsion separation rate due to increased viscosity at high protein levels. The negative coefficients (Table 2.4) and the downward curves (Figure 2.8) for the non-linear blending terms AC and BC show that there is synergism between lactose with β-casein, and between trehalose with β-casein, meaning that these mixtures can keep a low separation rate. The quantity of lactose or trehalose has no effect on stability, as indicated by the small coefficient for the model term AB.

Overall the desired result from an emulsion system is ideally to produce a low viscosity, high T_g' which when dried corresponds to a high T_g, low mean particle size and low separation rate. A fine balance can be achieved whereby a low viscosity, highly stable emulsion system can be produced that is not susceptible to physicochemical deteriorative changes that are caused by low glass transition temperature. Results indicate that protein contents of 5% w/w or 7.5% w/w are optimal to produce stable nanoemulsions. At 10% w/w protein viscosity is too high which would be difficult to spray dry, and at 2.5% protein, due to low viscosity, separation rate is greatest (Table 2.2). This study has demonstrated how to statistically optimise β-casein stabilised nanoemulsion systems.

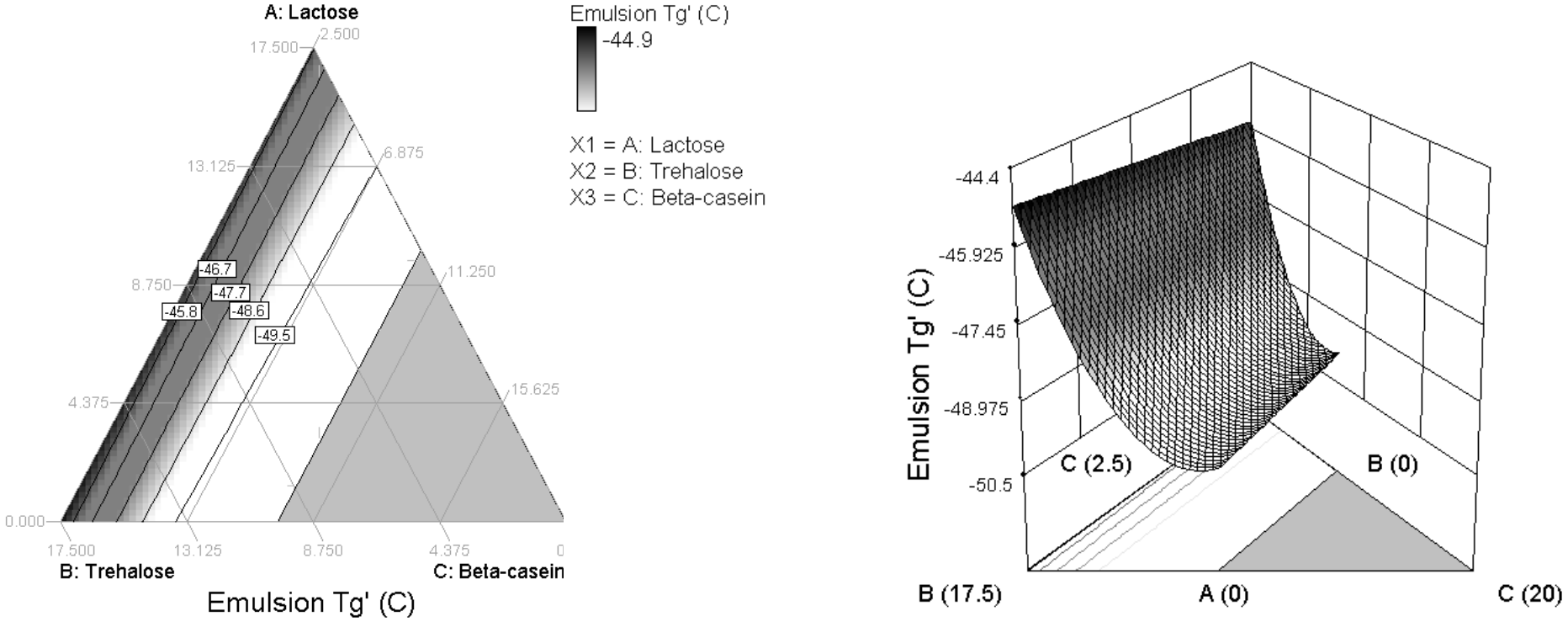

Figure 2.7 Contour and response surface plots of glass transition temperature of maximally freeze-concentrated solids in nanoemulsions (T_g') comprising of lactose, trehalose, and β-casein.

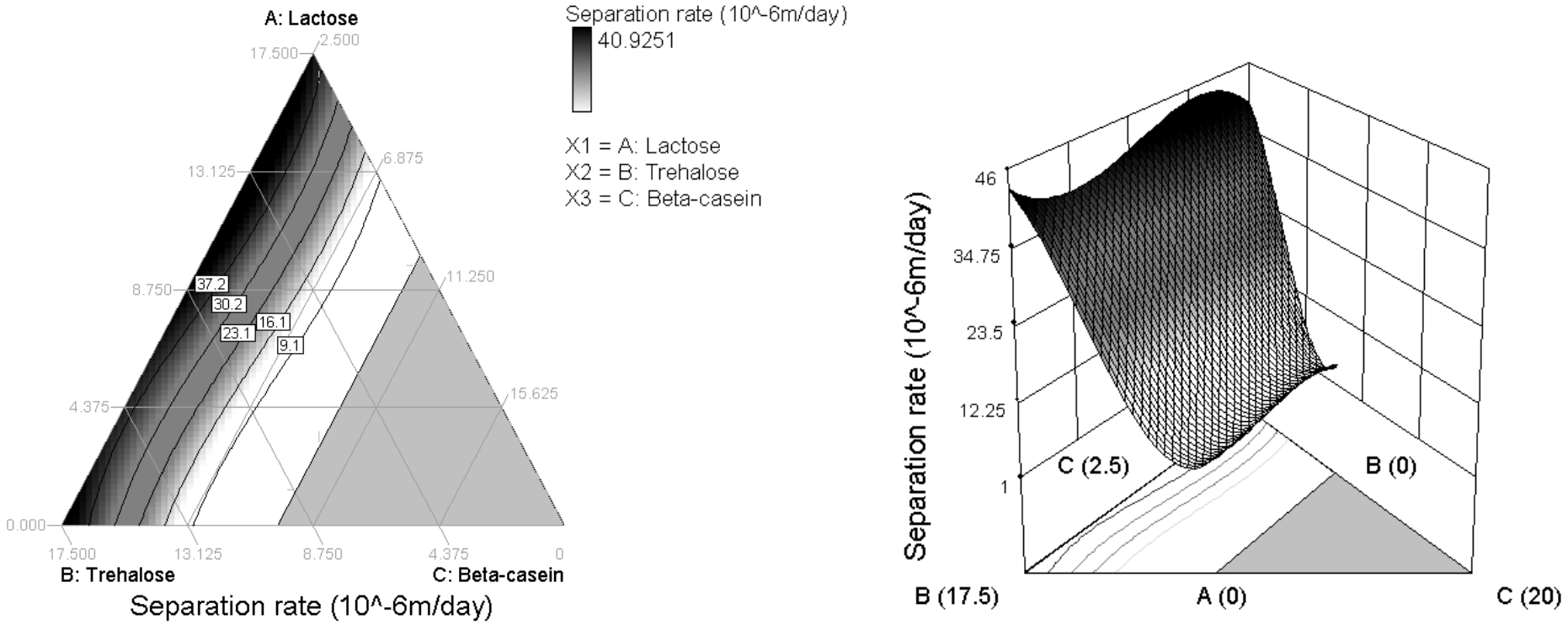

Figure 2.8 Contour and response surface plots of separation rate in nanoemulsions comprising of lactose, trehalose, and β-casein.

2.4 Conclusions

A statistical mixture design was successfully used for the formulation of nanoemulsions based on optimisation of continuous phase parameters of viscosity and glass transition. The study showed that increasing β-casein content in mixtures containing lactose and trehalose, significantly (P <0.0001) increased viscosity and decreased glass transition T_g'. A similar trend was observed in β-casein stabilised nanoemulsions containing lactose and trehalose. This indicates that the physical properties of the continuous phase are a primary factor influencing the stability and functionality of subsequent emulsions. Nanoemulsion mean particle size (P <0.0115) and stability (P <0.0001) were significantly increased with increasing β-casein content. It was postulated that the increased stability was due to the effect of increased viscosity that reduced the separation rate of the dispersed phase according to Stokes' law. Modulation of glass transition temperatures through selection of ingredients, and their concentrations, may be beneficial in powdered products to combat the phenomena of stickiness and crystallisation during storage.

Statistical experimental mixture design can be a useful tool in the formulation of nanoemulsions. It reduces the workload by giving a set number of experiments, and determines and analyses the impact of each component in the mixture.

Chapter 3 - Physicochemical properties of spray dried nanoemulsions with varying final water and sugar contents

Published as:

Maher, P.G., Roos, Y.H., and Fenelon, M.A. 2014. Physicochemical properties of spray dried nanoemulsions with varying final water and sugar contents. *Journal of Food Engineering* 126: 113–119.

Journal of Food Engineering 126 (2014) 113–119

Contents lists available at ScienceDirect

Journal of Food Engineering

journal homepage: www.elsevier.com/locate/jfoodeng

Physicochemical properties of spray dried nanoemulsions with varying final water and sugar contents

Patrick G. Maher [a,b], Yrjö H. Roos [b], Mark A. Fenelon [a,*]

[a] Teagasc Food Research Centre, Moorepark, Fermoy, Co. Cork, Ireland
[b] Food Technology, School of Food and Nutritional Sciences, University College Cork, Cork, Ireland

ARTICLE INFO

Article history:
Received 10 June 2013
Received in revised form 30 October 2013
Accepted 1 November 2013
Available online 12 November 2013

Keywords:
Microfluidization
Homogenization
Spray drying
Glass transition
Lactose crystallization
Free fat

ABSTRACT

The objective of this study was to investigate the physicochemical properties of spray dried nanoemulsions having different final water and sugar contents. Formulations consisting of lactose or a 70:30 mixture of lactose: sucrose (23.9%), sodium caseinate (5.1%) and sunflower oil (11.5%) in water were heat treated (100 °C, 30 s), homogenized (17 MPa) or microfluidized (100 MPa) and spray dried at two different outlet temperatures (80 or 90 °C). Nanoemulsions produced by microfluidization were more stable and less viscous than control emulsions and had lower solvent extractable free fat. Increasing dryer outlet temperature reduced water content, water activity, particle size, tapped bulk density, with a consequent increase of onset temperature of glass transition (T_g) and crystallization (T_c) of lactose in powders. Reduction of fat globule size by microfluidization lowered T_c of lactose, an effect attributed to the lower level of protein in the continuous phase. Partial replacement of lactose with sucrose decreased T_g and delayed crystallisation. The study demonstrated that the physical properties of powders can be altered by reducing the fat globule size of emulsions pre spray drying.

© 2013 Elsevier Ltd. All rights reserved.

1. Introduction

Spray drying is a method of food preservation based on dehydration to final water contents of <3% to reduce physical, chemical or biological deteriorative changes (Gharsallaoui et al., 2007). In many cases foods are dried in the form of an emulsion (Fäldt and Bergenståhl, 1996a,b), examples of which include: whole milk powder and milk based nutritional powders (e.g., infant formula), medical and therapeutic beverages. Protein is the main emulsifier in these emulsion systems and the amount of protein required to emulsify the fat phase depends on a number of factors including the amphiphilic nature of the protein, the concentration of both fat and protein phases, and mechanical forces used to disrupt the fat into smaller particles (Floury et al., 2000; Hogan et al., 2001b; Vega et al., 2007; Vega and Roos, 2006). High mechanical forces used during the process of microfluidization can be used to produce nanoemulsions (20–200 nm) which are more stable to creaming and sedimentation than conventional emulsions (1–100 μm); this has been attributed to the greater influence of Brownian motion in systems where gravity induced creaming or sedimentation (Huang et al., 2010; Solans et al., 2005) can occur. Moreover, lipid droplets with decreasing particle size are less likely to flocculate and coalesce due to a reduction in attractive forces between them (McClements, 2005). Consequently, nanoemulsions are increasingly being used in the food industry as delivery systems for non-polar bioactive lipids. Bioavailability of lipids in these systems is increased compared to conventional emulsions due to the smaller fat globule size and higher surface-to-volume ratio (Acosta, 2009; McClements, 2011); nanoemulsions are therefore useful for improving the bioactivity of lipophilic ingredients that are normally poorly absorbed.

The composition of the continuous phase of emulsions has a significant impact on viscosity, stability, and glass transition temperature as reported by Maher et al. (2011). Nanoemulsions have a greater interface area for protein to adsorb to, leaving less protein in the continuous phase. Other constituents of the continuous phase of dairy based beverages often include low molecular weight sugars, such as lactose and sucrose. The molecular and physicochemical properties of sugars, when superimposed on the properties of the dispersed phase, affect subsequent dried ingredient functionality both during and after reconstitution. For instance, sucrose will crystallize readily when exposed to high temperatures and relative humidities (Yu et al., 2007) and thus can be used to modulate certain glass forming structures in food. However, there is a critical humidity at a given temperature at which crystallization may occur (RH_c) (Burnett et al., 2004) and it is important to identify this humidity as it will determine the humidity range the powders can be stored at. Sugars (lactose and sucrose) are

* Corresponding author. Address: Food Chemistry & Technology Department, Teagasc Food Research Centre, Moorepark, Fermoy, Co. Cork, Ireland. Tel.: +353 2542355.
E-mail address: mark.fenelon@teagasc.ie (M.A. Fenelon).

0260-8774/$ - see front matter © 2013 Elsevier Ltd. All rights reserved.
http://dx.doi.org/10.1016/j.jfoodeng.2013.11.001

Abstract

The objective of this study was to investigate the physicochemical properties of spray dried nanoemulsions having different final water and sugar contents. Formulations consisting of lactose or a 70:30 mixture of lactose: sucrose (23.9%), sodium caseinate (5.1%), and sunflower oil (11.5%) in water were heat treated (100 ℃, 30 s), homogenised (17 MPa) or microfluidised (100 MPa), and spray dried at two different outlet temperatures (80 or 90 ºC). Nanoemulsions produced by microfluidisation were more stable and less viscous than control emulsions and had lower solvent extractable free fat. Increasing dryer outlet temperature reduced water content, water activity, particle size, tapped bulk density, with a consequent increase of onset temperature of glass transition (T_g) and crystallisation (T_{cr}) of lactose in powders. Reduction of fat globule size by microfluidisation lowered T_{cr} of lactose, an effect attributed to the lower level of protein in the continuous phase. Partial replacement of lactose with sucrose decreased T_g and delayed crystallisation. The study demonstrated that the physical properties of powders can be altered by reducing the fat globule size of emulsions pre-spray drying.

3.1 Introduction

Spray drying is a method of food preservation based on dehydration to final water contents of <3% to reduce physical, chemical or biological deteriorative changes (Gharsallaoui et al., 2007). In many cases, foods are dried in the form of an emulsion (Fäldt and Bergensåthl, 1996b, a), examples of which include: whole milk powder and milk based nutritional (e.g., infant formula), medical and therapeutic beverages. Protein is the main emulsifier in these emulsion systems and the amount of protein required to emulsify the fat phase depends on a number of factors including, the amphiphilic nature of the protein, the concentration of both fat and protein phases, and mechanical forces used to disrupt the fat into smaller particles (Floury et al., 2000; Hogan et al., 2001b; Vega and Roos, 2006; Vega et al., 2007). High mechanical forces used during the process of microfluidisation can be used to produce nanoemulsions (20 – 200 nm), which are more stable to creaming and sedimentation than conventional emulsions (0.2 – 100 μm); this has been attributed to the greater influence of Brownian motion in systems where gravity induced creaming or sedimentation (Solans et al., 2005; Huang et al., 2010) can occur. Moreover, lipid droplets with decreasing particle size are less likely to flocculate and coalesce due to a reduction in attractive forces between them (McClements, 2005). Consequently, nanoemulsions are increasingly being used in the food industry as delivery systems for non-polar bioactive lipids. Bioavailability of lipids in these systems is increased compared to conventional emulsions due to the smaller fat globule size and higher surface-to-volume ratio (Acosta, 2009; McClements, 2011); nanoemulsions are, therefore, useful for improving the bioactivity of lipophilic ingredients that are normally poorly absorbed.

The composition of the continuous phase of emulsions has a significant impact on viscosity, stability, and glass transition temperature as reported by Maher et al. (2011). Nanoemulsions have a greater interface area for protein to adsorb to, leaving less protein in the continuous phase. Other constituents of the continuous phase of dairy based beverages often include low molecular weight sugars, such as lactose and sucrose. The molecular and physicochemical properties of sugars, when superimposed on the properties of the dispersed phase, affect subsequent dried ingredient functionality both during and after reconstitution. For instance, sucrose will crystallise readily when exposed to high temperature and relative humidity (Yu et al., 2007) and, thus, can be used to

modulate certain glass forming structures in food. However, there is a critical humidity at a given temperature at which crystallisation may occur (RH_c) (Burnett et al., 2004), and it is important to identify this humidity as it will determine the humidity range the powders can be stored at. Sugars (lactose and sucrose) are often combined with dairy solids to meet nutritional and structural requirements in the diet. They have the advantage of availability at low cost, low viscosity in concentrated solutions, and ability to produce a good glass upon spray drying. They are often combined with milk proteins such as casein, which have the advantage of being amphiphilic and having good heat stability and emulsifying properties (Hogan et al., 2001a; Huck-Iriart et al., 2011). Sodium caseinate readily adsorbs at the fat surface in emulsion systems which increases fat encapsulation, causing decreased free fat. This reduces the hydrophobicity on the surface of powders making them more wettable, flowable, dispersible, and reduces lipid oxidation (Fäldt and Bergensåthl, 1996b; Hardas et al., 2000; Kim et al., 2005).

The effect of reducing the fat globule size (FGS) in emulsions has been investigated previously (Sheu and Rosenberg, 1995; Mongenot et al., 2000; Soottitantawat et al., 2003). These studies looked at volatile retention, whereas the current study investigated the physicochemical properties of spray dried conventional and nanoemulsions with different sugar and water contents. Powders were analysed for differences in free fat, glass transition, crystallisation, and water sorption characteristics. The objective of this study was to investigate the functionality of spray dried nanoemulsions and show how their physical characteristics differ from powders made from conventional emulsions.

3.2 Materials and Methods

3.2.1 Materials

The materials used were lactose (Glanbia, Kilkenny, Ireland), sucrose (purchased from local market), sodium caseinate (Kerry Ingredients, Listowel, Ireland) and sunflower oil (Trilby Trading, Drogheda, Ireland). Analytical grade petroleum ether (BP 40 – 60 ºC) was purchased from Sigma-Aldrich (Sigma-Aldrich, Wicklow, Ireland). The protein content of the sodium caseinate was 89.8%, as determined by the Kjeldahl method (IDF, 2001) and using a nitrogen-protein ratio of 6.38.

3.2.2 Methods

3.2.2.1 Emulsion preparation

Batches (30 kg) of oil-in-water emulsions were formulated with lactose or 70: 30 lactose: sucrose mixture (23.9%), sodium caseinate (5.1%) and sunflower oil (11.5%). A coarse emulsion was made by mixing these ingredients with a high shear mixer (Silverson Machines Ltd., UK) at 60 ºC. The mixture was then subjected to high-temperature short-time pasteurisation (100 ºC, 30 s) using a Microthermics tubular heat exchanger (Model 25HV; NC, USA). Control emulsions were produced using an in-line two stage homogeniser (model NS20006H, GEA Niro, Soavi, Parma, Italy) at a first stage pressure of 13.79 MPa and a second stage pressure of 3.45 MPa. Nanoemulsions were produced using a microfluidiser (model M-110EH, Microfluidics, Newton, MA, USA) at 100 MPa and 60 ºC in a Y-shaped interaction chamber and one pass. Control and nanoemulsions were spray dried using a single stage pilot-scale spray dryer (Anhydro F1 Lab, Copenhagen, Denmark) equipped with a two-fluid nozzle atomisation system (Type 1/8 JAC 316ss) and counter-flow drying. The inlet temperature of the dryer was set at 185 ºC and the outlet temperature was set at either 80 ºC or 90 ºC, with a water evaporation rate of ~20 kg/h to give high and low moisture powders, respectively. An experimental design is given in Table 3.1 showing the 8 different powder types that were produced. The first letter represents the sugar used (L or S), the second letter the emulsion type (C or N), and the number represents the air outlet temperature from the dryer in degrees Celsius (80 or 90).

3.2.2.2 Particle size analysis

Mean fat globule size (FGS), D[4,3] (De Brouckere mean), of each control emulsion was determined using a laser-light diffraction unit (Mastersizer S, Malvern Instruments Ltd, Worcestershire, UK), equipped with 300 RF lens. The optical parameters chosen were a particle and dispersant refractive index of 1.46 (oil) and 1.33 (water), respectively. Samples were measured post- homogenisation and post- reconstitution. Mean powder particle size, D[4,3], was determined by laser diffraction with the dry powder feeder (Malvern Mastersizer).

Mean (z-average) FGS of nanoemulsions was measured using an intensity distribution by a Zetasizer Nano system (Malvern Instruments, Inc., Worcester, UK). Measurements were carried out at 25 ºC and at a scattering angle of 173º. Samples taken post-homogenisation were compared to reconstituted powder samples after dilution to a solids content of 0.5% (w/w) using distilled water to avoid the effects of multiple scattering.

3.2.2.3 Apparent viscosity measurements

Apparent viscosity measurements of control and nanoemulsions pre- and post-homogenisation (40% solids) were carried out using a controlled stress rheometer (AR G2 rheometer, TA Instruments, Crawley, UK), equipped with a concentric cylinder geometry. The temperature was controlled by a Peltier apparatus (± 0.1 ºC). Samples (17 mL) were pre-sheared at 500 s^{-1} for 1 min, followed by equilibration for 2 min. Samples were then sheared from 5 to 500 s^{-1} over 3 min, held at 500 s^{-1} for 1 min, and then sheared from 500 to 5 s^{-1} over 3 min. Measurements were carried out at 55 ºC to replicate the temperature of the emulsions pre-drying. The apparent viscosity was taken at 500 s^{-1}.

Powders, reconstituted at 12.5% solids, were analysed using an AR G2 rheometer equipped with a 60 mm stainless steel parallel plate. Samples (~2 mL) were measured according to the above procedure at 25 ºC and a shear rate of 300 s^{-1}.

3.2.2.4 Emulsion stability

A LumiFuge 116 stability analyser (L.U.M. GmbH, Berlin, Germany) was used to measure the separation rate of conventional emulsions and nanoemulsions at 25 ºC. The Lumifuge is an analytical centrifuge that continually measures the light transmitted through a sample over the total length of a measurement cell. The samples (0.4 mL aliquots) were placed in polycarbonate sample cells and centrifuged (285 × *g*) for ~7.2 h, simulating ~3 months of separation under normal gravity. Separation rates were determined using the software package SepView 4.1 (L.U.M GmbH). The velocity of the separation of individual particles (mm/d) was measured.

3.2.2.5 Physicochemical properties of powders

Powder water content was determined using a halogen moisture analyser (HR-83 Halogen, Mettler Toledo, Switzerland). Water activity was measured with a Novasina LabMASTER-aw (Novatron Scientific Ltd, West Sussex, UK). Tapped bulk density of powders was determined according to the standard method (IDF, 1995). Solvent extractable free fat content of powders was determined by the GEA Niro analytical method No. A 10 a (GEA Niro, 2005).

3.2.2.6 Differential scanning calorimetry

Onset temperatures of glass transition and crystallisation (T_g and T_{cr}, respectively) of control and nanoemulsion powders were measured with a Q2000 differential scanning calorimeter (DSC), (TA Instruments, Crawley, UK). Approximately 10 mg samples were hermetically sealed in aluminium pans. Heat flow measurements were made by scanning from 0 – 100 °C at a ramp rate of 5 °C/min, cooled to 0 ºC at 10 °C/min, and re-heated to 140 ºC at 5 °C/min. T_g and T_{cr} were measured on the second heating scan that confirmed the reversibility of the glass transition. An empty pan was used as the reference. The DSC was calibrated with indium standards.

3.2.2.7 Dynamic vapour sorption

Sorption isotherms of powders were obtained using a DVS-1 analyser (Surface Measurement Systems, London, UK), equipped with a Cahn microbalance. Experiments were carried out at 25ºC. Approximately 30 mg samples of powders were placed in the sample pan and an empty pan was used as a reference. Samples were humidified from 0% relative humidity (RH) to 90% RH and back to 0% RH in increments of 10% RH steps in a two-cycle procedure. RH was changed after reaching stable weights when the dm/dt (slope of the changing mass with time) was <0.001 mg/min for at least 10 min, or exceeded the step time of 360 min. Accurate RH readings were obtained by mixing dry nitrogen gas (200 mL/min) with saturated water vapour in the correct proportion using

mass flow controllers. Graphs of water uptake over time for each powder were obtained using the DVS Data Analysis Suite.

3.2.3 Statistical analysis

A 2^3 factorial design was used with 3 varying factors at 2 levels. Spray drying experiments were carried out in triplicate. Analysis of Variance (ANOVA) was carried out using Minitab 15 (Minitab Ltd, Coventry, UK) statistical package. A single factor ANOVA test was used to determine significant changes in results between replicate trials. Fisher's one-way multiple comparison tests were used to compare different levels. Results are deemed statistically significant if $P < 0.05$.

Table 3.1 2^3 factorial experimental design and coding system of powders.

Powder	Sugar	Emulsion type	Dryer Outlet Temp (ºC)
LC80	Lactose	Control	80
LC90	Lactose	Control	90
LN80	Lactose	Nanoemulsion	80
LN90	Lactose	Nanoemulsion	90
SC80	Lactose/Sucrose	Control	80
SC90	Lactose/Sucrose	Control	90
SN80	Lactose/Sucrose	Nanoemulsion	80
SN90	Lactose/Sucrose	Nanoemulsion	90

3.3 Results and Discussion

3.3.1 Particle size analysis

A monomodal particle size distribution was observed for all samples prepared using either a microfluidiser or a standard homogeniser. The mean FGS for LN samples was significantly ($P < 0.05$) lower, i.e., 156 nm determined by dynamic light scattering, than that for the LC samples, i.e., mean particle size, D[4,3], of 1150 nm measured by laser diffraction (Table 3.2). Comparing the FGS of emulsions pre-drying (Table 3.2) with that

of the reconstituted powder for the same sample (Table 3.3) suggests that atomisation of emulsions through a low pressure two-fluid nozzle did not affect FGS during drying.

According to Fang & Dalgleish (1993), the maximum surface coverage of casein (2% w/w) on soybean oil (20% w/w) is 3 $mg.m^{-2}$ for a mean particle size of 320 nm. In the current study the protein: fat ratio was 4 times higher than this, verifying that more than sufficient protein was present to cover the fat droplets. This suggests that increased mechanical shear was the main reason for FGS decrease (Hogan et al., 2001b).

3.3.2 Apparent viscosity measurements

Decreasing FGS by microfluidisation (samples LN and SN) resulted in a significant (P <0.05) reduction in viscosity (Table 3.2). This is in agreement with Floury et al. (2000) who showed that decreasing the FGS with a high pressure homogeniser decreased the viscosity of oil-in-water emulsions. Small FGS and low viscosity of emulsions pre-spray drying reduce the likelihood of air inclusion in powder particles, caused by droplet ballooning during drying (Drusch, 2007), and, thus, the size of powder particles, resulting in less fat on the powder surface (Rosenberg et al., 1990). No significant (P >0.05) differences in viscosity of reconstituted powders were observed (Table 3.3).

3.3.3 Emulsion stability

Nanoemulsions were significantly (P <0.05) more stable to separation compared to control emulsions (Table 3.3), when reconstituted at 12.5% w/w. The creaming rate was 0.54 mm/d for LC80 and LC90 samples compared to 0.21 mm/d and 0.19 mm/d for LN80 and LN90 samples, respectively. These results confirmed predictions made from Stokes' law (Stokes, 1851), where particles of greater diameter separate from the continuous phase at a faster rate than smaller sized particles. Achieving a FGS <1 μm has been identified as an important target to increase emulsion stability and reduce free fat in finished powder (Sheu and Rosenberg, 1995; Hogan et al., 2001a).

Table 3.2 Comparison of mean fat globule size (FGS), D[4,3], and pre- and post-homogenisation/microfluidisation apparent viscosity (for control emulsion and nanoemulsions) pre- spray drying.

Sample	Mean FGS[1]	D[4,3][2]	Apparent viscosity	
			Pre- homogenisation/ microfluidisation	Post- homogenisation/ microfluidisation
	(nm)	(nm)	(mPa.s)	(mPa.s)
LC	-	1150 ± 90	9.0 ± 0.4	8.4 ± 0.6
LN	156 ± 2	-	9.0 ± 0.4[a]	8.0 ± 0.3[b]
SC	-	1330 ± 230	8.8 ± 0.3	8.5 ± 0.5
SN	154 ± 10	-	8.8 ± 0.3[a]	7.7 ± 0.5[b]

[1]Mean FGS measured by dynamic light scattering.

[2]D[4,3] measured by laser diffraction.

[(a-b)] Values within a row not sharing a common letter differ significantly (P <0.05). Otherwise, no significant difference.

3.3.4 Physical properties of powders

The water content and water activity of powders decreased with increasing outlet temperature of the spray dryer (Masters, 1991; Pisecky, 1997), except for samples SC80 and SC90 (Table 3.4). Increasing dryer outlet temperature led to a significantly (P <0.05) lower mean powder particle size and tapped bulk density for all powders. Similar results were seen by De Vilder et al. (1976), where a decrease in bulk density was observed with increasing dryer outlet temperature for whole milk powder. Control and nanoemulsion powders did not have significantly (P >0.05) different water content, water activity, particle size or bulk density. Solvent extractable free fat content of all powders ranged between 0.29 and 2.95% (Table 3.4). Powders LC80 and LN80 had reduced free fat compared to LC90 and LN90 powders. It has been reported that higher dryer outlet temperatures cause increased air vacuole expansion, leading to increased surface crack formation and, thus, increased free fat (De Vilder et al., 1976; Kelly et al., 2002). Additionally, the free fat content of LN80 and LN90 powders were significantly (P <0.05) lower than that for LC80 and LC90 (Table 3.4) powders. It is suggested that this is due to the smaller oil droplets in nanoemulsions being less likely to be ruptured during the

atomisation process, coupled with the smaller oil droplets being more efficiently embedded within the powder wall matrix and, thus, less likely to be extracted by solvent during testing. Similar results were reported by Millqvist-Fureby (2003) and Jafari et al. (2008a) who showed that decreasing FGS of emulsions using microfluidisation pre- spray drying caused a reduction in free fat content. A study by Aguilar and Ziegler (1994) showed that powders with a lactose concentration of greater than 40% w/w help reduce extractable free fat content. Free fat on the surface of powders increases hydrophobicity, reduces solubility in water and promotes lipid oxidation (Pisecky, 1997), and so is an important powder property to minimise.

Table 3.3 Mean fat globule size (FGS), D[4,3], apparent viscosity and creaming rate measurements for reconstituted powders at 12.5% w/w solids.

Sample	Mean FGS[1] (nm)	D[4,3][2] (nm)	Apparent Viscosity (mPa.s)	Creaming rate (mm/d)
LC80	-	1198 ± 5	2.0 ± 0.1[a]	0.5 ± 0.1[a]
LC90	-	1125 ± 10	2.0 ± 0.1[a]	0.5 ± 0.1[a]
LN80	154 ± 2	-	1.9 ± 0.1[a]	0.2 ± 0.0[b]
LN90	155 ± 3	-	2.2 ± 0.3[a]	0.2 ± 0.0[b]
SC80	-	1058 ± 10	2.0 ± 0.0[a]	0.5 ± 0.1[c]
SC90	-	1085 ± 24	2.0 ± 0.1[a]	0.5 ± 0.1[c]
SN80	151 ± 2	-	1.9 ± 0.1[a]	0.2 ± 0.0[b]
SN90	149 ± 3	-	1.9 ± 0.1[a]	0.2 ± 0.0[b]

[1]Mean FGS measured by dynamic light scattering.

[2]D[4,3] measured by laser diffraction.

[(a-c)] Values within a column not sharing a common letter differ significantly (P <0.05).

3.3.5 Differential scanning calorimetry

Onset temperature of glass transition (T_g) and crystallisation (T_{cr}) increased significantly (P <0.05) with increasing dryer outlet temperature (Table 3.5), due to reduced water contents and, thus, plasticisation effects (Haque and Roos, 2004; Omar and Roos, 2007). No significant difference (P >0.05) in T_g was observed between different powder types LC80 and LN80, or LC90 and LN90, however T_{cr} was significantly (P <0.05) lower for

LN80 and LN90 compared to LC80 and LC90. It is proposed that this was due to the smaller FGS of the nanoemulsion pre- spray drying compared to the control emulsion. As the fat globules were smaller post- microfluidisation, there was more surface area for the protein to adsorb to, reducing the concentration of protein in the continuous phase and, thus, protein to lactose ratio; consequently the lactose molecules were freer to rearrange and crystallise upon heating. In a study by Thomas et al. (2004b) it was found that increasing the quantity of β-lactoglobulin in freeze dried lactose/β-lactoglobulin mixtures caused lactose crystallisation to occur at a higher water activity, compared to pure lactose. The authors postulated that this was due to the presence of increased protein on the surface of the powder particles, giving limited access of water vapour to the lactose. Similar results were obtained by McCarthy et al. (2013) where infant formula powders with lower protein content and lower protein on the powder surface (as measured by XPS), absorbed less water prior to lactose crystallisation.

The values of T_g and T_{cr} for powders made from control-, (SC) or nano-, (SN) emulsions containing sucrose were not significantly different (P >0.05) (Table 3.5). In contrast, the T_g and T_{cr} of powders containing sucrose (SC and SN) was significantly (P <0.05) different from powders containing lactose (LC and LN). The T_g of pure sucrose (67 ºC) is lower than pure lactose (105 ºC) as reported by Liu et al. (2007) and Potes et al. (2012), respectively, and so partial replacement of lactose with sucrose had a plasticising effect which reduced T_g. In contrast, the presence of sucrose caused the T_{cr} to increase. This delay in crystal growth may have been due to changes in the molecular environment in the development of the lattice structure after the addition of sucrose. Similar results were obtained by Mazzobre et al. (2001) in a lactose/trehalose system where the presence of trehalose caused a T_{cr} increase. Also, Roe and Labuza (2005) showed that the addition of a small quantity of trehalose to sucrose increased T_{cr} significantly. This may be expected as trehalose has a higher T_g than sucrose and, therefore, its addition increases both T_g and T_{cr}. The findings in the current study indicated that the addition of a sugar with a smaller T_g (sucrose) to a sugar with a larger T_g (lactose) can increase T_{cr}, even though T_g of the mixture is decreased. Therefore, the T_{cr} of a sugar mixture is always greater than that of the individual sugar, even if one sugar has a plasticising effect on T_g.

Table 3.4 Comparison of properties of control to nanoemulsion powders.

Powder	Moisture content (%)	Water activity (-)	D[4,3] (μm)	Tapped bulk density (g/mL)	Free fat (%)
LC80	2.3 ± 0.2^{a}	0.19 ± 0.02^{a}	92.1 ± 2.4^{a}	0.42 ± 0.01^{a}	2.3 ± 0.6^{a}
LC90	1.8 ± 0.1^{b}	0.16 ± 0.02^{b}	83.9 ± 2.6^{b}	0.36 ± 0.02^{b}	3.0 ± 0.2^{a}
LN80	2.3 ± 0.1^{a}	0.19 ± 0.02^{a}	90.9 ± 0.3^{a}	0.39 ± 0.00^{c}	0.4 ± 0.1^{b}
LN90	1.9 ± 0.1^{a}	0.15 ± 0.01^{b}	79.4 ± 3.6^{b}	0.34 ± 0.01^{b}	0.6 ± 0.2^{b}
SC80	1.6 ± 0.4^{b}	0.12 ± 0.03^{c}	102.1 ± 5.0^{c}	0.43 ± 0.02^{a}	1.1 ± 0.9^{c}
SC90	1.6 ± 0.2^{b}	0.13 ± 0.03^{c}	89.1 ± 1.1^{a}	0.37 ± 0.01^{b}	2.2 ± 1.5^{a}
SN80	1.8 ± 0.4^{b}	0.17 ± 0.03^{a}	97.1 ± 4.1^{c}	0.38 ± 0.01^{b}	0.3 ± 0.2^{b}
SN90	1.3 ± 0.3^{b}	0.12 ± 0.02^{c}	86.8 ± 1.2^{a}	0.34 ± 0.01^{b}	0.4 ± 0.1^{b}

$^{(a-c)}$ Values within a column not sharing a common letter differ significantly (P <0.05).

3.3.6 Dynamic vapour sorption

The water sorption kinetics of low moisture powders are shown in Figure 3.1 (LC80 & LN80) and Figure 3.2 (SC80 & SN80). Results are presented on a Solids-Non-Fat (SNF) basis because fat does not absorb water. Two complete sorption and desorption cycles show the difference in water sorption pre- and post- crystallisation of lactose. In Figure 3.1, the profile for the first sorption/desorption cycle is different from the second cycle. In cycle 1, sorption of water from 0 – 40% RH (below T_g) occurred without change in structure and most likely due to surface adsorption only. At a RH of 50% a significant increase in water sorption occurred showing that structural changes, associated with a glass transition, allowed water to enter the bulk of the powder because of increased molecular mobility (Burnett et al., 2004). Water diffusion increases in polar hydrophilic matrices (Palzer, 2010) and has been shown to increase with increasing water activity up to the point of lactose crystallisation in SMP and WMP (Murrieta-Pazos et al., 2011). Also, above T_g, sugar and protein molecules can cancel their own hydrogen bonds as they become mobile, which allows water to find additional bonding sites. Above T_g, amorphous materials will relax to their more thermodynamically stable crystalline state. At 70% RH, a reduction in mass of sorbed water from ~15.5% to ~5.5% was observed

due to the crystallisation of amorphous lactose. Crystalline lactose generally has less water vapour sorption capacity and diffusivity than amorphous lactose due to decreased void space, free energy, surface area, and permeability (Burnett et al., 2006; Palzer, 2010). Water is, thus, released as unbound or free water. The RH at which this loss of mass occurred was the crystallisation humidity (RH_c). During the crystalline phase (~480 to 600 min), water was sorbed to the powder upon humidification from 70 – 90% RH. The second cycle showed no decrease in mass upon humidification, indicating no further crystallisation (Burnett et al., 2004; Burnett et al., 2006). The second sorption cycle shows a lower uptake of water compared to the first cycle due to water sorption occurring at the surface only post- crystallisation (Saltmarch and Labuza, 1980).

Table 3.5 Onset temperature of glass transition (T_g) and onset temperature of lactose crystallisation (T_{cr}) for control and nanoemulsion powders.

Powder	T_g (ºC)	T_{cr} (ºC)
LC80	58 ± 1^{a}	130 ± 4^{a}
LC90	60 ± 0^{b}	134 ± 2^{b}
LN80	57 ± 1^{a}	125 ± 3^{c}
LN90	60 ± 0^{b}	131 ± 1^{a}
SC80	54 ± 1^{c}	141 ± 0^{d}
SC90	53 ± 1^{c}	141 ± 0^{d}
SN80	54 ± 1^{c}	140 ± 0^{d}
SN90	53 ± 0^{c}	143 ± 3^{d}

$^{(a\text{-}d)}$ Values within a column not sharing a common first letter superscript differ significantly (P <0.05)

In Figure 3.2; cycle 1, the presence of sucrose, i.e., in powders SC80 and SN80, increased the RH (80%) at which crystallisation occurred (~500 min). Water was absorbed up to ~21% and upon crystallisation the mass of sorbed water reduced to ~15%. Post-crystallisation, the water uptake increased to ~23% at 90% RH. The 6% loss in water was less than that observed for LC80 and LN80 (Figure 3.1; cycle 1), indicating that the

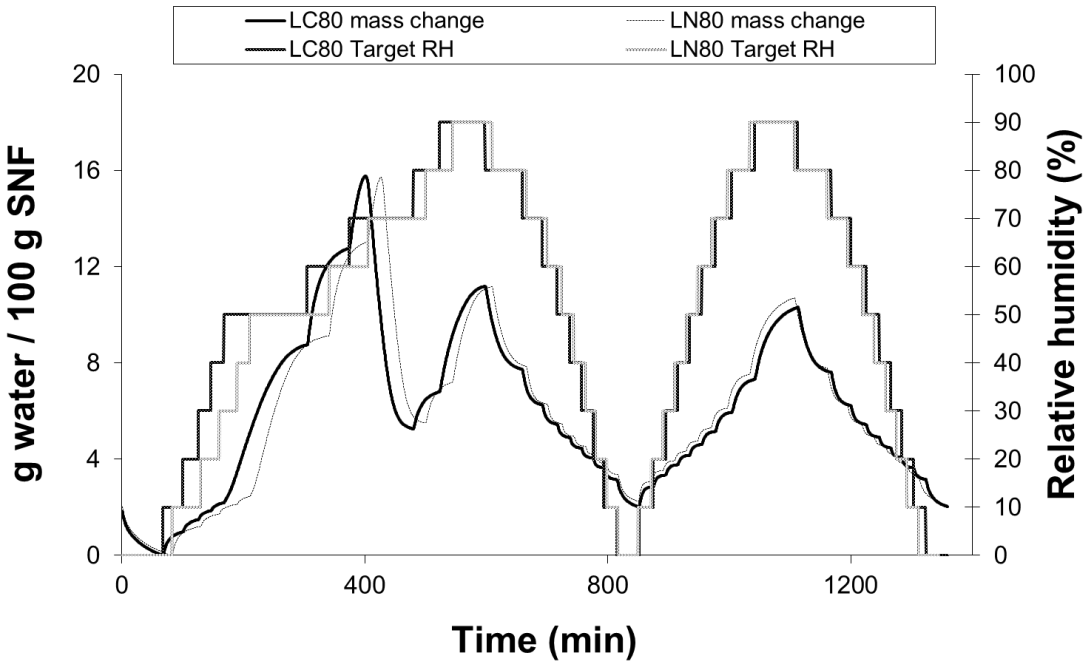

Figure 3.1 Moisture sorption kinetics comparison (0–90–0 % RH for 2 cycles) of high moisture powders with lactose (LC80 and LN80) measured on a Solids-Non-Fat (SNF) basis.

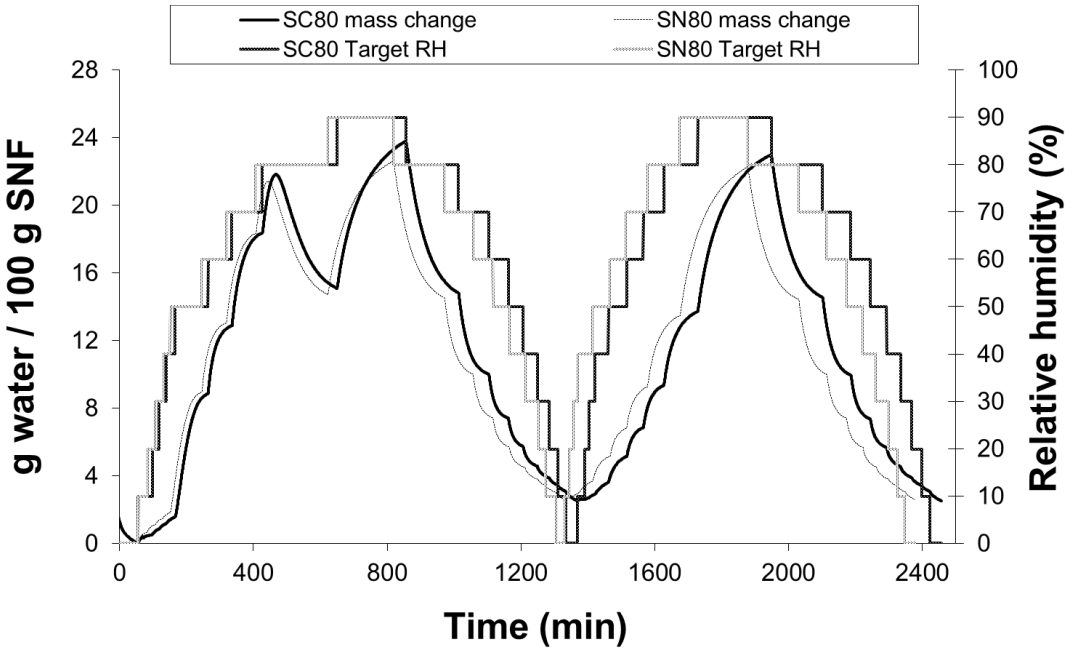

Figure 3.2 Moisture sorption kinetics comparison (0–90–0 % RH for 2 cycles) of high moisture powders with lactose: sucrose (SC80 and SN80) measured on a Solids-Non-Fat (SNF) basis.

presence of sucrose resulted in a higher RH_c and that only the lactose fraction crystallised. This agreed with the DSC results (Table 3.5), where the T_{cr} values for the SC80 and SN80 powders were higher than the LC80 and LN80. Similar to that observed in Figure 3.1, no reduction in mass was observed during the second sorption step in Figure 3.2, indicating that crystallisation was completed during the first sorption step in cycle 1. The timescale of the sorption/desorption kinetics showed that the SC80 and SN80 took longer than LC80 and LN80 to complete their 2 cycles (2400 min compared to 1400 min). No differences were observed between the LC80 and LN80 in Figure 3.1 and SC80 and SN80 in Figure 3.2.

The irreversibility of the morphological change from amorphous to crystalline is visible in Figures 3.1 and 3.2, as the sorption steps in cycle 1 are much different from the subsequent desorption/sorption/desorption steps. An increase of ~2.2% water was bound to LC80 and LN80 post- desorption (Figure 3.1), compared to an increase of ~2.5% water bound to SC80 and SN80 post- desorption (Figure 3.2). Figure 3.2 differs from Figure 3.1 in that crystallisation was reduced when sucrose partially replaced lactose. Also, at 90% RH in cycle 1 the mass of sorbed water at 90% RH was greater than pre- crystallisation (23% compared to 11%). This may be due to the sucrose not crystallising and able to absorb more water in its amorphous state. Sucrose has a higher solubility than lactose and so can sorb more water. The results indicate that only the lactose portion of SC80 and SN80 crystallised as the decrease in mass is ~70% of that for LC80 and LN80.

3.4 Conclusions

Spray dried nanoemulsions had reduced free fat and lower lactose T_{cr}, due to more protein on the fat surface and, hence, less protein in the continuous phase with the lactose. Sucrose reduced T_g but increased T_{cr} when present with lactose in powders, demonstrating that systems comprising of mixed sugars crystallise at higher temperature and humidity, regardless of the effect of individual sugars on T_g. These results show that the physical properties of powders can be altered by simply changing the FGS of emulsions pre- spray drying.

Chapter 4 - Microstructure and lactose crystallisation properties in spray dried nanoemulsions

Published as:

Maher, P.G., Auty, M.A.E., Roos, Y.H., Zychowski, L.M., and Fenelon, M.A. 2015. Microstructure and lactose crystallization properties in spray dried nanoemulsions. *Food Structure* 3: 1-11.

FOOD STRUCTURE 3 (2015) 1–11

Available online at www.sciencedirect.com

ScienceDirect

journal homepage: www.elsevier.com/locate/foostr

Microstructure and lactose crystallization properties in spray dried nanoemulsions

P.G. Maher [a,b], M.A.E. Auty [a,*], Y.H. Roos [b], L.M. Zychowski [a,b], M.A. Fenelon [a]

[a] Food Chemistry & Technology Department, Teagasc Food Research Centre, Moorepark, Fermoy, Co. Cork, Ireland
[b] Food Technology, School of Food and Nutritional Sciences, University College Cork, Cork, Ireland

ARTICLE INFO

Article history:
Received 17 July 2014
Received in revised form
3 October 2014
Accepted 9 October 2014
Available online 29 October 2014

Keywords:
Lactose crystallization
Dynamic vapour sorption
Polarized light microscopy
Confocal laser scanning microscopy
Cryo-scanning electron microscopy

ABSTRACT

The objective of this study was to characterize lactose crystallization behaviour and microstructure of spray dried nanoemulsions with different fat globule sizes (FGS). Powders of the same composition (57.7% w/w lactose, 12.3% w/w sodium caseinate, 27.7% w/w sunflower oil, and 2.3% w/w water) but different FGS (mean diameters 1100 nm and 155 nm) prior to spray drying were manufactured. Differences in lactose crystallization were studied using dynamic vapour sorption (DVS) and polarized light microscopy (PLM). Crystallization kinetics was modelled using the Avrami and Yang equations. Results showed that lactose crystallized in three dimensions and more rapidly in powders with a smaller FGS. PLM images showed a higher rate of lactose crystal formation for smaller FGS powders when stored for 4 days at 55% relative humidity. Confocal laser scanning microscopy (CLSM) and cryo-scanning electron microscopy (Cryo-SEM) images indicated the more evenly distributed small fat globules inside powder particles prepared from spraydried nanoemulsions. The surface of powder particles was uneven and ruptured post lactose crystallization. Crystals appeared after humidification and were assumed to be anhydrous α- and β-lactose in a 5:3 molar ratio. Results showed powder particles of the same composition were altered in lactose crystallization characteristics by changing the FGS of emulsions pre spray drying.
© 2014 Elsevier Ltd. All rights reserved.

1. Introduction

In dairy products, the degree of lactose crystallization has a significant effect on ingredient and food properties, such as texture and flavour. Crystallization of lactose in milk powders results in lumping and caking which has a negative impact on powder reconstitution (Lai & Schmidt, 1990). Component crystallization also causes the release of entrapped lipids in powders (Fäldt & Bergenståhl, 1996; Shimada, Roos, & Karel, 1991) making them more susceptible to oxidation.

Various methods can be used to quantify crystallization of amorphous sugars. Isothermal differential scanning calorimetry (DSC) was used by Kedward, MacNaughtan, Blanshard, and Mitchell (1998) and Roos and Karel (1990) to determine the crystallization of freeze dried lactose and sucrose at low water contents (<5%) and high temperatures (365–400 K). X-ray diffraction (XRD) was used by Jouppila, Kansikas, and Roos (1997) and Miao and Roos (2005) to monitor crystallization kinetics of lactose, trehalose and lactose/trehalose mixtures. Mahlin, Berggren, Alderborn, and Engstrom (2004) used atomic force microscopy (AFM) to quantify crystallization.

* Corresponding author. Tel.: +353 2542442.
E-mail address: mark.auty@teagasc.ie (M.A.E. Auty).
http://dx.doi.org/10.1016/j.foostr.2014.10.001
2213-3291/© 2014 Elsevier Ltd. All rights reserved.

Abstract

The objective of this study was to characterise lactose crystallisation behaviour and microstructure of spray dried nanoemulsions with different fat globule sizes (FGS). Powders of the same composition (57.7% w/w lactose, 12.3% w/w sodium caseinate, 27.7% w/w sunflower oil, and 2.3% w/w water) but different FGS (mean diameters 1100 nm and 160 nm) prior to spray drying were manufactured. Differences in lactose crystallisation were studied using dynamic vapour sorption (DVS) and polarised light microscopy (PLM). Crystallisation kinetics was modelled using the Avrami and Yang equations. Results showed that lactose crystallised in three dimensions and more rapidly in powders with a smaller FGS. PLM images showed a higher rate of lactose crystal formation for smaller FGS powders when stored for 4 days at 55% relative humidity. Confocal laser scanning microscopy (CLSM) and cryo-scanning electron microscopy (Cryo-SEM) images indicated the more evenly distributed small fat globules inside powder particles prepared from spray dried nanoemulsions. The surface of powder particles was uneven and ruptured post- lactose crystallisation. Crystals appeared after humidification and were assumed to be anhydrous α- and β-lactose in a 5:3 molar ratio. Results showed powder particles of the same composition were altered in lactose crystallisation characteristics by changing the FGS of emulsions pre- spray drying.

4.1 Introduction

In dairy products, the degree of lactose crystallisation has a significant effect on ingredient and food properties, such as texture and flavour. Crystallisation of lactose in milk powders results in lumping and caking, which has a negative impact on powder reconstitution (Lai and Schmidt, 1990). Component crystallisation also causes the release of entrapped lipids in powders (Shimada et al., 1991; Fäldt and Bergenståhl, 1996), making them more susceptible to oxidation.

Various methods can be used to quantify crystallisation of amorphous sugars. Isothermal differential scanning calorimetry (DSC) was used by Roos and Karel (1990) and Kedward et al. (1998) to determine the crystallisation of freeze dried lactose and sucrose at low water contents (<5%) and high temperatures (365 – 400 K). X-ray diffraction (XRD) was used by Jouppila et al. (1997) and Miao and Roos (2005) to monitor crystallisation kinetics of lactose, trehalose and lactose/trehalose mixtures. Mahlin et al. (2004) used atomic force microscopy (AFM) to quantify crystallisation.

Lactose crystallisation can be measured by gravimetric means by monitoring changes in mass of powder samples upon humidification (Iglesias and Chirife, 1978; Lai and Schmidt, 1990; Jouppila and Roos, 1994b). Crystallisation results in sorbed water release, which is measured from mass decrease in a humidified powder (Burnett et al., 2004; Burnett et al., 2006). This method is most successfully used at ambient temperatures, where the crystallisation rate is quite slow and can be easily monitored (Kedward et al., 2000).

Crystallisation kinetics can be modelled using various relationships. The Avrami equation (Avrami, 1939, 1940) has been used by several researchers (Arvanitoyannis and Blanshard, 1994; Kedward et al., 2000; Mazzobre et al., 2003; Haque and Roos, 2005). Derivative models from the Avrami equation include the Yang equation (Yang et al., 2010), and Urbanovici-Segal equation (Urbanovici and Segal, 1990). The Urbanovici-Segal equation includes a parameter r ($r > 0$) that determines how far the model deviates from the Avrami equation (Soutari et al., 2012). Other kinetic models used to determine lactose crystallisation are the Williams-Landel-Ferry (WLF) equation (Roos and Karel, 1991b), and the Hoffman equation (Arvanitoyannis and Blanshard, 1994). The Arrhenius equation can be used to determine the activation energy (E_A) required for crystallisation

(Schmidt et al., 1999). The Avrami equation determines the rate constant (k) and exponent (n) that, respectively, determine how fast the material crystallises and in how many dimensions. Powders stored at increasing temperature and humidity crystallise at faster rates (Soutari et al., 2012).

Polarised light microscopy (PLM) is a useful technique in distinguishing crystalline from non-crystalline material (Hartel, 2001), and can be used to directly measure the rate of crystal growth. Mazzobre at al. (2003) used polarised light videomicroscopy (PLV), in conjunction with DSC, to determine the isothermal crystallisation kinetics of lactose and lactose-trehalose mixtures. The PLV method proved a useful way of directly observing individual crystal growth and morphological aspects that were undetectable by DSC.

The distribution of fat globules has a significant effect on functional properties of dairy powders (Pisecky, 1997). Techniques such as CLSM and cryo-SEM are useful in highlighting microstructural differences, which help explain why dairy powders have various functional properties. CLSM is widely used for studying the microstructure of cheese, milk powder, and chocolate (Auty et al., 2001). McKenna (1997) examined whole milk powder using CLSM. Kelly et al. (2014) used CLSM to analyse the distribution of fat droplets in powder samples where different fat blends were stabilised by sodium caseinate. These authors dual-labelled samples with Nile Red/Fast Green FCF to show the distribution of fat and protein, respectively, throughout the powder particles. Air vacuoles were also visible in powders in images produced by CLSM. SEM techniques have been developed to examine the outer and inner structures of foods (Soottitantawat et al., 2003). SEM has been used in studies of microencapsulation properties of powder structures stabilised by sodium caseinate (Fäldt and Bergenståhl, 1996; Hogan et al., 2001a, b). Cryo-SEM is a useful technique in analysing nano-sized particles embedded in food matrices (Dudkiewicz et al., 2011).

The objectives of the present study were (i) to investigate the effects of reducing the FGS of emulsions prior to spray drying on water-induced lactose crystallisation during storage; and (ii) to characterise powder microstructure using correlative microscopy techniques (PLM, CLSM and cryo-SEM) to help explain differences of the physical properties of the powders.

4.2 Materials and Methods

4.2.1 Materials

Two powders containing 57.7% w/w lactose, 12.3% w/w sodium caseinate, 27.7% w/w sunflower oil, and 2.3% water were used (Maher et al., (2014)). The powders differed in their mean FGS as they were both homogenised (60 °C with a single pass) at different pressures prior to spray drying. Conventional emulsions were produced using in-line two stage homogenisation (model NS20006H, GEA Niro, Soavi, Parma, Italy), at first and second stage pressures of 13.79 MPa and 3.45 MPa, respectively, giving a FGS of ~1100 nm. Nanoemulsions were produced by microfluidisation with a microfluidiser (model M-110EH, Microfluidics, Newton, MA, USA) at 100 MPa, giving a FGS of ~155 nm. All emulsions were spray dried at the same conditions (inlet/outlet dryer temperatures of 185 °C/80 °C) with a single stage pilot-scale spray dryer (Anhydro F1 Lab, Copenhagen, Denmark), equipped with a two-fluid nozzle atomisation system (Type 1/8 JAC 316ss) and counter-flow drying. Resulting powders were labelled C and N for conventional emulsion powders (FGS ~1100 nm) and nanoemulsions powders (FGS ~155 nm), respectively.

4.2.2 Methods

4.2.2.1 Dynamic vapour sorption

Water sorption isotherms of powders were obtained from the DVS Data Analysis Suite in Microsoft Excel using a DVS-1 analyser (Surface Measurement Systems, London, UK) equipped with a Cahn microbalance. Powder samples (~30 mg) were placed in the sample pan with an empty pan used as a reference. Samples were humidified at 55% relative humidity (RH) on the DVS for two days (48 h) for C and N at 25ºC. Mixing dry nitrogen gas (200 mL/min) with saturated water vapour in the correct proportion using mass flow controllers was used to get accurate RH readings. Samples measured were from three replicate spray drying trials.

4.2.2.2 Polarised light microscopy

Samples were examined using an Olympus BX51 light microscope (Olympus BX-51, Olympus Corporation, Tokyo, Japan) with a 10x dry objective lens using polarised light. Digital images (TIFF, 8-bit) were taken using a Jenoptik C14 Imagic camera, and captured. Powders were analysed pre- and post- lactose crystallisation following storage over a saturated solution of $Mg(NO_3)_2$ (55% RH) for 4 days at 20 ℃. Crystalline regions appeared as bright areas on the micrographs.

4.2.2.3 Confocal laser scanning microscopy

Visualisation of powder particles was carried out using a Leica TCS SP5 confocal laser scanning microscope (CLSM; Leica Microsystems CMS GmbH, Wetzlar, Germany). Powder samples were placed onto a glass slide and labelled using a mixture of Fast Green and Nile Red or Nile Red alone (Auty et al., 2001). The dye mixture comprised Fast Green (aq. 0.01 g/0.1 L) and Nile Red dissolved in polyethylene glycol, molecular weight 400 (0.1g/0.1 L), mixed in a ratio that allowed diffusion of the dye molecules into the powder particles whilst maintaining particle integrity and preventing solubilisation. Based on trial and error, pre- and post- lactose crystallised powders were labelled, respectively, with 1:40 or 1:20 ratios of Fast Green to Nile Red. Dual excitation using 488nm/633nm was utilised for all Nile Red and Fast Green mixtures, while single excitation at 488 nm was used for the Nile Red images. Representative images of each sample were taken using 63x oil immersion objective with numerical aperture 1.4. Z-stacks were obtained in order to generate a three-dimensional structure of the particle, and to identify surface fat staining. Red and Green pseudo-coloured images (8-bit), 512 x 512 pixels in size, were acquired using a zoom factor of 1. A minimum of four z-stacks were taken per sample, with representative micrographs being shown. Samples were measured pre- and post-lactose crystallisation (55% RH for 4 days).

4.2.2.4 Cryo-scanning electron microscopy (Cryo-SEM)

Cryo-SEM was used to examine the microstructure of powders. Powders were sprinkled onto the surface of OCT embedding compound (Agar Scientific Ltd, UK) on a slotted

aluminium stub, then plunge-frozen into liquid nitrogen slush at − 210 °C and transferred under vacuum to the cold stage using the Alto 2500 cryo-transfer device (Gatan Ltd., Oxford, UK). A cold scalpel was used to fracture samples. Samples were cooled to − 125 °C, after sublimation at − 95 °C for 2 min, sputter coated with platinum prior to transfer to the cold stage for imaging at − 125 °C. A Zeiss Supra 40VP field emission scanning electron microscope (Carl Zeiss SMT Ltd., Cambridge, UK), operating at 2 kV and a working distance of 6 mm, was used to obtain secondary electron images. Representative micrographs were taken in order to visualise surface characteristics, including surface fat and lactose crystals, where present. Samples were analysed pre- and post- lactose crystallisation (55% RH for 4 days).

4.2.2.5 Statistical analysis

Spray drying experiments were carried out in triplicate. One-way analysis of variance (ANOVA) was used with Minitab 15 (Minitab Ltd., Coventry, UK) to determine significant differences between lactose crystallisation kinetics of both sets of powders by Fisher's one-way multiple comparison test. Results were deemed statistically significant if $P < 0.05$.

4.3 Results and Discussion

4.3.1 Water sorption kinetics

Water sorption kinetics of powders C and N were measured by DVS at 55% RH and 25 °C. These conditions were chosen since Burnett et al. (2004) showed that below 30% RH lactose crystallisation will not occur and above 58% RH lactose crystallisation is nearly instantaneous.

Figure 4.1a shows the mean water uptake in powders from 3 replicate samples on a solids-non-fat (SNF) basis over a 2880 min (48 h) period. It is shown that there was no difference in initial water sorption behaviour of the powders. The mean maximum sorption rate of water in the first 60 min was 7.4 g water/100 g SNF for C, and 7.9 g water/100 g SNF for N. Maximum water sorption occurred in ~140 min, upon which

there was a decrease in mass and, therefore, evidence for onset of lactose crystallisation (Burnett et al., 2004; Burnett et al., 2006). Powders C and N shown in Figure 4.1a crystallised at different rates, with lactose crystallising faster in N than in C. The mass of water decreased until full crystallisation was achieved towards the end of the run. The mean crystallisation rate of lactose in each powder showed 0.9 g water/100 g SNF lost per hour for C and 1.9 g water/100 g SNF lost per hour for N (measured between 700 and 760 min). The onset (m_0) and end points (m_∞) of lactose crystallisation were found by calculating the intersection point of tangent lines to the respective baselines using the experimental data in Figure 4.1a. The mean onset points for C and N were 483 min and 424 min, respectively, showing that N started to crystallise before C. N also had a mean end point of 1098 min compared to a mean end point of 1240 min for C. This clearly showed that lactose crystallised faster in powders from nanoemulsions (674 min in total) than in powders from conventional emulsions (757 min in total). This result was similar to that of Maher at al. (2014) who found using Differential Scanning Calorimetry (DSC) that lactose in powders from nanoemulsions crystallised at significantly (P <0.05) lower temperatures than in powders from conventional emulsions. Maher at al. (2014) explained that this was due to nanoemulsions having a smaller FGS, meaning that there was more surface area for protein to adsorb to, leaving less protein in the continuous lactose phase.

More detailed quantitative analysis of lactose crystallisation was achieved by converting the experimental data to the fraction crystallised over time, and subsequent results were analysed statistically. This was calculated by comparing the mass of water absorbed by the powder at a given time (m_t) to the mass of absorbed water at the end of crystallisation (m_∞) and the mass of water absorbed at the onset of crystallisation (m_0). Then:

$$Crystallisation = \theta_t = \frac{m_0 - m_t}{m_0 - m_\infty} \tag{4.1}$$

The resulting isotherm is shown in Figure 4.1b and is the mean of 3 replicate powders of each type (C and N). The time has been normalised so that the onset of lactose crystallisation is time zero and the y-axis has been normalised to reflect the crystallisation fraction. Before lactose crystallisation, the crystalline fraction was assumed to be zero and it was assumed to be one after crystallisation. Various different equations have been used

in literature to model crystallisation kinetics, the most common of which is the Avrami model (1939):

$$\theta_t = 1 - \exp(-kt^n) \tag{4.2}$$

Here, k is the rate constant (min^{-1}) and n is the Avrami exponent. The rate constant (k) quantifies how fast the crystals grow indicating the stability of the system (Gaisford et al., 2009), and the Avrami exponent (n) defines the mechanism of crystallisation. The Avrami rate constant mainly depends on the crystallisation temperature (Kawamura, 1979) and typically follows an Arrhenius-type temperature dependency. It takes both nucleation and crystal growth into account (Sharples, 1966). An Avrami exponent value of 1 represents nucleation and crystal growth from surfaces, a value of 2 represents crystal growth from edges, and a value of 3 indicates crystal growth in three dimensions. Non-integer n values can also be obtained and they represent mixed crystallisation mechanisms (Cahn, 1956; Soutari et al., 2012). The sigmoidal shape of the curve in Figure 4.1b is typical of those produced using the Avrami equation. The larger the Avrami exponent (n) the more sigmoidal the crystallisation curve (Avrami, 1940). Transformation rates are low at the beginning and end of the transformation, but rapid in between. Initially there is a slow rate due to the time required to form a significant number of nuclei of the new phase. The nuclei grow rapidly into particles, during the intermediate phase, and consume the old phase while nuclei continue to form in the remaining parent phase. When the transformation is nearly complete, there is less material to transform to nuclei and the production of new particles becomes slow. Also, the already existing particles touch each other forming a boundary where growth stops. This is not accounted for in the Avrami model as it assumes a constant crystal growth rate, which is why the model breaks down as complete crystallisation approaches (Soutari et al., 2012).

The experimental data was also modelled using a modified version of the Avrami equation from Yang et al. (2010):

$$\theta_t = 1 - \frac{1}{1 + kt^n} \tag{4.3}$$

The same equation was derived by Tobin et al. (1974). Crystallisation isotherms were fitted to Equations 4.2 and 4.3 and the results were compared to the experimental data in

Table 4.1. The Avrami model was found to better describe the experimental crystallisation process than the Yang model. The mean Avrami rate constants of 1.1 x 10^{-8} min^{-1} (C) and 1.2 x 10^{-7} min^{-1} (N) are significantly different (P <0.05), showing that lactose in powders from nanoemulsions crystallised faster than in conventional emulsions (Table 4.1). The Avrami integers are very close to 3, indicating the crystals are growing in three dimensions (Soutari et al., 2012).

Half-times of lactose crystallisation are useful in predicting the storage stability of lactose containing products (Jouppila et al., 1997). The crystallisation half-time is calculated using the rate constant (k) and exponent (n) in the following equation:

$$t_{1/2} = \left(\frac{\ln 2}{k}\right)^{\frac{1}{n}} \quad (4.4)$$

The $t_{1/2}$ values, calculated using the Avrami k and n values, were very similar to those found experimentally (Table 4.1). High coefficients of determination (R^2) and similar $t_{1/2}$ values indicate that the Avrami equation models the experimental data to a high degree of accuracy. Figure 4.1b shows that Avrami crystallisation values are very similar to experimental values.

Values found using the Yang equation were less accurate than those from the Avrami equation (Table 4.1). The coefficient of determination was lower and the $t_{1/2}$ was much different to the experimental value. The exponents (n) of 4.39 (C) and 4.31 (N) were greater and rate constants (k) were lower than Avrami constants. Similar results were reported by Al-Mulla (2007), who found that the Yang (or Tobin) model did not fit as well as the Avrami model because it gave higher n values and lower R^2 values for the crystallisation of polymers.

The rate constants (k) obtained in this study (1.1 – 12 x 10^{-8} min^{-1}) were much lower than those obtained by Schmidt et al. (1999), who measured the crystallisation kinetics of amorphous lactose at 25 °C in the range 52.5 – 57.5% RH (5.6 – 15.5 x 10^{-3} min^{-1}). Jouppila et al. (1997) found that the Avrami model did not work for SMP at 53.8% RH, but did work at humidity ≥ 66.2%. The rate constants for SMP were lower (1.1 x 10^{-10} min^{-1}), with a corresponding increase in crystallisation half-time (40 h) compared to the powders in this study, even at the higher RH of 66.2%.

Table 4.1 Summary of kinetic parameters obtained by fitting the crystallisation isotherms to the Avrami model and Yang model.

Powder	Avrami				Yang				Experimental
	k (min^{-1})	n (-)	$t_{1/2}$ (min)	R^2 (-)	k (min^{-1})	n (-)	$t_{1/2}$ (min)	R^2 (-)	$t_{1/2}$ (min)
C	1.1×10^{-8} [a]	3.06 [a]	363 [a]	0.995	7.3×10^{-12} [a]	4.39 [a]	323 [a]	0.976	368 [a]
N	1.2×10^{-7} [b]	2.76 [b]	287 [b]	0.985	2.3×10^{-9} [a]	4.31 [a]	262 [b]	0.970	285 [b]

[a-b] Values within a column not sharing a common letter differ significantly (P <0.05) by one-way ANOVA.

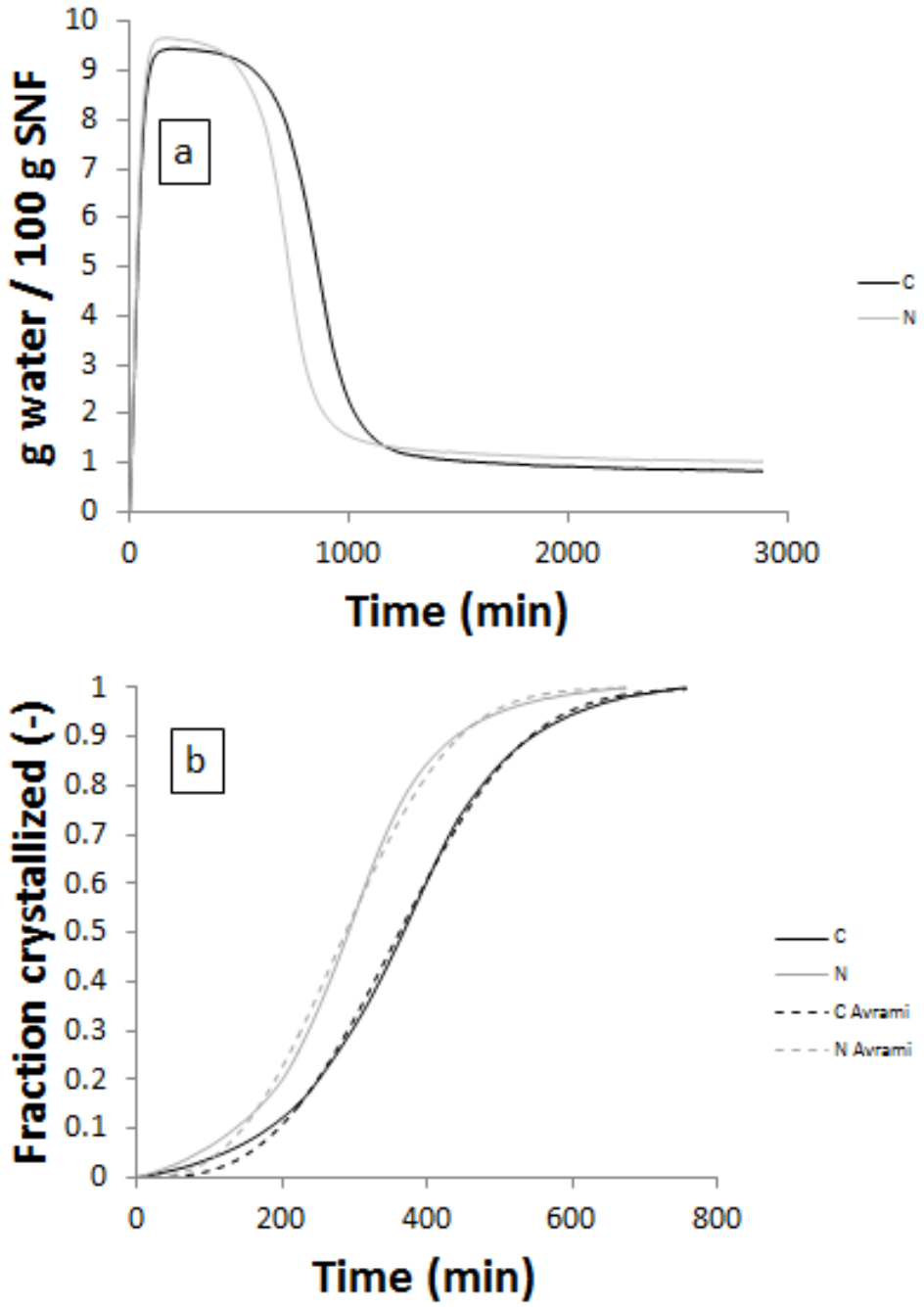

Figure 4.1 a) Dynamic vapour sorption graph of control (C) and nanoemulsion (N) powders held at 55% RH for 48 h showing lactose crystallisation. b) Crystallisation isotherms for C and N at 25 °C for experimental data and those calculated using the Avrami equation.

Similar Avrami indexes were obtained for SMP (~3), indicating crystal growth in three dimensions.

Overall, this shows that protein had a significant effect on lactose crystallisation kinetics. When protein was not present, lactose crystallised quickly (Schmidt et al., 1999). The 11% sodium caseinate in this study caused delayed lactose crystallisation, and increasing the protein content to 35% (for SMP) further delayed lactose crystallisation (Jouppila et al., 1997). It is postulated that nanoemulsions have less non-adsorbed protein than conventional emulsions due to their smaller FGS giving increased surface area for protein adsorption. Therefore, this study suggests that not only is the total amount of protein important, but the amount of non-adsorbed protein that has the most significant effect on lactose crystallisation.

To the authors' best knowledge, no other studies have compared crystallisation of lactose in powders with significantly different FGS. The best comparison can be made with McCarthy et al. (2013) who showed that lactose crystallisation occurred at lower water contents with decreasing protein content (i.e., less protein in the continuous phase) for infant formula powders. Similar results were found by Thomas et al. (2004b), who found that increasing β-lactoglobulin contents increased the humidity at which lactose crystallised in β-lactoglobulin/lactose mixtures.

4.3.2 Microscopy

4.3.2.1 Polarised light microscopy

Figure 4.2 shows PLM images of powders C and N when stored in a desiccator over a saturated salt solution of $Mg(NO_3)_2$ at 55% RH for 0, 1, 2, 3, and 4 days. The micrographs are consistent with results obtained from DVS, showing that lactose crystals formed more quickly in powder N than powder C over 4 days. Both powders at day 0 showed no evidence of lactose crystals. This was in contrast to other studies (Roetman, 1979; Haque and Roos, 2005; McCarthy et al., 2013) that showed lactose crystals present in fresh powders. At day 1, no crystals were seen in powder C but some small isolated crystals were seen in powder N (Figure 4.2d). At day 2, some crystals had formed in powder C (Figure 2e) with increased growth of crystals on the edges of powder particles

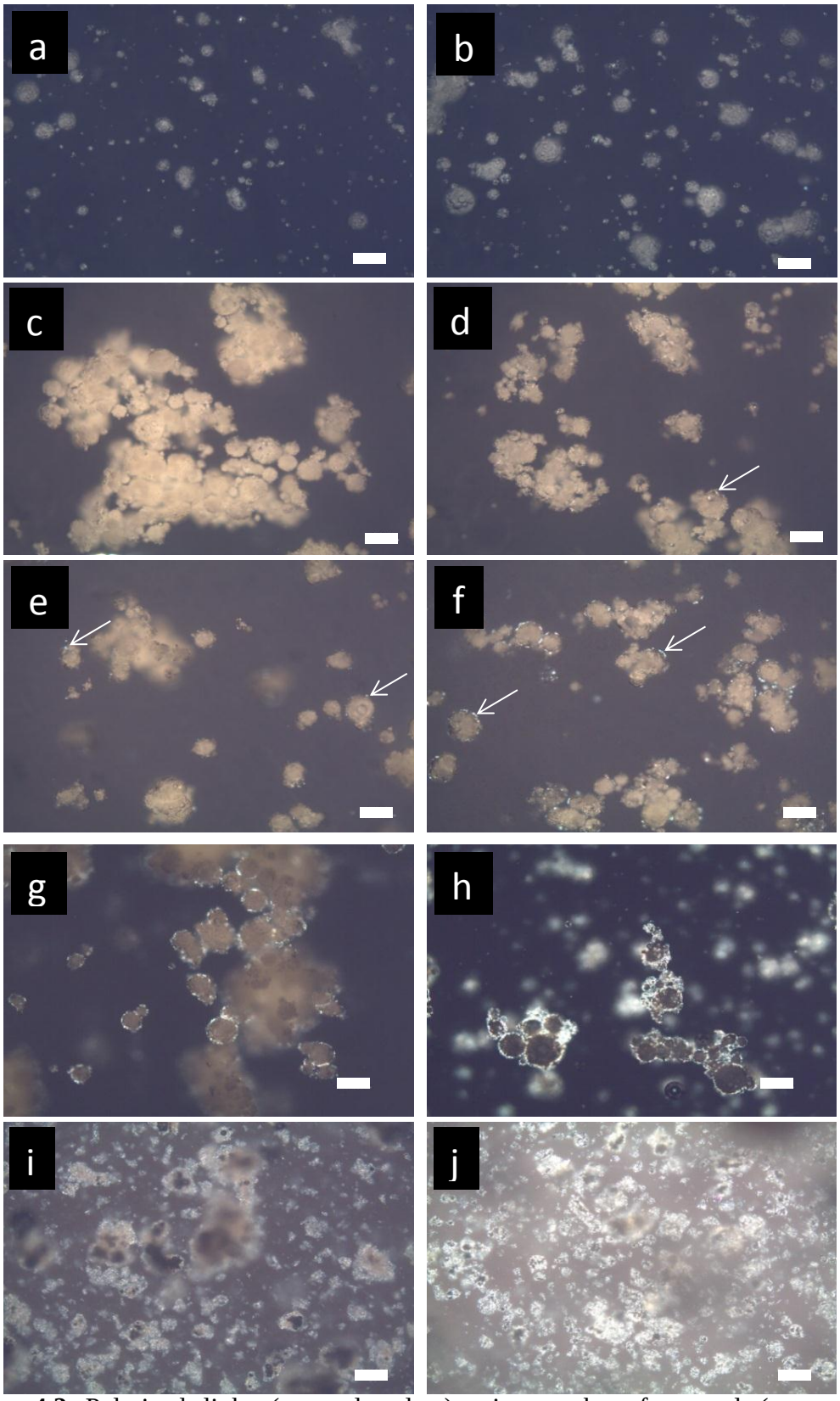

Figure 4.2 Polarised light (crossed polars) micrographs of control (a,c,e,g,i) and nanoemulsion (b,d,f,h,j) powders. after storage for 0 (a,b), 1 (c,d), 2 (e,f), 3 (g,h) and 4 (i,j) days at 55% relative humidity. Arrows indicate small crystals, scale bar =100 μm.

In powder N (Figure 2f). Surface crystals are evident in powder C at day 3 (Figure 4.2g) but there are noticeably more crystals present in powder N (Figure 4.2h). By day 4, both powders C and N showed crystallisation throughout the particles.

4.3.2.2 Confocal laser scanning microscopy

Confocal laser scanning microscopy results are shown in Figure 4.3. Labelling with Nile Red/Fast Green highlighted the fat and protein phases of the powder and showed air vacuoles as dark regions within the particle (Figure 4.3a, b, arrows). Discrete spherical fat droplets, most of which are 1 - 5 μm in diameter, were clearly seen within powder C (Figure 4.3a). By contrast, fat droplets in powder N were small (Figure 4.3b); although some individual droplets (~0.2 - 1 μm diameter) were visible, there was considerable co-localisation of the Nile Red and Fast Green signals, indicating that most fat droplets were below the resolution limit of the CLSM. The protein phase of both powders is shown in red. The protein is more clearly observed in powder C than powder N, due to the fat globules being less numerous and evenly spaced, allowing more gaps for the protein phase to be visualised. Very little surface fat was visible for either powder (Figure 4.3a, b), in contrast with some agglomerated whole milk powder particles that have shown evidence of surface fat pooling (McKenna, 1997). No evidence of lactose crystals was found in fresh powders (Figure 4.3a, b).

Powders stored after 4 days at 55% RH are shown in Figure 4.3c, d, e, f. Particles from both powders appeared to have deformed and were more agglomerated than fresh powders. Figure 4.3c shows large free fat droplets (arrows) >5 μm in diameter, as well as fat droplets and pools within the particles. Powder N shows generally less free fat but had more obvious elongated or needle-shaped crystals seen by negative contrast (Figure 4.3d, arrows). The protein signal was fairly weak and appeared localised at the surface and outer edges of the particles (Figure 4.3 c, d). This may be due to high level of lactose crystallisation preventing the stain from diffusing into the particle core.

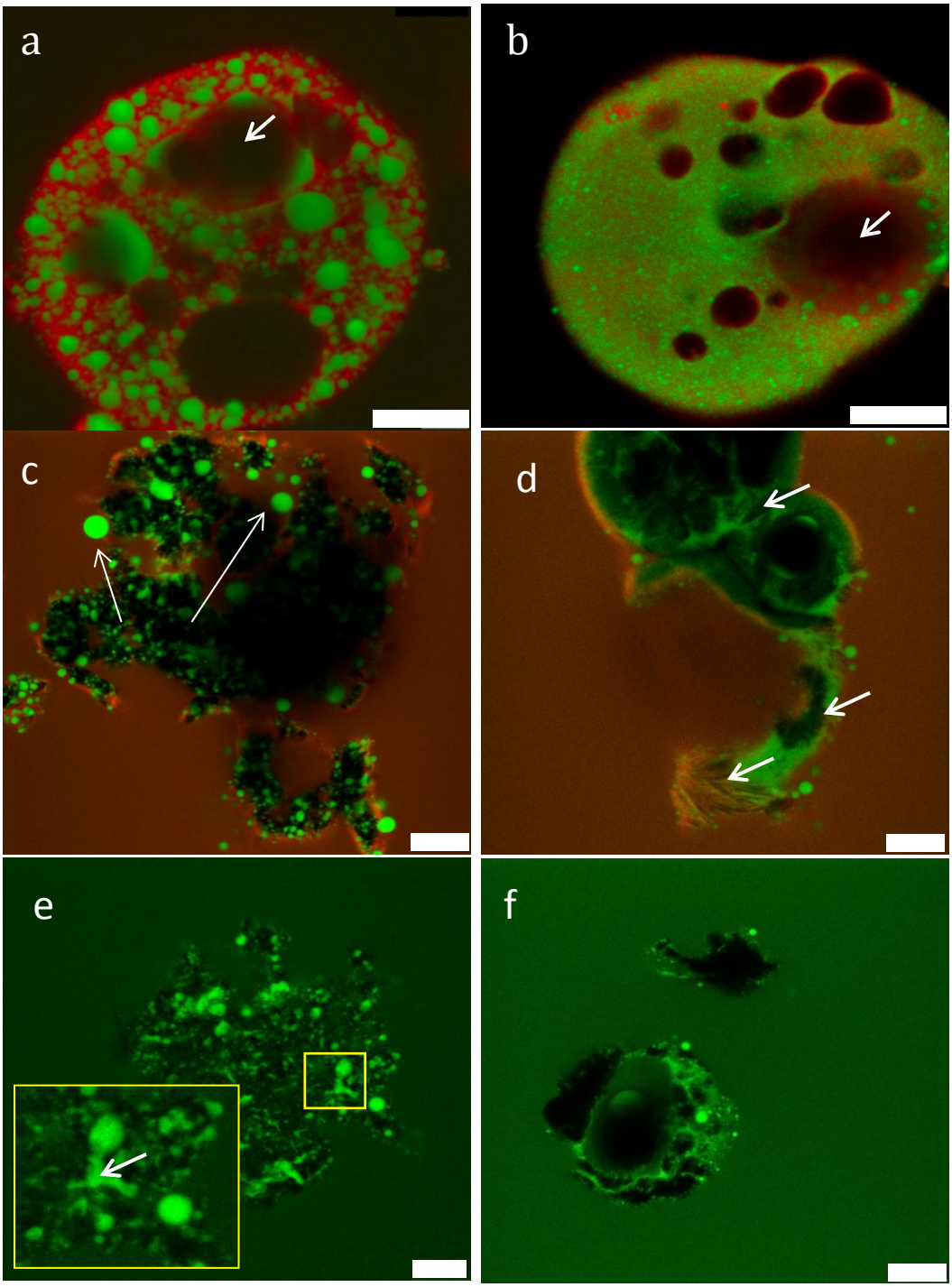

Figure 4.3 Confocal laser scanning micrographs of showing internal microstructures of control (a,c,e) and nanoemulsion (b,d,f) powders after storage for 0 (a,b) and 4 (c,d,e,f) days at 55% relative humidity. Figure 4.3 a – d are fluorescently labelled with Nile Red/Fast Green to show fat (green) and protein (red); Figure 4.3 e & f are labelled with Nile Red to show fat phase. Arrows indicate air vacuoles (a, b), discrete fat droplets (c) and solid lactose crystals (d). Fig 4.3e inset shows irregularly shaped coalesced fat regions. Scale bars =100 μm.

4.3.2.3 Cryo-scanning electron microscopy

It is important to characterise the outer topography of particles as it can give information on flow properties of spray dried powders (Soottitantawat et al., 2003). Cryo-SEM images are presented in Figures 4.4 and 4.5. The surface morphology of fresh powders from C and N powders is shown in Figures 4.4a and 4.4b, respectively. The surfaces of all powders appeared to be very smooth with little indentation and powder rupture, similar to data of Hogan et al. (2001b) who also used sodium caseinate as an emulsifier. Sodium caseinate is a very efficient emulsifier and dominates the powder surface, even in small concentrations, due to a higher surface activity of protein in water during the drying process (Fäldt and Bergenståhl, 1996). Very little solvent extractable free fat was measured previously by Maher et al. (2014), with powder N (0.4%) having a significantly (P <0.05) lower FF content than powder C (2.3%). There was little evidence of free fat on the surface of these powders. Fractured particles are shown in Figure 4.4c, d, e, f. The advantage of cryo-SEM is that the air vacuoles are easily visible and well preserved. Both powders showed high levels of occluded air in the form of rounded vacuoles (Figure 4.4c, d, arrows), although powder N appeared to have slightly larger vacuoles and thinner cross-walls than powder C. Vacuoles were distributed evenly throughout the powder particles and were mostly in the size range 5 – 50 μm.

Conventional emulsion powders (C) have an uneven distribution of oil droplets spread throughout the powder particles, whereas nanoemulsion powders (N) have an even distribution of much smaller oil droplets. The size of the oil droplets was ~1100 nm for C and ~155 nm for N. The smaller oil droplets in nanoemulsions were more embedded in the matrix and, therefore, less likely to be extracted upon addition of solvent. No evidence of lactose crystals was found in any of the fresh powders. Higher magnifications revealed the powder wall structure at the nano-scale (Figure 4.4e, f, g, h). In powder C, spherical fat droplets, mostly 200 nm to 5 μm in diameter, are seen embedded within the wall matrix (Figure 4.4e, f, arrows). Fat droplets were smaller in powder N (<200 nm diameter) and could only be seen at very high magnifications (Figure 4.4h, arrow).

The powders were also examined by cryo-SEM post- lactose crystallisation (Figure 4.5). At low magnification, agglomeration (or melding) of powder particles was evident (Figure 4.5a, b). Higher magnification revealed the presence of radiating clusters of

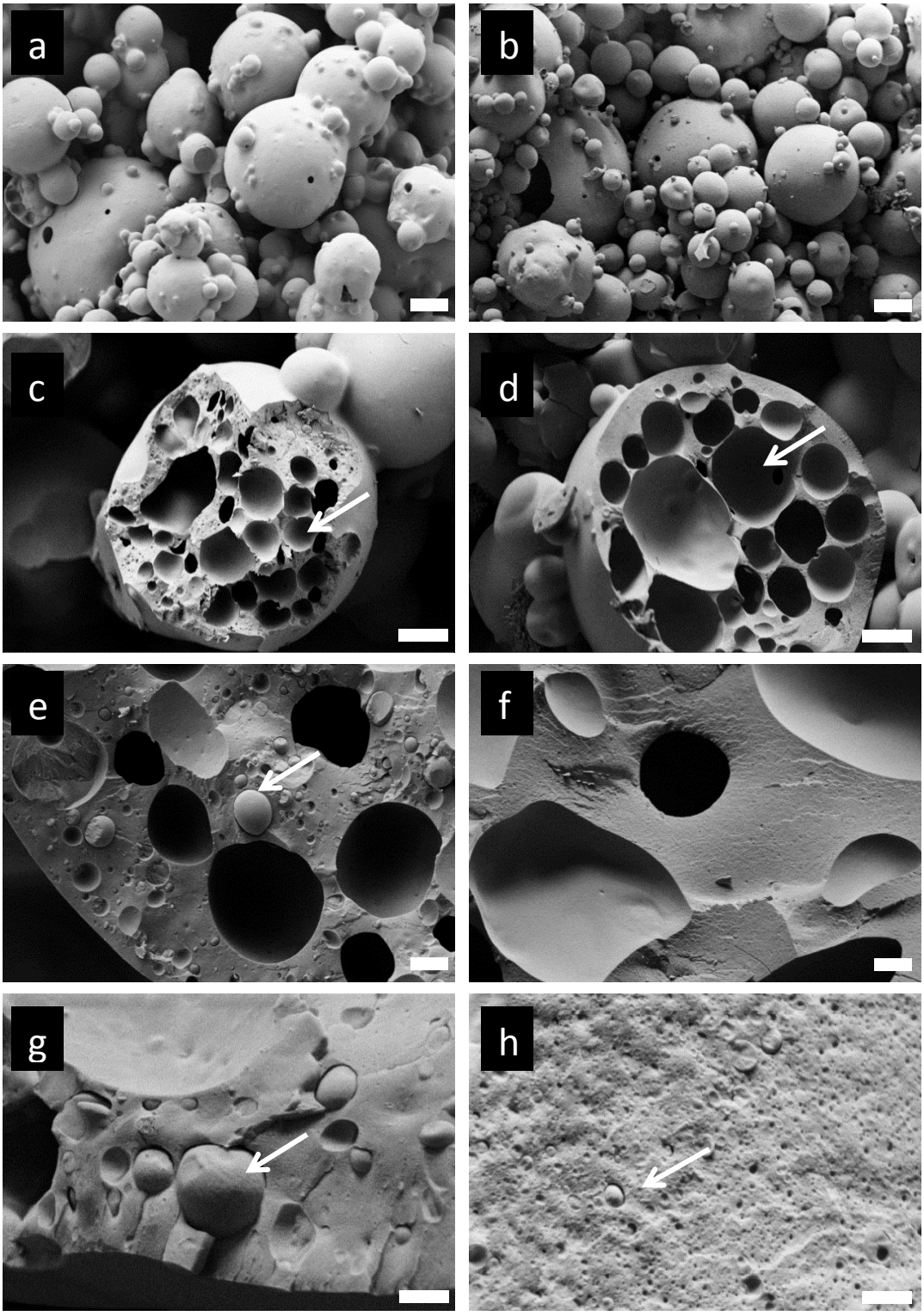

Figure 4.4 Cryo-scanning electron micrographs of control (a,c,e,g) and nanoemulsion (b,d,f,h) powders prior to crystallisation. Images show powder particle surface morphology (a,b) and interior features of fractured particles (c – h). Arrows indicate air vacuoles (c,d) and fat droplets (e,g,h). Scale bars =20 μm (a,b), 10 μm (c,d), 2 μm (e,f) and 500 nm (g,h).

needle-like crystals on powder surfaces (Figure 4.5c, d). Surfaces of lactose-crystallised powders were more uneven with various indentations and holes. The irregular surface, as a result of lactose crystallisation, was also observed by Murrieta-Pazos et al. (2011). Fäldt and Bergenståhl (1996) found using electron spectroscopy for chemical analysis (ESCA), that a protein film dominates the powder surface even after lactose crystallisation. Solid bridges formed between particles after lactose crystallisation, making them agglomerate and cluster, which is in contrast to the more discrete individual particles from the fresh powder. No large crystals were observed on the powder surface. Fäldt and Bergenståhl (1996) postulated that fat globules reduce the size of lactose crystals formed after humidification. Fractured particles showed crystals embedded within the wall and also projecting into vacuoles (Figure 4.5e, f, arrows). There was little evidence of intact spherical fat droplets in either powder, suggesting that they had been disrupted by lactose crystals. This observation is consistent with CLSM results which showed irregular fat pools dispersed within the powder particles (Figure 4.3e), and highlights the advantage of a correlative microscopy approach. Cryo-SEM had the advantages of good structural preservation and high resolution, but could not easily distinguish between fat, protein or amorphous lactose. CLSM revealed the distribution of fat in powders more clearly, while PLM revealed the onset and progress of crystallisation over time and confirmed DVS data which indicated that powders prepared from nanoemulsions crystallised at a faster rate.

Combining cryo-SEM with CLSM and PLM, thus, provided a powerful set of tools for characterising the microstructures of dairy powders.

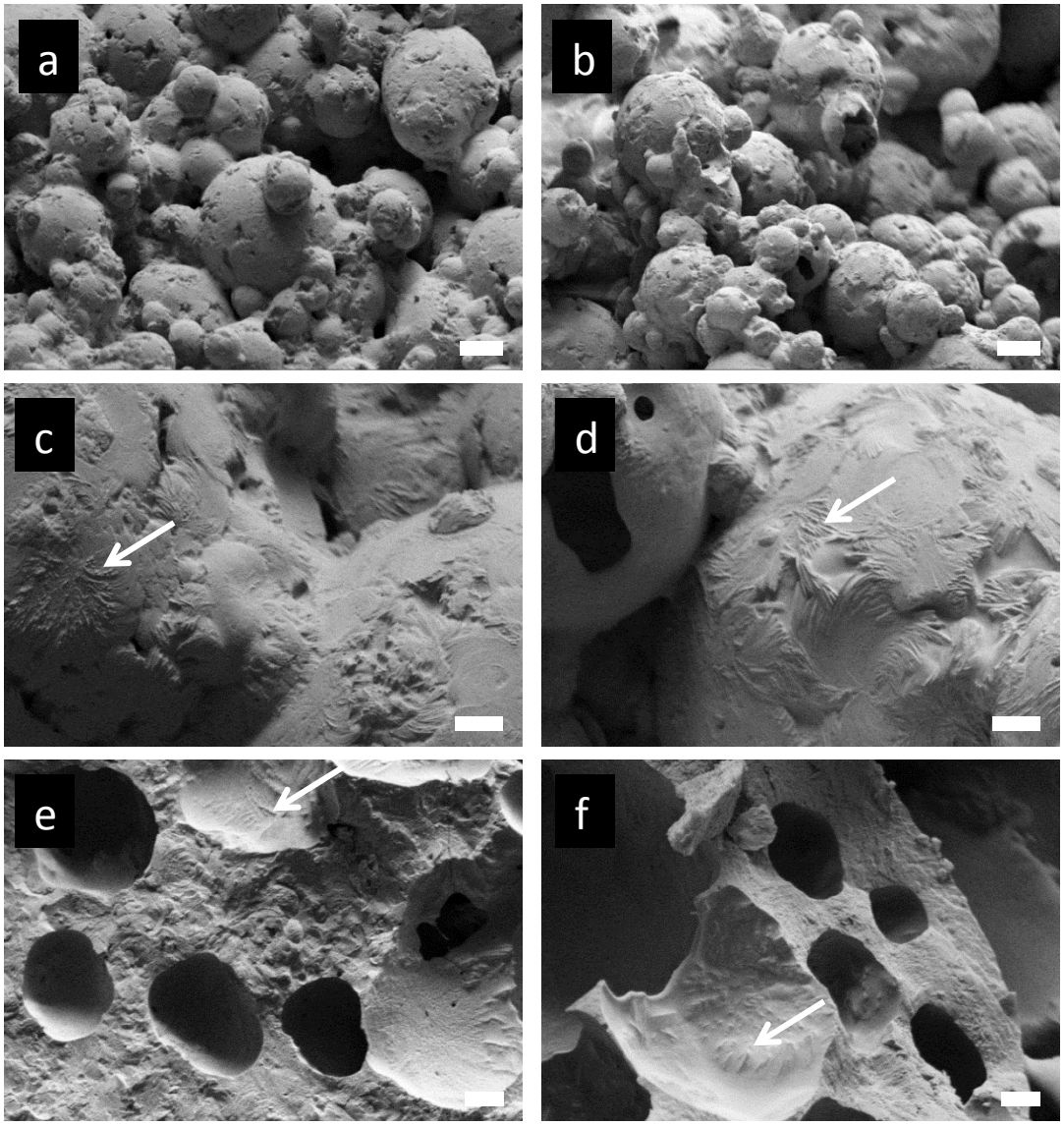

Figure 4.5 Cryo-scanning electron micrographs of control (a,c,e) and nanoemulsion (b,d,f) powders after storage for 4 days at 55% relative humidity showing crystals (arrowed) on the powder surfaces (a,b,c,d) and also interior of fractured particles. Scale bars =20 μm (a,b), 5 μm (c,d) and 2 μm (e,f).

4.4 Conclusions

Powders prepared from nanoemulsions crystallised significantly (P <0.05) more quickly than those prepared from conventional emulsions, as measured using DVS. Rates were calculated with the Avrami equation and crystals were found to form in three dimensions. Evidence of crystal growth was observed with PLM and showed the same trend as results from DVS. CLSM and cryo-SEM show differences in powder structure with powders from nanoemulsions having smaller fat globules that are evenly distributed throughout powder particles. It is suggested that reduced protein in the continuous phase with lactose contributed to observed increase in crystallisation rate in powders prepared from nanoemulsions. Elongated lactose crystals (probably a mixture 5:3 molar ratio of α– and β-lactose) were observed post- humidification at 55% RH, initially at the surface, but progressively occurring within the particles. To the authors' knowledge, there have been no studies on powders prepared from nanoemulsions using CLSM, SEM, or cryo-SEM that show the distribution of fat globules within the particles *in situ*. This paper provides a useful insight into how reducing the FGS of emulsions pre- spray drying impacts upon the physical properties of powders.

Chapter 5 - Levels of pentanal and hexanal in spray dried nanoemulsions

Accepted for publication as:

Maher, P.G., Roos, Y.H., Kilcawley, K.N., Auty, M.A.E., and Fenelon, M.A. 2015. Levels of pentanal and hexanal in spray dried nanoemulsions. *LWT - Food Science and Technology* In Press.

Abstract

Lipid oxidation can adversely alter sensory and nutritional attributes of fats preserved in food powders. The aim of this study was to compare the extent of lipid oxidation in spray dried conventional emulsions and nanoemulsions. Powders containing lactose or lactose/sucrose (7:3) (57.9 g/100 g), sodium caseinate (12.4 g/100 g), sunflower oil (27.9 g/100 g) and water (1.8 g/100 g) were manufactured from control emulsions (D[4, 3] ~1100 nm) and nanoemulsions (FGS ~155 nm). A gas chromatographic headspace solid-phase microextraction (HS-SPME) method was validated and subsequently used to determine levels of volatile compounds pentanal and hexanal as indicators of lipid oxidation in powders stored over a 24 month period. Occluded air was significantly (P <0.05) lower and interstitial air significantly higher (P <0.05) in powders made from nanoemulsions. Levels of pentanal and hexanal were significantly (P <0.05) reduced in powders made from nanoemulsions compared to those from control emulsions, due to their altered structure, lower porosity, and lower free fat. Partial replacement of lactose with sucrose may have also reduced pentanal and hexanal.

5.1 Introduction

Lipid oxidation in food results in altered nutrition, flavour, and texture causing deterioration of quality and reduced shelf life (Sun, Wang, Chen, & Li, 2011). Primary and secondary indicators of lipid oxidation are measured by the food industry to monitor the stability of fat containing products. Hydroperoxides are formed in primary oxidation while low molecular weight aldehydes result from secondary oxidation. Aldehydes limit stability of food products due to undesirable off-flavours (Esterbauer, 1993; Stapelfeldt, Mortensen, & Skibsted, 1997a), therefore their quantification provides a useful method of measuring lipid oxidation.

Different techniques have been used to monitor lipid oxidation in food products. Romeu-Nadal, Castellote, & López-Sabater (2004) developed a static headspace gas chromatography (SHGC) method with a flame ionization detector (FID) to determine volatile compounds (propanal, pentanal and hexanal) in infant formula as indicators of oxidation. Solid-phase microextraction (SPME) was developed in the early 1990's as a quick and accurate method to extract and concentrate volatile organic compounds in various food products (Pawliszyn, 2000). For headspace extraction, SPME utilizes a silica fibre coated with different adsorbent or absorbent materials that are exposed to the headspace of a sample in a specialized headspace (HS) vial under controlled conditions (temperature, agitation and time). Once equilibration is reached, the absorbed/adsorbed compounds are subsequently desorbed from the fibre in the GC inlet at high temperatures and introduced to the column for separation and detection. The technique has been used to determine the quantity of saturated aldehydes, particularly hexanal, in infant formula (Fenaille, Visani, Fumeaux, Milo, & Guy, 2003; García-Llatas, Lagarda, Romero, Abellán, & Farré, 2007; Przygonski, 2003; Romeu-Nadal et al., 2004). It is also used to quantify volatiles produced from milk, cheese, whey powder, and spray dried emulsions (Damerau, Kamlang-ek, Moisio, Lampi, & Piironen, 2014; Tunick, Iondola, & Van Hekken, 2013). Pentanal and hexanal are also breakdown products of *n*-6 polyunsaturated fatty acid from oxidation of sunflower oil-in-water emulsions (van Ruth, Roozen, Posthumus, & Janse, 1999).

Various studies have shown the effect that the molecular environment in oil-in-water emulsions has on lipid oxidation, such as emulsifier type (Fomuso, Corredig, & Akoh,

2002) and droplet charge (Mancuso, McClements, & Decker, 1999; Mei, McClements, & Decker, 1999; Mei, McClements, Wu, & Decker, 1998). Also, it has been reported that droplets of a smaller fat globule size (FGS) give rise to greater levels of lipid oxidation due to an increased surface area for oxygen and free radicals to penetrate the droplets; Fritsch (1994) attributed this effect to a large oil/water interfacial area. Similarly, Nakaya et al. (2005) found that the oxidative stability of soybean oil triacylglycerol (TAG) in oil-in-water emulsions decreased with increasing oil droplet size. In contrast, Osborn and Akoh (2004) showed that oil droplet size had no effect on primary or secondary lipid oxidation. Few studies are available comparing volatiles produced, during prolonged storage (24 months), in powders made from conventional emulsions (FGS >1000 nm) to those from nanoemulsions (FGS <200 nm). Horn, Nielsen, Jensen, Horsewell, & Jacobsen (2012) compared lipid oxidation of fish oil in sodium caseinate stabilized and whey protein isolate stabilized emulsions produced using two-stage valve homogenization and microfluidization. However, the authors did not vary the fat globule size (FGS) of emulsions, but varied the homogenization/microfluidization pressure and number of passes to produce emulsions with the same FGS. No significant differences were found in secondary oxidation of sodium caseinate stabilized emulsions, and the metal chelating ability of sodium caseinate was cited as the main antioxidant in the system. Other studies have shown how non-reducing sugars inhibit lipid oxidation (Sims, Fioriti, & Trumbetas, 1979; Sims, 1994; Ponginebbi, Nawar, & Chinachoti, 1999) and reducing sugars promote lipid oxidation (Yamauchi, Aoki, Sugiuri, Kato, & Ueno, 1982; Yamauchi, Goto, Kato, & Ueno, 1984; Shimada, Fujikawa, Yahara, & Nakamura, 1992). Porosity can also affect lipid oxidation, with Keogh et al. (2001) showing that the degree of casein aggregation has an inverse effect on porosity and, thus, an inverse effect on the amount of lipid oxidation in powders.

The objective of the present study was to investigate the effect of (i) reducing FGS of emulsions prior to spray drying, and (ii) varying sugar composition on pentanal and hexanal development in powders stored for 24 months.

5.2 Materials and Methods

5.2.1 Materials

Four powders were selected from those by produced Maher, Roos, & Fenelon (2014), which were produced from spray drying at the same conditions (inlet/outlet dryer temperatures of 185 °C/90 °C) in a single stage spray dryer (Anhydro F1 Lab, Copenhagen, Denmark). Powders with two different sugar compositions and two different mean fat globule size (FGS) were compared (Table 5.1). Powders consisted of lactose (L) or a 70:30 mixture of lactose: sucrose (S) (57.9 g/100 g), sodium caseinate (12.4 g/100 g), sunflower oil (27.9 g/100 g) and water (1.8 g/100 g). Control emulsions (C) and nanoemulsions (N) were produced using homogenization (17.24 MPa) or microfluidization (100 MPa), respectively, prior to spray drying. Coding system of powders is given in Table 5.1. Immediately after production, all powders were stored in sealed aluminium cans (10 cm wide, 11 cm high) under nitrogen gas (<25 mL/L oxygen in total).

Canned powders were stored for 12 months at 10 °C prior to initial measurement. Following this, triplicate analysis of powders from one experiment were done at each time point over an 8 week period (weeks 0, 1, 2, 4, and 8) at regular and accelerated storage conditions of 20 ºC and 50 ºC. Powders from the three replicate spray drying experiments were stored for 12 further months at 20 °C and were measured at the end of product shelf life (24 months) to determine final aldehyde concentrations.

Table 5.1 Experimental design and coding system of powders

Powder	Sugar	Emulsion type
LC	Lactose	Control
LN	Lactose	Nanoemulsion
SC	Lactose/Sucrose	Control
SN	Lactose/Sucrose	Nanoemulsion

5.2.2 Reagents

Standard solutions of volatile compounds valeraldehyde (pentanal), capronaldehyde (hexanal), and internal standard (IS) ethyl butyrate were made with dissolution of Milli-Q water (Millipore, Le Mont-sur-Lausanne, Switzerland). All standards were purchased from Sigma Aldrich (Sigma-Aldrich, Wicklow, Ireland).

5.2.3 Methods

5.2.3.1 HS-SPME and gas chromatographic – flame ionisation detector (GC-FID)

The procedure was a modified version of that described by García-Llatas, Lagarda, Romero, Abellán, & Farré (2007), who measured the volatile compounds hexanal and pentane in infant formula. Powder (0.5 g) was added to 4,250 μL Milli-Q water and 250 μL IS (1 μg/mL ethyl butyrate in Milli-Q water), i.e., a dilution factor of 10, into an amber La-Pha-Pack 20 mL screw capped vial with a silicone/PTFE liner (Apex Scientific Ltd., Maynooth, Co. Kildare, Ireland).

Sample equilibration was performed for 30 min using a CTC Analytics CombiPal Autosampler (JVA Analytical Ltd, Dublin, Ireland) at 40 ºC with pulsed agitation (4 s and 250 rpm) to favour volatile release. Above 40 ºC the matrix composition may be altered, which would favour hydroperoxide decomposition (Frankel, Hu, & Tappel, 1989).

After equilibration, a 75 μm Carboxen™/polydimethylsiloxane (CAR/PDMS) fibre (Supelco, Bellefonte, PA, USA), previously conditioned at 300 ºC for 1 h, was exposed to the sample headspace (45 min) for analyte extraction using the CTC. The CAR/PDMS was chosen as it has a large capacity, is bipolar and is especially sensitive for small molecules (García-Llatas, Lagarda, Romero, Abellán, & Farré, 2007; Marsili, 1999, 2000). The fibre was retracted and injected *via* a merlin microseal (Sigma Aldrich Ireland Ltd, Arklow, Ireland), on a 1177 injector on a Varian 3800 GC (Aquilant Analytical Services, Clondalkin, Dublin 22, Ireland) using a Supelco SPME inlet (Sigma Aldrich Ireland Ltd) at 250 ºC and desorbed for 5 min (splitless mode for 2 min) with a Zebron ZB-WAX (30 m x 0.25 mm ID x 0.50 μm) column (Phenomenex, Macclesfield, Cheshire, UK). Volatile compounds were separated under the following conditions: carrier gas:

helium 1 mL/min, initial column temperature was 75 ºC held for 8 min, followed by heating to 240 ºC at 30 ºC/min, and holding at 240 ºC for 2 min giving a total run time of 15.5 min. A flame ionization detector (FID) was used at 300 ºC. Quantifying the peak area of each aldehyde and comparing it to that of the IS was achieved using Varian Star Workstation software (Aquilant Analytical Services, Condalkin, Dublin 22, Ireland) allowed the concentration of aldehydes to be determined in μg/mL solution, using the standard curves generated for each aldehyde (Table 5.2). Results were reported as ng aldehyde/g powder. Blank samples (air) were run between each sample to verify that no carryover occurred. Samples were measured in triplicate.

5.2.3.2 Particle density, occluded air and interstitial air

The particle density was measured with a pycnometer (AcuPyc 1340, Micromeritics, Norcross, GA, USA). The method uses helium to measure the particle density of an air-free volume of a known weight of powder (GEA Niro, 2006). The occluded air (V_{OA}), measured in mL/100 g, is defined as the difference between the volume of a given mass of particles and the volume of the same mass of air-free solids. It is calculated from the equation:

$$V_{OA} = \frac{100}{D_{particle}} - \frac{100}{D_{solids}} \quad (5.1)$$

Here, $D_{particle}$ is the measured particle density (g/mL) and D_{solids} is the calculated density of powder solids (g/mL). The interstitial air (V_{IA}), measured in mL/100 g, is defined as difference between the volume of a given mass of particles and the volume of the same mass of 100 x tapped powder. It is calculated from the equation:

$$V_{IA} = \frac{100}{D_{powder}} - \frac{100}{D_{particle}} \quad (5.2)$$

Here, D_{powder} is the powder bulk density (g/mL) measured after 100 taps. Samples were measured in triplicate.

5.2.3.3 Cryo-scanning electron microscopy (Cryo-SEM)

Powders were examined using cryo-SEM. Powders were sprinkled onto the surface of OCT embedding compound (Agar Scientific Ltd, UK) on a slotted aluminium stub. The sample was then plunge-frozen into liquid nitrogen slush (− 210 °C) and transferred under vacuum to the cold stage using the Alto 2500 cryo-transfer device (Gatan Ltd., Oxford, UK). Samples were fractured using a cold scalpel. After sublimation at − 95 °C for 2 min, the sample was cooled to − 125 °C, sputter coated with platinum and transferred to the cold stage for imaging at − 125 °C. Secondary electron images were obtained using a Zeiss Supra 40VP field emission scanning electron microscope (Carl Zeiss SMT Ltd., Cambridge, UK) operating at 2 kV and a working distance of 6 mm.

5.2.4 Statistical analysis

Data for 24 month powder samples, from triplicate spray drying experiments, were transformed prior to analysis by factors $x^{-0.9}$ and $x^{-1.14}$ for pentanal and hexanal, respectively, as recommended by the Box Cox plot on Design Expert® software version 7.1.3 (Stat-Ease Inc., Minneapolis, MN, U.S.A.) to normalise the data. Following transformation, one-way analysis of variance (ANOVA) was used with Minitab 15 (Minitab Ltd., Coventry, UK) to determine significant differences between four different treatments. Fisher's one-way multiple comparison test were used to compare different levels. Results were deemed statistically significant if $P < 0.05$.

5.3 Results and Discussion

5.3.1 HS-SPME GC-FID method optimisation and validation

The optimum settings to maximize the response of pentanal and hexanal from the GC were determined by varying factors such as sample concentration (0.05, 0.1, 0.2, 0.5, and 1.0 g powder/5 g solution (Milli-Q water)), equilibration time (2, 5, 10, 15, 30, and 60 min), and sampling time (5, 15, 30, 45, and 60 min). Optimization of all parameters was performed, using the sample LN, to determine which conditions could maximize the response from the GC. The optimum conditions were found to be a sample concentration

of 0.5 g powder/5 g solution, equilibration time of 30 min, and a sampling time of 45 min. The time taken to run each sample was approximately 1.5 h, with the equilibration time of 30 min, sampling time of 45 min, and 15.5 min of GC analysis.

The method was validated using a similar protocol to Romeu-Nadal et al. (2004) and García-Llatas et al. (2007). The detection limits and quantification limits of pentanal, and hexanal were estimated in accordance with the American Society Guidelines (MacDougall & Crummett, 1980), defined as 3 and 10 times the height of the noise level of blank samples, respectively (Table 2). The detection limit for hexanal of 3.89 ng was similar to the 3.63 ng value reported by García-Llatas et al. (2007) using SPME. The detection limit for pentanal was 0.09 ng (Table 5.2), which was lower than that reported by Romeu-Nadal et al. (2004) using a static headspace method, demonstrating that HS-SPME is a more sensitive technique than HS alone.

A standard curve was produced for both aldehydes (Table 5.2). A constant amount of IS (250 μl, 1000 ng/mL) was added with increasing amounts of aldehydes (0 – 200 ng/mL) to Milli-Q water in each sample (5 mL in total). The peak-area ratio of either aldehyde to that of the IS, as denoted by y, were compared to the concentration of each aldehyde, as denoted by x (Table 5.2). There was a linear increase in peak-area ratio with increasing analyte concentration in the range pentanal (0 – 200 ng/mL), and hexanal (0 – 200 ng/mL). Linearity results are given in Table 5.2 with the high coefficients of determination (r^2) showing a high degree of linearity for each aldehyde.

The precision of the method was expressed as the relative standard deviation (RSD) of 5 replicate measurements. The reproducibility was determined by measuring the same sample 5 times on the same day. Results are shown in Table 5.2 and they meet the acceptable precision standards proposed by Horwitz (1982) for analyte concentrations in the range 10 – 1000 ng/mL for the two volatiles studied.

Quantities of each aldehyde standard equivalent to the measured concentration of each aldehyde from a powder sample were added to powder samples and measured. The quantity of aldehyde measured should in theory be 100% greater than that of the powder sample alone. Recovery percentages were within the acceptable range of 94 and 106% for the two aldehydes (Table 5.2).

Table 5.2 Analytical parameters for pentanal and hexanal.

	Pentanal	Hexanal
Sensitivity		
Detection limit (ng)	0.09	3.89
Quantification limit (ng)	0.30	12.96
Linearity (y = ax + b)		
a: Slope	0.0125	0.0123
b: Intercept	-0.0588	-0.1292
R^2: Determination coefficient	0.994	0.985
Precision		
Repeatability[a] (n =5)	16.3 ± 1.6	49.5 ± 3.5
R.S.D. (%)	9.69	7.01
Reproducibility[b] (n =5)	16.0 ± 1.4	50.8 ± 5.6
R.S.D. (%)	9.03	10.97
Accuracy		
Present (ng/mL)	28.38	105.30
Added (ng/mL)	28.38	105.30
Recovery (n =5)	94.36%	105.24%

y is the area of aldehyde/area of internal standard; x is the amount of aldehyde (ng/mL).

R.S.D. is the relative standard deviation.

[a] Repeatability expressed as mean (ng/mL) ± standard deviation.

[b] Reproducibility expressed as mean (ng/mL) ± standard deviation.

5.3.2 Pentanal and hexanal in powders

The validated method with optimized parameters described above was used to determine the quantities of pentanal and hexanal in each powder sample after long term storage (24 months). A study was first performed where powders from one spray drying experiment, previously stored for 12 months at 10 °C, were analyzed (in triplicate) after accelerated storage for 8 weeks at 20 °C and 50 °C. At week 0 (12 months in total) results show that LN had significantly (P <0.05) lower pentanal and hexanal than LC (Figure 5.1 and 5.2). Odour thresholds for aldehydes in water are 6 ng/mL for pentanal and 13.8 ng/mL for hexanal (Devos, 1990). Pentanal and hexanal levels in this study were converted from ng/g to ng/mL by dividing results by 10 so that a meaningful comparison could be made. Therefore, at week 0 LC is over the odour threshold for pentanal and hexanal, LN is

slightly over the odour threshold for hexanal and under the odour threshold for pentanal. At week 0, SC and SN are below the odour threshold for pentanal and above the odour threshold for hexanal. Powders partially containing sucrose have significantly (P <0.05) lower amounts of pentanal and hexanal than powders without sucrose (SC compared to LC). LN and SN are not significantly different (P >0.05). Powders stored at both temperatures increased significantly (P <0.05) in pentanal and hexanal from week 0 to week 8 (Figure 5.1 and 5.2). At week 8 all powders are above their odour thresholds for pentanal and hexanal, with powders made from nanoemulsions being significantly lower (P <0.05) in pentanal and hexanal than powders made from control emulsions (Figure 5.1 and 5.2). The inhibiting effect of sucrose at week 8 is less significant than week 0.

The influence of increasing powder storage temperature (50 ℃ rather than 20 ℃) over the time period analyzed had little increasing effect on aldehyde level as was expected (Klinkesorn, Sophanodora, Chinachoti, McClements, & Decker, 2005), with only one sample having higher pentanal and hexanal at 50 ℃ than 20 ℃ (SN compared to SC at week 2; Figure 5.1 and 5.2). Other studies report no increase in lipid oxidation at increasing storage temperatures, possibly due to a decrease in solubility of oxygen in oil at increased temperatures leading to reduced rates of autoxidative peroxide formation (Hogan, O'Riordan, & O'Sullivan, 2003), or that increased storage temperatures increase the antioxidant capacities of proteins (whey and casein), thereby improving the oxidative stability of these emulsions (Taylor & Richardson, 1980; Tong, Sasaki, McClements, & Decker, 2000). Sodium caseinate has been shown by various studies to be an effective encapsulant with high encapsulation efficiencies (Fäldt & Bergensåthl, 1995; Fäldt & Bergenståhl, 1996; Kim & Morr, 1996b). As surface fat is more readily oxidized than encapsulated fat (Hardas, Danviriyakul, Foley, Nawar, & Chinachoti, 2000), maximizing encapsulation efficiency helps minimize lipid oxidation.

Powders measured at the end of shelf life (24 months old, stored at 10 ℃ for 12 months followed by 20 ℃ for 12 months) from three separate spray drying experiments were analyzed for pentanal and hexanal. The quantities of pentanal and hexanal were significantly (P <0.05) lower in powders from nanoemulsions (LN and SN) compared to powders from control emulsions (LC and SC) (Table 5.3), showing the beneficial effect

of reducing FGS of emulsions pre spray drying on lipid oxidation. Similar to week 8 in the first study, although mean values were lower, there was no significant difference (P >0.05) between powders containing sucrose and powders not containing sucrose. Aldehyde levels in this study are above odour thresholds for all powders.

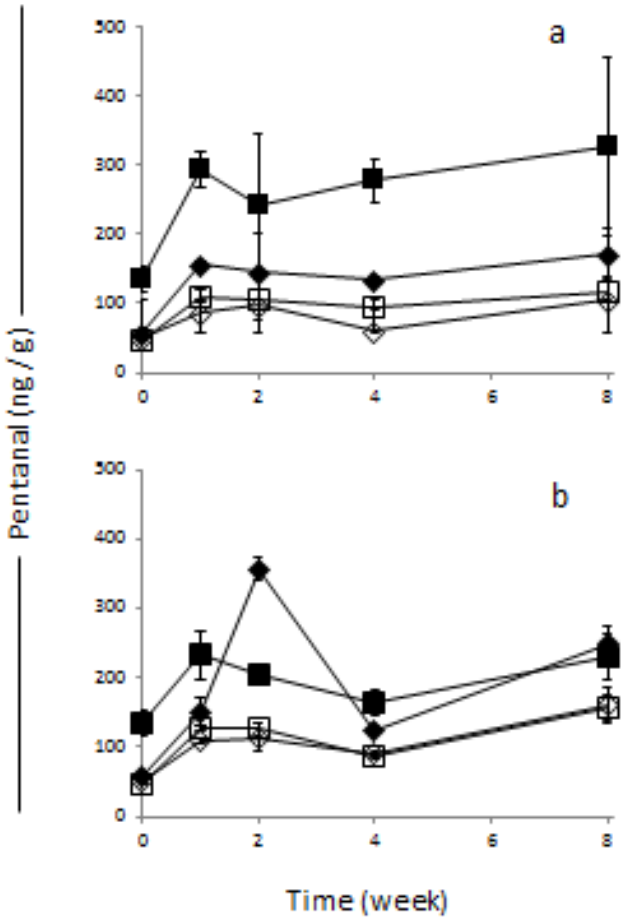

Figure 5.1 Pentanal content of powders (LC ■, LN □, SC⧫, SN ◊) stored at (a) 20 ℃ and (b) 50 ℃ for 8 weeks after prior storage at 10 ℃ for 12 months. Values presented are the mean ± standard deviation of three replicates from one spray drying experiment.

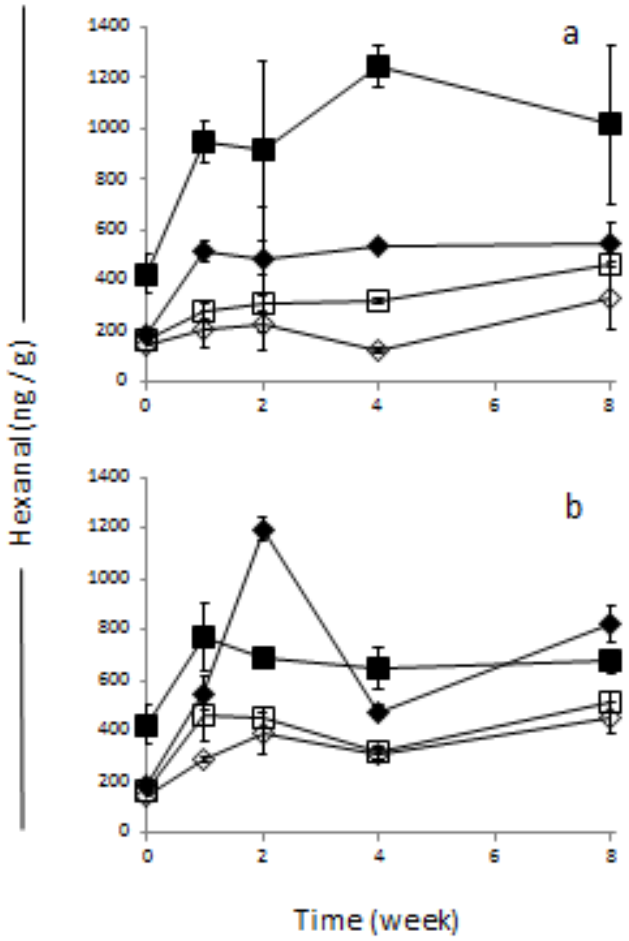

Figure 5.2 Hexanal content of powders (LC ■, LN □, SC⧫, SN ◊) stored at (a) 20 ℃ and (b) 50 ℃ for 8 weeks after prior storage at 10 ℃ for 12 months. Values presented are the mean ± standard deviation of three replicates from one spray drying experiment

5.3.3 Effect of varying sugar composition

The effect of the partial replacement of 30% of the lactose with sucrose was studied (Table 5.1). Sucrose (non-reducing sugar) has been shown to reduce lipid oxidation of linoleic acid in oil-in-water emulsions stabilized by Tween-20 (Ponginebbi et al., 1999), and reduce oxidation of safflower in oil-in-water emulsions stabilized by an anionic surfactant (Sims, 1994; Sims et al., 1979). The main reason for the inhibiting effect of sucrose in oil-in water emulsions is due to its free radical scavenging ability, (McClements & Decker, 2000).

In the first study, at week 0 the presence of sucrose in powders caused a significant (P <0.05) decrease in pentanal and hexanal. Although pentanal and hexanal levels increased

from week 0 to week 8 when sucrose was present, the antioxidant effect of sucrose-containing powders compared to non-sucrose-containing powders was not present at week 8. After 24 months, results showed that there was no significant (P >0.05) difference between SC & LC, and SN and LN when using one-way ANOVA. However, it was noticed that each comparative batch (i.e. comparing batches from trial 1 to each other, trial 2 to each other etc.) showed reduced levels of aldehydes for SC compared to LC (results not shown), thereby showing that there may be some reducing effect. Pentanal and hexanal were lower in SN compared to LN, however not significantly (P >0.05) lower, indicating that FGS reduction had a greater effect on aldehyde reduction than sugar composition.

Table 5.3 Mean pentanal and hexanal contents (ng/g) of powders after 24 months storage (12 months each at 10 and 20 °C), and mean particle density, occluded air, and interstitial air in powders from triplicate spray drying trials.

Sample	Pentanal ng/g	Hexanal ng/g	$D_{particle}$ g/100 mL	V_{OA} mL/100 g	V_{IA} mL/100 g
P-value	(0.045)	(0.005)	(0.001)	(0.001)	(0.001)
LC	400 [a]	717 [a]	0.77 [b]	52.6 [b]	146.6 [c]
LN	178 [b]	317 [b]	0.82 [a]	44.7 [c]	161.5 [a]
SC	324 [ab]	514 [a]	0.67 [c]	71.7 [a]	143.4 [d]
SN	184 [b]	298 [b]	0.77 [b]	52.8 [b]	152.3 [b]

[a-b] Values within a column not sharing a common letter differ significantly (P <0.05) by one-way ANOVA.

5.3.4 Porosity of powders

The particle density of powders from nanoemulsions were significantly (P <0.05) higher compared to control powders i.e. comparing LC to LN and SC to SN (Table 5.3). This led

to powders with significantly (P <0.05) lower occluded air (V_{OA}) and higher interstitial air (V_{IA}). High degrees of V_{OA} can be seen in Figure 5.3a (LC) and Figure 5.3b (LN). Occluded air (porosity) is affected by factors such as atomization conditions, total solids concentration, and foaming characteristics of the concentrate. Sodium caseinate has a high foaming capacity (Sánchez & Patino, 2005) meaning that air is easily incorporated into the feed before drying. Oil reduces the foaming of concentrates and a pneumatic two-fluid nozzle atomizer (as used in this study) is expected to give higher porosity than either disc or pressure nozzle types. Keogh et al. (2001) studied the effect of varying the porosity of powders on the oxidation of fish oil. The porosity was varied by using different caseins with different degrees of aggregation; sodium caseinate (low aggregation), calcium caseinate (medium aggregation), and skimmed milk powder (high aggregation). High aggregation led to low porosity and low aggregation led to high porosity, with increasing porosity leading to significantly increased levels of fish oil oxidation. The high porosity values (>40 mL/100 g) in the current study (Table 5.3) are expected for a protein with low aggregation and high foaming ability (sodium caseinate), and a two-fluid nozzle type atomizer in a single stage spray dryer with a high outlet temperature (90 °C). The results show that pentanal and hexanal levels are significantly (P <0.05) reduced when porosity is reduced (i.e. nanoemulsion powders). Moreover, powders containing sucrose (SC and SN) had significantly (P <0.05) lower particle density and significantly (P <0.05) higher porosity than powders with lactose (LC and LN) i.e., comparing SC to LC and SN to LN (Table 5.3). This is correlated with increased powder size, D[4,3], (83.9, 79.4, 89.1, and 86.8 μm for LC, LN, SC, and SN, respectively), in powders containing sucrose as found by Maher et al. (2014). Although SC and SN had significantly higher porosity, this was generally not (except pentanal for SN compared to LN) correlated with increased aldehyde level, suggesting that sucrose may have some inhibiting effect on oxidation. Interstitial air (V_{IA}) increased significantly (P <0.05) for powders made from nanoemulsions and decreased significantly (P <0.05) for powders containing sucrose. The oxygen in the V_{IA} may have interacted with the powder free fat over time causing increased oxidation for conventional emulsions as they had higher free fat contents (3.0, 0.6, 2.2, and 0.4 g/100 g for LC, LN, SC, and SN, respectively; Maher et al., 2014).

5.3.5 Cryo-SEM

The structural differences between powders produced from control emulsions (LC) and nanoemulsions (LN) are shown in Figure 5.3a, b, c. Figure 5.3a (LC) shows large oil droplets of size ~ 1 μm randomly distributed throughout the powder particle. Figure 5.3b (LN) shows that oil droplets are not visible at the same magnification as Figure 5.3a. A higher magnification image of LN is shown in Figure 5.3c showing the smaller oil droplets throughout the powder particle. These droplets in Figure 5.3c are tightly embedded in the powder, and may be better protected against oxygen diffusion through the powder. Turchiuli et al. (2005) showed well dispersed fat droplets within the powder matrix reduces the oxidation of vegetable oil, measured by quantification of conjugated dienes. Increasing levels of free fat may make powders more susceptible to lipid oxidation (Sharma, Jana, & Chavan, 2012). As mentioned previously, Maher et al. (2014) showed that solvent-extractable free fat was lower for LN and SN (0.6 g/100 g and 0.4 g/100 g) than LC and SC (3.0 g/100 g and 2.2 g/100 g). This result is similar to Soottitantawat, Yoshi, Furata, Ohkawara, & Linko (2003) who showed that reducing the FGS of emulsions pre spray drying produces powders with reduced free fat and higher retention of encapsulated volatile compounds. The present study showed that increasing levels of solvent-extractable free fat in powders contributed to increased pentanal and hexanal. In this study, reduced powder particle porosity (with entrapped air being ~210 mL/L oxygen) and reduced free fat are thought to lower the rate of development of pentanal and hexanal during long term storage.

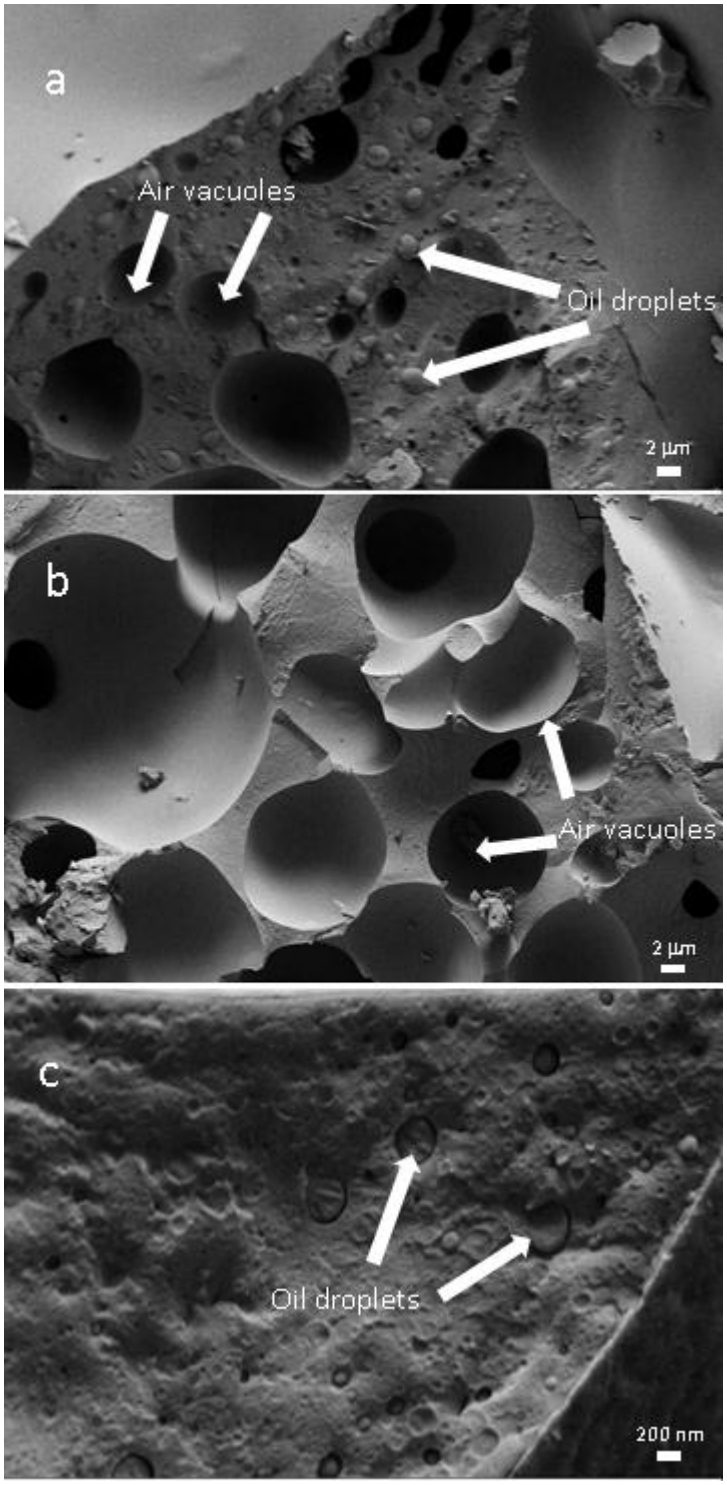

Figure 5.3 Cryo-scanning electron micrograph showing distribution of oil droplets and air vacuoles in powders LC (a) and LN (b & c).

5.4 Conclusions

HS-SPME has been shown to be a suitable technique for measuring pentanal and hexanal levels in fat-filled powders. Reducing FGS prior to spray drying caused a significant (P <0.05) decrease in porosity of powders, contributing to a reduction in pentanal and hexanal. Lower levels of pentanal and hexanal in powders made from nanoemulsions (LN and SN) were also attributed to lower free fat and smaller (~155 nm) oil droplets that were more embedded in the powder matrix. After 12 months storage at 10 °C, powders from nanoemulsions (LN) had pentanal levels below the odour threshold whereas powders from conventional emulsions had pentanal levels above the odour threshold. All powders increased in pentanal and hexanal content after 8 weeks storage and were above the odour thresholds for pentanal and hexanal. Results also indicate that partial replacement of lactose with sucrose may have an antioxidant effect. Overall, these results have shown that reducing the FGS of emulsions pre spray drying caused a significant (P <0.05) reduction in concentration of pentanal and hexanal in powders upon long term storage (24 months).

Chapter 6 - Overall discussion

6.1 Nanoemulsions

This thesis examined nanoemulsions in both liquid and powder forms. In the first part of the study (Chapter 2), liquid nanoemulsions were investigated. Nanoemulsions (30% w/w) were produced following optimisation of the carbohydrate/protein (lactose or trehalose/β-casein) continuous phase. A mixture design was created with design of experiments (DOE) software to create formulations (20% w/w) with β-casein (0 – 10% w/w) and lactose/trehalose (10 – 20% w/w) (Table 2.1). Factors such as viscosity and glass transition temperature of maximal freeze-concentration (T_g') were measured, and the optimisation function in the mixture design software was used to find the quantities of lactose and trehalose at fixed protein concentrations (2.5%, 5%, 7.5%, and 10% w/w) that maximise and minimise viscosity and T_g' (Table 2.2). Sunflower oil (10% w/w) was added to these optimised formulations and microfluidised at 67 MPa to produce nanoemulsions.

In carbohydrate/protein mixtures, viscosity increased exponentially with increasing protein content, due to increased interactions between hydrated protein molecules (Boye et al., 1997), and the ability of protein molecules to absorb and swell (Damodaran, 1997) (Table 2.1; Figure 2.1). T_g' decreased with increasing protein content because of increased viscosity resulting in retarded ice formation, leaving more unfrozen water to cause a plasticising effect (Roos and Karel, 1991a) (Table 2.1; Figure 2.2). The ice melting temperature at maximal freeze-concentration (T_m') increased with increasing protein content also due to retarded ice formation at increased viscosity (Table 2.1; Figure 2.3). These mixtures were freeze dried and their glass transition temperature (T_g) measured, with T_g of powders increasing with increasing protein content (Table 2.1; Figure 2.4). Generally, high T_g' in a liquid system corresponds to high T_g (post-dehydration), and low T_g' corresponds to low T_g. Therefore, the quantity of protein, in either liquid or dehydrated systems, strongly affects the glass transition temperature of that system.

For emulsion systems, the mean particle size increased significantly (P <0.05) with increasing protein content (Table 2.2; Figure 2.5), possibly due to the layering effect of increasing protein according to self-consistent field (SCF) theory where the protein concentration goes above a certain threshold value causing multilayer condensation of

self-associating protein onto the oil droplet surface (Dickinson, 1997a). Similar to carbohydrate/protein mixtures, T_g' of nanoemulsions decreased with increasing protein content and viscosity of nanoemulsions increased, with values being greater than mixture viscosity due to the higher solids content following the addition of sunflower oil (Table 2.2; Figure 2.7). Stability of nanoemulsions increased with increasing protein content (Table 2.2; Figure 2.8) due to increased viscosity (Table 2.2; Figure 2.6). Stokes' law shows that particles suspended in higher viscosity systems separate at lower rates Nanoemulsions are more stable to creaming/sedimentation on storage compared to conventional emulsions, due to the effects of Brownian motion being stronger than gravitational forces. Experimental separation velocity compared well with those calculated from Stokes' equation, validating the emulsion stability results (Table 2.2).

Overall, an ideal emulsion should have a low viscosity, mean particle size and separation rate, and a high T_g' which corresponds to a high T_g when dried. A fine balance can be achieved whereby a low viscosity, highly stable emulsion system can be produced, which when dried is not susceptible to physico-chemical deteriorative changes associated with low glass transition temperature. Optimisation of the continuous phase using mixture design software is a useful tool in designing stable nanoemulsion systems. It can also be used to design systems with certain exact desired characteristics.

6.2 Physical properties of nanoemulsions

The second part of this thesis investigated the properties of powders produced from spray drying nanoemulsions and compared them to powders from spray dried conventional emulsions (Chapters 3-5). As described in Chapter 3, emulsions/nanoemulsions were heat treated (100 °C, 30 s), homogenised (17 MPa) or microfluidised (100 MPa), and spray dried at two different outlet temperatures (80 and 90 °C). Powders comprised of (on a dry basis) ~60% w/w carbohydrate (lactose or lactose/sucrose), ~29% w/w sunflower oil, and ~11% w/w sodium caseinate. The effect of varying the water content and sugar composition of these powders was also investigated (Table 3.1). The post-homogenisation emulsions (Table 3.2) and reconstituted powders (Table 3.3) showed that nanoemulsions had significantly (P <0.05) smaller (~155 nm) FGS than conventional emulsions (~1100 nm), due to the higher pressure used and higher shearing forces from

microfluidisation. The smaller FGS of nanoemulsions gave them greater stability to separation and hence lower creaming rates (0.2 compared to 0.54 mm/d) as expected from Stokes' law (Table 3.3). Maintaining a FGS <1 μm is important to increase emulsion stability and reduce free fat in the finished powder (Sheu and Rosenberg, 1995; Hogan et al., 2001a). In Chapter 3, powders from nanoemulsions had significantly (P <0.05) lower free fat than powders from conventional emulsions (Table 3.4), possibly due to the greater stability of nanoemulsions during the spray drying process, and oil droplets (~155 nm) being more embedded in the powder matrix making fat less extractable upon the addition of solvent. Similar results were reported by Millqvist-Fureby (2003) and Jafari et al. (2008a). Powders dried at a higher outlet temperature (90 °C) had significantly (P <0.05) lower water content, water activity, powder particle size, and tapped bulk density (Table 3.5).

DSC results showed the plasticising effect of water and sucrose, resulting in powders with reduced T_g (Table 3.5). Sucrose was found to delay crystallisation of lactose as no crystallisation peak was observed upon heating (Table 3.5). With no sucrose present, lactose crystallised at significantly (P <0.05) lower temperatures in powders made from nanoemulsions compared to powders made from conventional emulsions (Table 3.5). The authors have postulated that this is due to less protein present in the continuous phase with lactose, as more protein is required to stabilise fat droplets of a smaller size (greater surface area). Other studies have shown how increasing protein content of emulsions delayed lactose crystallisation (Thomas et al., 2004b; McCarthy et al., 2013). DVS results showed that powders containing sucrose (lactose: sucrose, 70:30) caused lactose to crystallise at higher humidity than powders with lactose as the only carbohydrate (Figures 3.1 & 3.2). This is similar to the DSC result and shows that the presence of sucrose interferes with the crystallisation of lactose, whether it is induced by high temperature or humidity.

These results show that by changing the FGS of emulsions pre- spray drying, the physical properties of powders of the same composition can be altered. Powders made from nanoemulsions, while exhibiting no difference in T_g, had lower T_{cr} than powders made from conventional emulsions, making them more stable during storage. The partial replacement of lactose with a small quantity of sucrose had the negative effect of reducing the T_g which makes the powder more likely to stick to the spray dryer wall

during processing, reducing yield. However, these powders have the advantage of better stability during storage because lactose is less likely to crystallise when sucrose is present.

6.3 Microstructure and its effect on lactose crystallisation

A more detailed investigation of lactose crystallisation was studied in Chapter 4, where a comparison of crystallization kinetics and powder microstructure (pre- and post-crystallisation) was made. A nanoemulsion powder was compared to a conventional emulsion powder in a DVS at 25 °C and 55% RH, and crystallisation kinetics were modelled with the Avrami equation (Avrami, 1939, 1940) (Figure 4.1). Crystals formed in three dimensions (based on Avrami exponent, n) with crystallisation rates (Avrami rate constant, k) being 1.2×10^{-7} min^{-1} for the nanoemulsion powder compared to 1.1×10^{-8} min^{-1} for the conventional emulsion powder (Table 4.1). Polarised light microscopy was used to visually observe crystal growth in powders stored in a desiccator over a saturated salt solution of $Mg(NO_3)_2$ (55% RH) for 4 days at 20 °C. The same trend was observed as in DVS, with lactose crystals forming more quickly in nanoemulsion powders (Figure 4.2). Results are similar to those from DSC in Chapter 3 and are explained by the same reasoning. These results show not only the importance of the total amount of protein, but the significance of the amount of protein in the continuous phase which affects lactose crystallisation rate i.e. the more protein in the continuous phase, the slower the lactose crystallisation rate. Avrami rate constant values (k) were lower than for pure amorphous lactose (0% protein) (Schmidt et al., 1999) and higher than in SMP (~35% protein) (Jouppila et al., 1997), demonstrating that increased protein content results in reduced rates of lactose crystallisation.

Confocal laser scanning microscopy (CLSM) (Figure 4.3) and cryo-scanning electron microscopy (cryo-SEM) (Figures 4.4 & 4.5) techniques showed the even distribution of smaller oil droplets through powders made from nanoemulsions. Fresh powders had a smooth surface and showed no evidence of lactose crystals with very little surface fat observed. After humidification at 55% RH, elongated lactose crystals were observed at the powder surface and moving progressively towards the powder interior. Nanoemulsion

powders appeared to have a stronger structure with more intact air vacuoles and less rupturing of fat droplets.

To the authors' knowledge, there are no studies on powders prepared from nanoemulsions which use CLSM, SEM, or cryo-SEM to observe the fat globule distribution within particles *in situ*. The results in this thesis (Chapter 4) show that correlative microscopy techniques provide a useful insight into how reducing the FGS of emulsions, pre- spray drying, affect physical properties of powders. Other studies have shown that increasing protein content delays lactose crystallisation, but this study is unique in the that the systems have the same composition and only differ in terms of microstructure caused by different homogenisation pressures pre- spray drying. Increased rates of lactose crystallisation are negative for storage stability; however, one benefit is that powders appeared less ruptured than conventional emulsion powders following crystallisation. One potential area for future investigation is examining the stability of vitamins, both water- and fat-soluble, in powdered nanoemulsion systems and comparing them to those from powdered conventional emulsions both pre- and post- lactose crystallisation.

6.4 Pentanal and hexanal produced in nanoemulsion powders

In Chapter 5, the effect of reducing the fat globule size (FGS) of oil droplets and varying the sugar composition in powders on lipid oxidation was studied (Table 5.1). A headspace-solid phase microextraction (HS-SPME) method was validated (Table 5.2), and used to determine the aldehyde (pentanal and hexanal) content in powders stored over 24 months (end of shelf life). Results showed that reducing the FGS caused a significant (P <0.05) reduction in pentanal and hexanal levels in powders upon storage (Table 5.3). This may be due to significantly (P <0.05) lower porosity (V_{OA} from pycnometer), significantly (P <0.05) lower free fat, and because smaller oil droplets are more embedded in the powder matrix (Table 5.3). Cryo-SEM images (Figure 5.3) show the high degree of porosity in powders, verifying the results measured from the pycnometer (>40 mL/100 g). Some evidence of reduced lipid oxidation was observed when lactose was partially replaced by sucrose (Table 5.3). Sucrose is a free radical scavenger (McClements and Decker, 2000) and has been shown in other studies to reduce lipid oxidation (Sims et al., 1979; Sims, 1994; Ponginebbi et al., 1999). These results show that

reducing the FGS of emulsions pre- spray drying caused a significant (P <0.05) reduction in concentration of pentanal and hexanal in powders upon long term storage (24 months), and that HS-SPME is a suitable technique to monitor lipid oxidation. Pentanal and hexanal levels were above their respective odour thresholds (Devos, 1990), therefore, highlighting the important impact of reducing FGS on lowering aldehyde levels to minimise negative sensory attributes occurring upon storage.

6.5 Overall conclusions

Overall, this research shows the impact that reducing the FGS has on emulsions and spray dried emulsions, and how the composition of the continuous phase is particularly important. Nanoemulsions can be designed to have optimal properties by using mixture design software which is of benefit for formulation of foods with certain desired characteristics. Nanoemulsions have reduced creaming rates compared to conventional emulsions, due to their smaller size. During atomisation, these smaller oil droplets are more stable to rupture leading to less free fat in the resulting powder, making them less likely to oxidise and improving their flowability and rehydration properties. Powders made from spray drying nanoemulsions also have a significantly altered microstructure, which has advantages and disadvantages. For storage stability, the main advantage is that lipid oxidation is reduced (due to lower free fat and lower porosity); however, a disadvantage is that the rate of lactose crystallisation is increased (due to less protein in continuous phase). These increased rates can be negated by the addition of some sucrose. Partial replacement of lactose with sucrose reduces T_g, which is negative for spray drying (in terms of powder stickiness), but delays lactose crystallisation and reduces lipid oxidation in powders, which is beneficial for long term storage of powders. This research provides a comprehensive account of the fundamental properties of nanoemulsions in liquid and dried forms.

Areas of potential future work include the following topics:

- Investigate stability of water-soluble and fat-soluble vitamins in dried nanoemulsion systems.
- Compare different proteins as emulsifiers for nanoemulsions.

- Further analyse crystallisation kinetics of conventional emulsion/nanoemulsion powders using a variety of sugars.
- Analyse surface composition and topography of nanoemulsion powders using X-ray Photoelectron Spectroscopy and Atomic Force Microscopy.
- Investigate oxidation of nanoemulsion powders using a variety of less stable oils (fish oils, PUFA's, etc.) for short term stability studies.

References

Abdelwahed, W., Degobert, G., Stainmesse, S., Fessi, H., (2006). Freeze-drying of nanoparticles: formulation, process and storage considerations. *Advanced Drug Delivery Reviews* 58(15), 1688-1713.

Abramovič, H., Butinar, B., Nikolič, V., (2007). Changes occurring in phenolic content, tocopherol composition and oxidative stability of Camelina sativa oil during storage. *Food Chemistry* 104(3), 903-909.

Acosta, E., (2009). Bioavailability of nanoparticles in nutrient and nutraceutical delivery. *Current Opinion in Colloid and Interface Science* 14(1), 3-15.

Aguilar, C.A., Ziegler, G.R., (1994). Physical and microscopic characterization of dry whole milk with altered lactose content. 1. Effect of lactose concentration. *Journal of Dairy Science* 77(5), 1189-1197.

Aguilera, J.M., del Valle, J.M., Karel, M., (1995). Caking phenomena in amorphous food powders. *Trends in Food Science & Technology* 6(5), 149-155.

Akoh, C.C., Min, D.B., (2008). *Food lipids: chemistry, nutrition, and biotechnology*. Marcel Decker Inc., New York, USA.

Al-Mulla, A., (2007). Isothermal crystallization kinetics of poly(ethylene terephthalate) and poly(methyl methacrylate) blends. *eXPRESS Polymer Letters* 1(6), 334-344.

Alamilla-Beltrán, L., Chanona-Pérez, J., Jiménez-Aparicio, A., Gutiérrez-López, G., (2005). Description of morphological changes of particles along spray drying. *Journal of Food Engineering* 67(1), 179-184.

Allen, J.C., Wrieden, W.L., (1982a). Influence of milk proteins on lipid oxidation in aqueous emulsion: I. Casein, whey protein and α-lactalbumin. *Journal of Dairy Research* 49(02), 239-248.

Allen, J.C., Wrieden, W.L., (1982b). Influence of milk proteins on lipid oxidation in aqueous emulsion: II. Lactoperoxidase, lactoferrin, superoxide dismutase and xanthine oxidase. *Journal of Dairy Research* 49(02), 249-263.

Anderson, D., Stoddart, J., (1966). Studies on uronic acid materials: Part XV. The use of molecular-sieve chromatography in studies on acacia senegal gum (Gum Arabic). *Carbohydrate Research* 2(2), 104-114.

Anderson, D., Howlett, J., McNab, C., (1985). The amino acid composition of the proteinaceous component of gum arabic (Acacia Senegal (L.) Willd.). *Food Additives & Contaminants* 2(3), 159-164.

Anton, N., Vandamme, T.F., (2011). Nano-emulsions and micro-emulsions: Clarifications of the critical differences. *Pharmaceutical Research* 28, 978-985.

Arvanitoyannis, I., Blanshard, J.M.V., (1994). Rates of crystallization of dried lactose-sucrose mixtures. *Journal of Food Science* 59(1), 197-205.

Augustin, M.A., Hemar, Y., (2009). Nano-and micro-structured assemblies for encapsulation of food ingredients. *Chemical Society Seviews* 38(4), 902-912.

Auty, M.A.E., Twomey, M., Guinee, T.P., Mulvihill, D.M., (2001). Development and application of confocal scanning laser microscopy methods for studying the distribution of fat and protein in selected dairy products. *Journal of Dairy Research* 68, 417-427.

Avrami, M., (1939). Kinetics of phase change. I. General theory. *Journal of Chemical Physics* 7, 1103-1112.

Avrami, M., (1940). Kinetics of Phase Change II. Transformation-Time Relations for Random Distribution of Nuclei. *Journal of Chemical Physics* 8, 212-224.

Baranauskienė, R., Venskutonis, P.R., Dewettinck, K., Verhé, R., (2006). Properties of oregano (*Origanum vulgare L.*), citronella (*Cymbopogon nardus G.*) and marjoram (*Majorana hortensis L.*) flavors encapsulated into milk protein-based matrices. *Food Research International* 39(4), 413-425.

Barbosa-Cánovas, G.V., Juliano, P., (2005). Physical and chemical properties of food powders., In: Onwulata, C.I. (Ed.), *Encapsulated and powdered foods*. Taylor and Francis Group, LLC., New York, NY, USA, pp. 39-71.

Barrefors, P., Granelli, K., Appelqvist, L.A., Bjoerck, L., (1995). Chemical characterization of raw milk samples with and without oxidative off-flavor. *Journal of Dairy Science* 78(12), 2691-2699.

Beatus, Y., Raziel, A., Rosenberg, M., Kopelman, I., (1985). Spray-drying microencapsulation of paprika oleoresin. *Lebensmittel-Wissenschaft und Technologie* 18, 28-34.

Bellows, R., King, C., (1973). Product collapse during freeze drying of liquid foods. *AIChE Symposium Series* 69, 33-41.

Bhandari, B.R., Dumoulin, E., Richard, H., Noleau, I., Lebert, A., (1992). Flavor encapsulation by spray drying: application to citral and linalyl acetate. *Journal of Food Science* 57(1), 217-221.

Bhandari, B.R., Datta, N., Howes, T., (1997). Problems associated with spray drying of sugar-rich foods. *Drying Technology* 15(2), 671-684.

Bhandari, B.R., Howes, T., (1999). Implication of glass transition for the drying and stability of dried foods. *Journal of Food Engineering* 40(1-2), 71-79.

Bhugra, C., Rambhatla, S., Bakri, A., Duddu, S.P., Miller, D.P., Pikal, M.J., Lechuga-Ballesteros, D., (2007). Prediction of the onset of crystallization of amorphous sucrose below the calorimetric glass transition temperature from correlations with mobility. *Journal of Pharmaceutical Sciences* 96(5), 1258-1269.

Biliaderis, C.G., Lazaridou, A., Mavropoulos, A., Barbayiannis, N., (2002). Water plasticizing effects on crystallization behaviour of lactose in a co-lyophilized amorphous polysaccharide matrix and its relevance to the glass transition. *International Journal of Food Properties* 5(2), 463-482.

Bimbenet, J., Bonazzi, C., Dumoulin, E., (2002). Drying of foodstuffs. *Drying 2002 - In: Proceeding of the 13th International Spray Drying Symposium*, 64-80.

Bowen, W., (1938). Spray drying. *Industrial & Engineering Chemistry* 30(9), 1001-1002.

Boye, J.I., Ma, C.Y., Harwalkar, V.R., (1997). Thermal denaturation and coagulation of proteins., In: Damodaran, S., Paraf, A. (Eds.), *Food proteins and their applications*. Marcel Dekker Inc., New York, NY, USA, pp. 25-56.

Buffo, R., Reineccius, G., (2000). Optimization of gum acacia/modified starch/maltodextrin blends for the spray drying of flavors. *Perfumer & Flavorist* 25(4), 45-54.

Buma, T., (1971). Free fat and physical structure of spray-dried whole milk. 5. Cohesion Determination, influence of particle size, moisture content and free-fat content. *Netherland Milk Dairy Journal* 25, 107-122.

Burnett, D., Thielmann, F., Booth, J., (2004). Determining the critical relative humidity for moisture-induced phase transitions. *International Journal of Pharmaceutics* 287, 123-133.

Burnett, D., Thielmann, F., Sokoloski, T., Brum, J., (2006). Investigating the moisture-induced crystallization kinetics of spray-dried lactose. *International Journal of Pharmaceutics* 313, 23-28.

Cahn, J.W., (1956). Transformation kinetics during continuous cooling. *Acta Metallurgia* 4, 572-575.

Caric, M., Kalab, M., (1987). Effects of drying techniques on milk powders quality and microstructure: a review. *Food Microstructure* 6, 171-180.

Chacon, M., Molpeceres, J., Berges, L., Guzman, M., Aberturas, M., (1999). Stability and freeze-drying of cyclosporine loaded poly (D, L lactide–glycolide) carriers. *European Journal of Pharmaceutical Sciences* 8(2), 99-107.

Chaiyasit, W., Elias, R.J., McClements, D.J., Decker, E.A., (2007). Role of physical structures in bulk oils on lipid oxidation. *Critical Reviews in Food Science and Nutrition* 47(3), 299-317.

Chen, H., Weiss, J., Shahidi, F., (2006). Nanotechnology in nutraceuticals and functional foods. *Food Technology* 3, 30-36.

Choi, M., Briancon, S., Andrieu, J., Min, S., Fessi, H., (2004). Effect of freeze-drying process conditions on the stability of nanoparticles. *Drying Technology* 22(1-2), 335-346.

Christensen, K., Pedersen, G., Kristensen, H., (2002). Physical stability of redispersible dry emulsions containing amorphous sucrose. *European Journal of Pharmaceutics and Biopharmaceutics* 53(2), 147-153.

Chronakis, I.S., (1998). On the molecular characteristics, compositional properties, and structural-functional mechanisms of maltodextrins: a review. *Critical Reviews in Food Science and Nutrition* 38(7), 599-637.

Ciron, C.I.E., Gee, V.L., Kelly, A.L., Auty, M.A., (2012). Modifying the microstructure of low-fat yoghurt by microfluidisation of milk at different pressures to enhance rheological and sensory properties. *Food Chemistry* 130(3), 510-519.

Couchman, P., Karasz, F., (1978). A classical thermodynamic discussion of the effect of composition on glass-transition temperatures. *Macromolecules* 11(1), 117-119.

Coultate, T.P., Coultate, T.P., Tom, P.C., (2002). *Food: the chemistry of its components*. Royal Society of Chemistry, Cambridge, UK.

Coupland, J.N., Zhu, Z., Wan, H., McClements, D.J., Nawar, W.W., Chinachoti, P., (1996). Droplet composition affects the rate of oxidation of emulsified ethyl linoleate. *Journal of the American Oil Chemists' Society* 73(6), 795-801.

Damerau, A., Kamlang-ek, P., Moisio, T., Lampi, A. M., & Piironen, V. (2014). Effect of SPME extraction conditions and humidity on the release of volatile lipid oxidation products from spray-dried emulsions. *Food Chemistry, 157*, 1-9.

Damodaran, S., (1997). Food proteins: an overview, In: Damodaran, S., Paraf, A. (Eds.), *Food proteins and their applications*. Marcel Decker Inc., New York, NY, USA, pp. 1-24.

Danviriyakul, S., McClements, D., Decker, E., Nawar, W., Chinachoti, P., (2002). Physical stability of spray-dried milk fat emulsion as affected by emulsifiers and processing conditions. *Journal of Food Science* 67(6), 2183-2189.

De Paz, E., Martín, Á., Estrella, A., Rodríguez-Rojo, S., Matias, A.A., Duarte, C.M., Cocero, M.J., (2012). Formulation of β-carotene by precipitation from pressurized ethyl acetate-on-water emulsions for application as natural colorant. *Food Hydrocolloids* 26(1), 17-27.

De Vilder, J., Martens, R., Naudts, M., (1976). Influence of process variables on some whole milk powder characteristics. *Milchwissenschaft* 31(7), 396-401.

Decker, E., (1998). Antioxidant mechanisms, In: Akoh, C.C., Min, D.B. (Eds.), *Food lipids: chemistry, nutrition and biotechnology*. Marcel Decker Inc., New York, NY, USA, pp. 397-421.

Deming, D.M., Teixeira, S.R., Erdman, J.W., (2002). All-trans β-carotene appears to be more bioavailable than 9-cis or 13-cis β-carotene in gerbils given single oral doses of each isomer. *Journal of Nutrition* 132(9), 2700-2708.

Desai, K.G.H., Park, H.J., (2005). Recent developments in microencapsulation of food ingredients. *Drying Technology* 23(7), 1361-1394.

Desobry, S.A., Netto, F.M., Labuza, T.P., (1997). Comparison of spray-drying, drum-drying and freeze-drying for β-carotene encapsulation and preservation. *Journal of Food Science* 62(6), 1158-1162.

Devos, M., (1990). *Standardized human olfactory thresholds.* IRL Press, Oxford University, UK.

Dickinson, E., Stainsby, G., (1982). Colloids in foods. *London: Applied Sci*, 33-66.

Dickinson, E., Whyman, R.H., Dalgleish, D.G., (1987). Colloidal properties of model oil-in-water food emulsions stabilized separately by α_{s1}-casein, β-casein and κ-casein, In: Dickinson, E. (Ed.), *Food emulsions and foams*. Royal Society of Chemistry, London, UK.

Dickinson, E., Rolfe, S.E., Dalgleish, D.G., (1988). Competitive adsorption of α_{s1}-casein and β-casein in oil-in-water emulsions. *Food Hydrocolloids* 2(5), 397-405.

Dickinson, E., Matsumara, Y., (1994). Proteins at liquid interfaces: role of the molten globule state. *Colloids & Surfaces: B* 3(1-2), 1-17.

Dickinson, E., (1997a). Properties of emulsions stabilized with milk proteins: overview of some recent developments. *Journal of Dairy Science* 80(10), 2607-2619.

Dickinson, E., (1997b). Aggregation processes, particle interactions and colloidal structure, In: Dickinson, E., Bergenståhl, B. (Eds.), *Food colloids: proteins, lipids and polysaccharides*. Royal Society of Chemistry, Cambridge, UK, pp. 107-126.

Dickinson, E., Golding, M., (1997). Depletion flocculation of emulsions containing unadsorbed sodium caseinate. *Food Hydrocolloids* 11(1), 13-18.

Dickinson, E., Golding, M., Povey, J.W., (1997). Creaming and flocculation of oil-in-water emulsions containing sodium caseinate. *Journal of Colloid and Interface Science* 185, 515-529.

Dickinson, E., Pawlowsky, K., (1998). Influence of k-carrageenan on the properties of a protein-stabilized emulsion. *Food Hydrocolloids* 12(4), 417-423.

Dickinson, E., (1999). Caseins in emulsions: interfacial properties and interactions. *International Dairy Journal* 9(3-6), 305-312.

Dobarganes, M.C., Velasco, J., (2002). Analysis of lipid hydroperoxides. *European Journal of Lipid Science and Technology* 104(7), 420-428.

Dóka, O., Ajtony, Z., Bicanic, D., Koehorst, Z., (2000). Assessing the extent of degradation in the UV radiation and heat-catalyzed oxidized whole milk powder: The UV photoacoustic and diffuse reflectance spectroscopies versus the peroxide value. *Applied Spectroscopy* 54(9), 1405-1408.

Dollo, G., Le Corre, P., Guerin, A., Chevanne, F., Burgot, J.L., Leverge, R., (2003). Spray-dried redispersable O/W emulsions to improve oral bioavailability of poorly soluble drugs. *European Journal of Pharmaceutical Sciences* 19(4), 273-280.

Downton, G.E., Flores-Luna, J.L., King, C.J., (1982). Mechanism of stickiness in hygroscopic, amorphous powders. *Industrial & Engineering Chemistry Fundamentals* 21(4), 447-451.

Drusch, S., (2007). Sugar beet pectin: A novel emulsifying wall component for microencapsulation of lipophilic food ingredients by spray-drying. *Food Hydrocolloids* 21(7), 1223-1228.

Dudkiewicz, A., Tiede, K., Loeschner, K., Jensen, L.H.S., Wierzbicki, R., Boxall, A.B.A., Molhave, K., (2011). Characterization of nanomaterials in food by electron microscopy. *Trends in Analytical Chemistry* 30(1), 28-43.

Dziezak, J.D., (1988). Microencapsulation and encapsulation ingredients. *Food Technology* 42(4), 136-151.

El-Sayed, T.M., Wallack, D.A., King, C.J., (1990). Changes in particle morphology during drying of drops of carbohydrate solutions and food liquids. 1. Effect of composition and drying conditions. *Industrial & Engineering Chemistry Research* 29(12), 2346-2354.

Elias, R.J., McClements, D.J., Decker, E.A., (2005). Antioxidant activity of cysteine, tryptophan, and methionine residues in continuous phase β-lactoglobulin in oil-in-water emulsions. *Journal of Agricultural and Food Chemistry* 53(26), 10248-10253.

Elias, R.J., Bridgewater, J.D., Vachet, R.W., Waraho, T., McClements, D.J., Decker, E.A., (2006). Antioxidant mechanisms of enzymatic hydrolysates of β-lactoglobulin in food lipid dispersions. *Journal of Agricultural and Food Chemistry* 54(25), 9565-9572.

Elias, R.J., McClements, D.J., Decker, E.A., (2007). Impact of thermal processing on the antioxidant mechanisms of continuous phase β-lactoglobulin in oil-in-water emulsions. *Food Chemistry* 104(4), 1402-1409.

Esterbauer, H., (1993). Cytotoxicity and genotoxicity of lipid-oxidation products. *American Journal of Clinical Nutrition* 57, 779S-785S.

Euston, S., Finnigan, S., Hirst, R., (2000). Aggregation kinetics of heated whey protein-stabilized emulsions. *Food Hydrocolloids* 14(2), 155-161.

Fäldt, P., Bergensåthl, B., Carlsson, G., (1993). The surface coverage of fat on food powders analysed by ESC (electron spectroscopy for chemical analysis). *Food Structure* 12, 225-234.

Fäldt, P., Bergensåthl, B., (1994). The surface composition of spray-dried protein-lactose powders. *Colloids and Surfaces A: Physiochemical and Engineering Aspects* 90(2-3), 183-190.

Fäldt, P., Bergensåthl, B., (1995). Fat encapsulation in spray dried food powders. *Journal of the American Oil Chemists' Society* 72, 171-176.

Fäldt, P., Bergensåthl, B., (1996a). Spray-dried whey protein/lactose/soybean oil emulsions. 2. Redispersability, wettability and particle structure. *Food Hydrocolloids* 10(4), 431-439.

Fäldt, P., Bergensåthl, B., (1996b). Spray-dried whey protein/lactose/soybean oil emulsions. 1. Surface composition and particle structure. *Food Hydrocolloids* 10(4), 421-429.

Fäldt, P., Bergenståhl, B., (1996). Changes in surface composition of spray-dried food powders due to lactose crystallization. *LWT - Food Science and Technology* 29(5–6), 438-446.

Fang, Y., Dalgleish, D.G., (1993). Casein adsorption on the surfaces of oil-in-water emulsions modified by lecithin. *Colloids and Surfaces B: Biointerfaces* 1(6), 357-364.

Fathi, M., Mozafari, M., Mohebbi, M., (2012). Nanoencapsulation of food ingredients using lipid based delivery systems. *Trends in Food Science & Technology* 23(1), 13-27.

Fenaille, F., Visani, P., Fumeaux, R., Milo, C., Guy, P.A., (2003). Comparison of mass spectrometry-based electronic nose and solid phase microextraction gas chromatography mass spectrometry technique to assess infant formula oxidation. *Journal of Agricultural and Food Chemistry* 51(9), 2790-2796.

Ferreira, I., Rocha, S., Coelho, M., (2007). Encapsulation of antioxidants by spray-drying. *Chemical Engineering Transactions* 11(9), 713-717.

Fitzpatrick, J.J., Iqbal, T., Delaney, C., Twomey, T., Keogh, M.K., (2004). Effect of powder properties and storage conditions on the flowability of milk powders with different fat contents. *Journal of Food Engineering* 64(4), 435-444.

Flink, J., (1983). Structure and structure transitions in dried carbohydrate materials, In: Peleg, M., Bagley, E.B. (Eds.), *Physical properties of foods*. AVI Publishing Co., Westport, CT, USA, pp. 473-521.

Floury, J., Desrumaux, A., Lardières, J., (2000). Effect of high-pressure homogenization on droplet size distributions and rheological properties of model oil-in-water emulsions. *Innovative Food Science & Emerging Technologies* 1(2), 127-134.

Fogler, B.B., Kleninschmidt, R.V., (1938). Spray drying. *Industrial & Engineering Chemistry* 30(12), 1372-1384.

Fomuso, L.B., Corredig, M., Akoh, C.C., (2002). Effect of emulsifier on oxidation properties of fish oil-based structured lipid emulsions. *Journal of Agricultural and Food Chemistry* 50(10), 2957-2961.

Foster, K.D., Bronlund, J.E., Paterson, A.H.J., (2005). The contribution of milk fat towards the caking of dairy powders. *International Dairy Journal* 15(1), 85-91.

Fox, P., (2001). Milk proteins as food ingredients. *International Journal of Dairy Technology* 54(2), 41-55.

Frankel, E.N., Hu, M.L., Tappel, A.L., (1989). Rapid headspace gas chromatography of hexanal as a measure of lipid peroxidation in biological samples. *Lipids* 24(11), 976-981.

Frankel, E.N., (1996). Antioxidants in lipid foods and their impact on food quality. *Food Chemistry* 57(1), 51-55.

Frankel, E.N., (1998). *Lipid oxidation*. The Oily Press, Dundee, Scotland.

Freudig, B., Hogekamp, S., Schubert, H., (1999). Dispersion of powders in liquids in a stirred vessel. *Chemical Engineering and Processing: Process Intensification* 38(4), 525-532.

Fritsch, C., (1994). Lipid oxidation - the other dimension. *Inform* 5, 423-436.

Fu, B., Labuza, T.P., (1993). Shelf-life prediction: theory and application. *Food Control* 4(3), 125-133.

Gaisford, S., Verma, A., Saunders, M., Royall, P.G., (2009). Monitoring crystallisation of drugs from fast-dissolving oral films with isothermal calorimetry. *International Journal of Pharmaceutics* 380, 105-111.

García-Llatas, G., Lagarda, M.J., Romero, F., Abellán, P., Farré, R., (2007). A headspace solid-phase microextraction method of use in monitoring hexanal and pentane during storage: Application to liquid infant foods and powdered infant formulas. *Food Chemistry* 101(3), 1078-1086.

GEA Niro, (2005). GEA Niro Method No.A 10 a: Surface free fat of powder.

GEA Niro, (2006). GEA Niro Method No.A 11 a: Particle Density, Occluded Air and Interstitial Air by Air Pycnometer.

Gharsallaoui, A., Roudaut, G., Chambin, O., Voilley, A., Saurel, R., (2007). Applications of spray-drying in microencapsulation of food ingredients: an overview. *Food Research International* 40(9), 1107-1121.

Gibbs, B.F., Kermasha, S., Alli, I., Mulligan, C.N., (1999). Encapsulation in the food industry: a review. *International Journal of Food Sciences and Nutrition* 50(3), 213-224.

Given Jr, P.S., (2009). Encapsulation of flavors in emulsions for beverages. *Current Opinion in Colloid & Interface Science* 14(1), 43-47.

Gordon, M., Taylor, J.S., (1952). Ideal copolymers and the second-order transitions of synthetic rubbers. i. non-crystalline copolymers. *Journal of Applied Chemistry* 2(9), 493-500.

Gouin, S., (2004). Microencapsulation: industrial appraisal of existing technologies and trends. *Trends in Food Science & Technology* 15(7), 330-347.

Guillén, M.A.D., Cabo, N., (2002). Fourier transform infrared spectra data versus peroxide and anisidine values to determine oxidative stability of edible oils. *Food Chemistry* 77(4), 503-510.

Guterres, S.S., Beck, R.C.R., Pohlmann, A.R., (2009). Spray-drying technique to prepare innovative nanoparticulated formulations for drug administration: a brief overview. *Brazilian Journal of Physics* 39(1A), 205-209.

Haque, M.K., Roos, Y.H., (2004). Water plasticization and crystallization of lactose in spray-dried lactose/protein mixtures. *Journal of Food Science* 69(1), FEP 23-29.

Haque, M.K., Roos, Y.H., (2005). Crystallization and x-ray diffraction of spray-dried and freeze-dried amorphous lactose. *Carbohydrate Research* 340, 293-301.

Hardas, N., Danviriyakul, S., Foley, J., Nawar, W., Chinachoti, P., (2000). Accelerated stability studies of microencapsulated anhydrous milk fat. *Lebensmittel-Wissenschaft und Technologie* 33, 506-513.

Hartel, R., (2001). Measurements of crystalline structure in foods, *Crystallization in foods*. Aspen Publishers, Gaithersburg, MD, USA, pp. 34-90.

Hartman, G.H., Akeson, W.R., Stahmann, M.A., (1967). Leaf protein concentrate prepared by spray-drying. *Journal of Agricultural and Food Chemistry* 15(1), 74-79.

Hecht, J.P., King, C.J., (2000). Spray drying: influence of developing drop morphology on drying rates and retention of volatile substances. 1. Single-drop experiments. *Industrial & Engineering Chemistry Research* 39(6), 1756-1765.

Hedegaard, R., Kristensen, D., Nielsen, J.H., Frøst, M.B., Østdal, H., Hermansen, J.E., Kröger-Ohlsen, M., Skibsted, L.H., (2006). Comparison of descriptive sensory

analysis and chemical analysis for oxidative changes in milk. *Journal of Dairy Science* 89(2), 495-504.

Higashiyama, T., (2002). Novel functions and applications of trehalose. *Pure Applied Chemistry* 74(7), 1263-1269.

Hogan, S.A., McNamee, B.F., O'Riordan, E.D., O'Sullivan, M., (2001a). Emulsification and microencapsulation properties of sodium caseinate/carbohydrate blends. *International Dairy Journal* 11(3), 137-144.

Hogan, S.A., McNamee, B.F., O'Riordan, E.D., O'Sullivan, M., (2001b). Microencapsulating properties of sodium caseinate. *Journal of Agricultural and Food Chemistry* 49, 1934-1938.

Hogan, S.A., O'Riordan, E.D., O'Sullivan, M., (2003). Microencapsulation and oxidative stability of spray-dried fish oil emulsions. *Journal of Microencapsulation* 20(5), 675-688.

Horn, A. F., Nielsen, N. S., Jensen, N.S., Horsewell, A., & Jacobsen, C. (2012). The choice of homogenisation equipment affects lipid oxidation in emulsions. *Food Chemistry, 134*(2), 803-810.

Horwitz, W., (1982). Evaluation of analytical methods used for regulation of foods and drugs. *Analytical Chemistry* 54(1), 67A-76A.

Huang, Q., Yu, H., Ru, Q., (2010). Bioavailability and delivery of nutraceuticals using nanotechnology. *Journal of Food Science* 75(1), R50-R57.

Huck-Iriart, C., Alvarez-Cerimedo, M., Candal, R., Herrera, M.L., (2011). Structures and stability of lipid emulsions formulated with sodium caseinate. *Current Opinion in Colloid and Interface Science* 16, 412-420.

IDF, (1995). Dried milk and dried milk products. Determination of bulk density. IDF standard 134A. Brussels, Belgium: International Dairy Federation.

IDF, (2001). Milk. Determination of nitrogen content, ISO 8969-2. IDF standard 20-2. Brussels, Belgium: International Dairy Federation.

Iglesias, H.A., Chirife, I., (1978). Delayed crystallization of amorphous sucrose in humidified freeze dried model systems. *Journal of Food Technology* 13, 137-144.

Jacobsen, C., (1999). Sensory impact of lipid oxidation in complex food systems. *Lipid/Fett* 101(12), 484-492.

Jacobsen, C., (2008). Omega-3s in food emulsions: overview and case studies. *Agro Food Industry Hi-Tech* 19(5), 9-13.

Jafari, S.M., He, Y., Bhandari, B., (2006). Nano-emulsion production by sonication and microfluidization—a comparison. *International Journal of Food Properties* 9(3), 475-485.

Jafari, S.M., He, Y., Bhandari, B., (2007a). Production of sub-micron emulsions by ultrasound and microfluidization techniques. *Journal of Food Engineering* 82(4), 478-488.

Jafari, S.M., He, Y., Bhandari, B., (2007b). Encapsulation of nanoparticles of *d*-limonene by spray drying: role of emulsifiers and emulsifying techniques. *Drying Technology* 25(6), 1069-1079.

Jafari, S.M., Assadpoor, E., Bhandari, B., He, Y., (2008a). Nano-particle encapsulation of fish oil by spray drying. *Food Research International* 41(2), 172-183.

Jafari, S.M., Assadpoor, E., He, Y., Bhandari, B., (2008b). Re-coalescence of emulsion droplets during high-energy emulsification. *Food Hydrocolloids* 22(7), 1191-1202.

Jo, C., Ahn, D., (1999). Fat reduces volatiles production in oil emulsion system analyzed by purge-and-trap dynamic headspace/gas chromatography. *Journal of Food Science* 64(4), 641-643.

Jouppila, K., Roos, Y.H., (1994a). Water sorption and time-dependent phenomena of milk powders. *Journal of Dairy Science* 77(7), 1798-1808.

Jouppila, K., Roos, Y.H., (1994b). Glass transitions and crystallization in milk powders. *Journal of Dairy Science* 77(10), 2907-2915.

Jouppila, K., Kansikas, J., Roos, Y.H., (1997). Glass transition, water plasticization, and lactose crystallization in skim milk powder. *Journal of Dairy Science* 80(12), 3152-3160.

Jung, D.M., Ebeler, S.E., (2003). Headspace solid-phase microextraction method for the study of the volatility of selected flavor compounds. *Journal of Agricultural and Food Chemistry* 51(1), 200-205.

Karagül-Yüceer, Y., Cadwallader, K.R., Drake, M., (2002). Volatile flavor components of stored nonfat dry milk. *Journal of Agricultural and Food Chemistry* 50(2), 305-312.

Kaushik, V., Roos, Y.H., (2007). Limonene encapsulation in freeze-drying of gum arabic-sucrose-gelatin systems. *LWT- Food Science and Technology* 40(8), 1381-1391.

Kawamura, K., (1979). The DSC thermal analysis of crystallization behaviour in palm oil. *Journal of the American Oil Chemists' Society* 56, 753-758.

Kedward, C.J., MacNaughtan, W., Blanshard, J.M.V., Mitchell, J.R., (1998). Crystallization kinetics of lactose and sucrose on isothermal differential scanning calorimetry. *Journal of Food Science* 63(2), 192-197.

Kedward, C.J., MacNaughtan, W., Mitchell, J.R., (2000). Isothermal and non-isothermal crystallization in amorphous sucrose and lactose at low moisture contents. *Carbohydrate Research* 329(2), 423-430.

Kelly, G.M., O'Mahony, J.A., Kelly, A.L., O'Callaghan, D.J., (2014). Physical characteristics of spray-dried dairy powders containing different vegetable oils. *Journal of Food Engineering* 122, 122-129.

Kelly, J., Kelly, P., Harrington, D., (2002). Influence of processing variables on the pyhsicochemical properties of spray dried fat-based milk powders. *Lait* 82, 401-412.

Kenyon, M.M., (1995). Modified starch, maltodextrin, and corn syrup solids as wall materials for food encapsulation, In: Risch, S.J., Reineccius, G.A. (Eds.), *Encapsulation and controlled release of food ingredients*. American Chemical Society: ACS symposium series, Washington DC, USA, pp. 42-50.

Keogh, M.K., O'Kennedy, B.T., Kelly, J., Auty, M.A., Kelly, P.M., Fureby, A., Haahr, A.M., (2001). Stability to oxidation of spray-dried fish oil powder microencapsulated using milk ingredients. *Journal of Food Science* 66(2), 217-224.

Kesisoglou, F., Panmai, S., Wu, Y., (2007). Application of nanoparticles in oral delivery of immediate release formulations. *Current Nanoscience* 3(2), 183-190.

Kim, E.H.J., Chen, X.D., Pearce, D., (2002). Surface characterization of four industrial spray-dried dairy powders in relation to chemical composition, structure and wetting property. *Colloids and Surfaces B: Biointerfaces* 26(3), 197-212.

Kim, E.H.J., Chen, X.D., Pearce, D., (2005). Effect of surface composition on the flowability of industrial spray-dried powders. *Colloids and Surfaces B: Biointerfaces* 46, 182-187.

Kim, Y.D., Morr, C.V., (1996a). Microencapsulation properties of gum arabic and several food proteins: spray dried orange oil emulsion particles. *Journal of Agricultural and Food Chemistry* 44(5), 1314-1320.

Kim, Y.D., Morr, C.V., (1996b). Microencapsulation properties of gum Arabic and several food proteins: spray-dried orange oil emulsion particles. *Journal of Agricultural and Food Chemistry* 44(5), 1314-1320.

Klinkesorn, U., Sophanodora, P., Chinachoti, P., McClements, D.J., Decker, E.A., (2005). Stability of spray-dried tuna oil emulsions encapsulated with two-layered interfacial membranes. *Journal of Agricultural and Food Chemistry* 53(21), 8365-8371.

Lai, H., Schmidt, S., (1990). Lactose crystallisation in skim milk powder observed by hydrodynamic equilibria, scanning electron micrroscopy and 2H nuclear magnetic resonance. *Journal of Food Science* 55(4), 994-999.

Landström, K., Alsins, J., Bergenståhl, B., (2000). Competitive protein adsorption between bovine serum albumin and β-lactoglobulin during spray-drying. *Food Hydrocolloids* 14(1), 75-82.

Langrish, T., Wang, E., (2006). Crystallisation of powders of spray-dried lactose, skim milk and lactose-salt mixtures. *International Journal of Food Engineering* 2(4), 1-15.

Leong, T., Wooster, T., Kentish, S., Ashokkumar, M., (2009a). Minimising oil droplet size using ultrasonic emulsification. *Ultrasonics Sonochemistry* 16(6), 721-727.

Leong, W.F., Che Man, Y.B., Lai, O.M., Long, K., Misran, M., Tan, C.P., (2009b). Optimization of processing parameters for the preparation of phytosterol microemulsions by the solvent displacement method. *Journal of Agricultural and Food Chemistry* 57(18), 8426-8433.

Li, Y., Le Maux, S., Xiao, H., McClements, D.J., (2009). Emulsion-based delivery systems for tributyrin, a potential colon cancer preventative agent. *Journal of Agricultural and Food Chemistry* 57(19), 9243-9249.

Liang, R., Shoemaker, C.F., Yang, X., Zhong, F., Huang, Q., (2013). Stability and bioaccessibility of β-carotene in nanoemulsions stabilized by modified starches. *Journal of Agricultural and Food Chemistry* 61(6), 1249-1257.

Lin, C.C., Lin, S.Y., Hwang, L.S., (1995). Microencapsulation of squid oil with hydrophilic macromolecules for oxidative and thermal stabilization. *Journal of Food Science* 60(1), 36-39.

Liu, X.D., Furuta, T., Yoshii, H., Linko, P., (2000). Retention of emulsified flavor in a single droplet during drying. *Food Science and Technology Research* 6(4), 335-339.

Liu, X.D., Atarashi, T., Furuta, T., Yoshii, H., Aishima, S., Ohkawara, M., Linko, P., (2001). Microencapsulation of emulsified hydrophobic flavors by spray drying. *Drying Technology* 19(7), 1361-1374.

Liu, Y., Bhandari, B.R., Zhou, W., (2007). Study of glass transition and enthalpy relaxation of mixtures of amorphous sucrose and amorphous tapioca starch syrup solid by differential scanning calorimetry (DSC). *Journal of Food Engineering* 81(3), 599-610.

Liu, Z.Q., Zhou, J.-h., Zeng, Y.-l., Ouyang, X.-l., (2004). The enhancement and encapsulation of *Agaricus bisporus* flavor. *Journal of Food Engineering* 65(3), 391-396.

Lloyd, M., Zou, J., Farnsworth, H., Ogden, L., Pike, O., (2004a). Quality at time of purchase of dried milk products commercially packaged in reduced oxygen atmosphere. *Journal of Dairy Science* 87(8), 2337-2343.

Lloyd, M., Zou, J., Ogden, L., Pike, O., (2004b). Sensory and nutritional quality of nonfat dry milk in long-term residential storage. *Journal of Food Science* 69(8), S326-S331.

MacDougall, D., Crummett, W.B., (1980). Guidelines for data acquisition and data quality evaluation in environmental chemistry. *Analytical Chemistry* 52(14), 2242-2249.

Madene, A., Jacquot, M., Scher, J., Desobry, S., (2006). Flavor retention and controlled release - A review. *International Journal of Food Science and Technology* 41(1), 1-21.

Maher, P.G., Fenelon, M.A., Zhou, Y., Kamrul Haque, M., Roos, Y.H., (2011). Optimization of β-Casein stabilized nanoemulsions using experimental mixture design. *Journal of Food Science* 76(8), C1108-C1117.

Maher, P.G., Roos, Y.H., Fenelon, M.A., (2014). Physicochemical properties of spray dried nanoemulsions with varying final water and sugar contents. *Journal of Food Engineering* 126(0), 113-119.

Mahlin, D., Berggren, J., Alderborn, G., Engstrom, S., (2004). Moisture-induced surface crystallization of spray-dried amorphous lactose particles studied by atomic force microscopy. *Journal of Pharmaceutical Sciences* 93(1), 29-37.

Mancuso, J.R., McClements, D.J., Decker, E.A., (1999). The effects of surfactant type, pH, and chelators on the oxidation of salmon oil-in-water emulsions. *Journal of Agricultural and Food Chemistry* 47(10), 4112-4116.

Mao, L., Xu, D., Yang, J., Yuan, F., Gao, Y., Zhao, J., (2009). Effects of small and large molecule emulsifiers on the characteristics of b-carotene nanoemulsions prepared by high pressure homogenization. *Food Technology and Biotechnology* 47(3), 336-342.

Mao, L., Yang, J., Xu, D., Yuan, F., Gao, Y., (2010). Effects of homogenization models and emulsifiers on the physicochemical properties of β-carotene nanoemulsions. *Journal of Dispersion Science and Technology* 31(7), 986-993.

Marsili, R.T., (1999). Comparison of solid-phase microextraction and dynamic headspace methods for the gas chromatographic-mass spectrometric analysis of light-induced lipid oxidation products in milk. *Journal of Chromatographic Science* 37, 17-23.

Marsili, R.T., (2000). Shelf-life prediction of processed milk by solid-phase microextraction, mass spectrometry, and multivariate analysis. *Journal of Agricultural and Food Chemistry* 48(8), 3470-3475.

Mason, T.G., Wilking, J., Meleson, K., Chang, C., Graves, S., (2006). Nanoemulsions: formation, structure, and physical properties. *Journal of Physics: Condensed Matter* 18(41), R635.

Masters, K., (1968). Spray Drying—The Unit Operation Today. *Industrial & Engineering Chemistry* 60(10), 53-63.

Masters, K., (1991). *Spray Drying*. Longman Scientific & Technical and John Wiley & Sons Inc., Essex, UK.

Matsuno, R., Adachi, S., (1993). Lipid encapsulation technology-techniques and applications to food. *Trends in Food Science & Technology* 4(8), 256-261.

Mazzobre, M.A.F., Aguilera, J.M., Buera, M.a.P., (2003). Microscopy and calorimetry as complementary techniques to analyze sugar crystallization from amorphous systems. *Carbohydrate Research* 338(6), 541-548.

Mazzobre, M.F., Soto, G., Aguilera, J.M., Buera, M.P., (2001). Crystallization kinetics of lactose in sytems co-lyofilized with trehalose. Analysis by differential scanning calorimetry. *Food Research International* 34, 903-911.

McCarthy, N.A., Gee, V.L., Hickey, D.K., Kelly, A.L., O'Mahony, J.A., Fenelon, M.A., (2013). Effect of protein content on the physical stability and microstructure of a model infant formula. *International Dairy Journal* 29(1), 53-59.

McClements, D.J., Decker, E.A., (2000). Lipid oxidation in oil-in-water emulsions: Impact of molecular environment on chemical reactions in heterogeneous food systems. *Journal of Food Science* 65(8), 1270-1282.

McClements, D.J., (2005). *Food emulsions: Principles, practice, and techniques* (2nd ed). CRC Press, Boca Raton, FL, USA.

McClements, D.J., Decker, E.A., Weiss, J., (2007). Emulsion-based delivery systems for lipophilic bioactive components. *Journal of Food Science* 72(8), R109-R124.

McClements, D.J., Decker, E.A., Park, Y., Weiss, J., (2009). Structural design principles for delivery of bioactive components in nutraceuticals and functional foods. *Critical reviews in Food Science and Nutrition* 49(6), 577-606.

McClements, D.J., (2011). Edible nanoemulsions: fabrication, properties, and functional performance. *Soft Matter* 7(6), 2297-2316.

McClements, D.J., Rao, J., (2011). Food-grade nanoemulsions: formulation, fabrication, properties, performance, biological fate, and potential toxicity. *Critical Reviews in Food Science and Nutrition* 51(4), 285-330.

McClements, D.J., (2012). Nanoemulsions versus microemulsions: terminology, differences, and similarities. *Soft Matter* 8(6), 1719-1729.

McKenna, A.B., (1997). Examination of whole milk powder by confocal laser scanning microscopy. *Journal of Dairy Research* 64, 423-432.

McNamee, B.F., O'Riordan, E.D., O'Sullivan, M., (1998). Emulsification and microencapsulation properties of gum arabic. *Journal of Agricultural and Food Chemistry* 46(11), 4551-4555.

McNamee, B.F., O'Riordan, E.D., O'Sullivan, M., (2001). Effect of partial replacement of gum arabic with carbohydrates on its microencapsulation properties. *Journal of Agricultural and Food Chemistry* 49(7), 3385-3388.

Mei, L., McClements, D.J., Wu, J., Decker, E.A., (1998). Iron-catalyzed lipid oxidation in emulsion as affected by surfactant, pH and NaCl. *Food Chemistry* 61(3), 307-312.

Mei, L., McClements, D.J., Decker, E.A., (1999). Lipid oxidation in emulsions as affected by charge status of antioxidants and emulsion droplets. *Journal of Agricultural and Food Chemistry* 47(6), 2267-2273.

Miao, S., Roos, Y.H., (2004). Nonenzymatic browning kinetics of a carbohydrate-based low-moisture food system at temperatures applicable to spray drying. *Journal of Agricultural and Food Chemistry* 52(16), 5250-5257.

Miao, S., Roos, Y.H., (2005). Crystallization kinetics and x-ray diffraction of crystals formed in amorphous lactose, trehalose, and lactose/trehalose mixtures. *Journal of Food Science* 70(5), E350-E358.

Millqvist-Fureby, A., Burns, N., Landström, K., Bergensåthl, B., (1999). Surface activity at the air-water interface in relation to surface composition of spray-dried milk protein-stabilized emulsions, In: Dickinson, E., Rodriguez-Patino, J. (Eds.), *Food emulsions and foams*. Royal Society of Chemistry, London, UK, pp. 236.

Millqvist-Fureby, A., Elofsson, U., Bergenståhl, B., (2001). Surface composition of spray-dried milk protein-stabilised emulsions in relation to pre-heat treatment of proteins. *Colloids and Surfaces B: Biointerfaces* 21(1), 47-58.

Millqvist-Fureby, A., (2003). Characterisation of spray-dried emulsions with mixed fat phases. *Colloids and Surfaces B: Biointerfaces* 31, 65-79.

Min, D., Ticknor, D., Lee, S., Reineccius, G., (1990). Effects of processing conditions and antioxidants on the oxidative stability and carbon dioxide formation in low fat dry milk. *Journal of Food Science* 55(2), 401-403.

Minemoto, Y., Hakamata, K., Adachi, S., Matsuno, R., (2002). Oxidation of linoleic acid encapsulated with gum arabic or maltodextrin by spray-drying. *Journal of Microencapsulation* 19(2), 181-189.

Mongenot, N., Charrier, S., Chalier, P., (2000). Effect of ultra sound emulsification on cheese aroma encapsulation by carbohydrates. *Journal of Agricultural and Food Chemistry* 48, 861-867.

Mora-Gutierrez, A., Farrell Jr., H.M., (2000). Sugar-casein interaction in deuterated solutions of bovine and caprine casein as determined by oxygen-17 and carbon-13 nuclear magnetic resonance: a case of preferential interactions. *Journal of Agricultural and Food Chemistry* 48, 3245-3255.

Moreau, D., Rosenberg, M., (1998). Porosity of whey protein-based microcapsules containing anhydrous milkfat measured by gas displacement pycnometry. *Journal of Food Science* 63(5), 819-823.

Moreau, D.L., Rosenberg, M., (1996). Oxidative stability of anhydrous milkfat microencapsulated in whey proteins. *Journal of Food Science* 61(1), 39-43.

Morr, C., Ha, E., (1993). Whey protein concentrates and isolates: processing and functional properties. *Critical Reviews in Food Science & Nutrition* 33(6), 431-476.

Mozafari, M.R., Flanagan, J., Matia-Merino, L., Awati, A., Omri, A., Suntres, Z.E., Singh, H., (2006). Recent trends in the lipid-based nanoencapsulation of antioxidants and their role in foods. *Journal of the Science of Food and Agriculture* 86(13), 2038-2045.

Murrieta-Pazos, I., Gaiani, C., Galet, L., Cuq, B., Desobry, S., Scher, J., (2011). Comparative study of particle structure evolution during water sorption: Skim and whole milk powders. *Colloids and Surfaces B: Biointerfaces* 87(1), 1-10.

Nakagawa, K., Surassmo, S., Min, S.-G., Choi, M.-J., (2011). Dispersibility of freeze-dried poly (epsilon-caprolactone) nanocapsules stabilized by gelatin and the effect of freezing. *Journal of Food Engineering* 102(2), 177-188.

Nakaya, K., Ushio, H., Matsukawa, S., Shimizu, M., Ohshima, T., (2005). Effects of droplet size on the oxidative stability of oil-in-water emulsions. *Lipids* 40(5), 501-507.

O' Dwyer, S.P., O' Beirne, D., Eidhin, D.N., O' Kennedy, B.T., (2013). Effects of sodium caseinate concentration and storage conditions on the oxidative stability of oil-in-water emulsions. *Food Chemistry* 138(2–3), 1145-1152.

O'Brien, R.D., Farr, W.E., Wan, P.J., (2000). "Shortening technology". Introduction to fats and oils technology, AOCS press, USA. *USA, AOCS press*.

Ohkawa, H., Ohishi, N., Yagi, K., (1978). Reaction of linoleic acid hydroperoxide with thiobarbituric acid. *Journal of Lipid Research* 19(8), 1053-1057.

Okuyama, K., Wuled Lenggoro, I., (2003). Preparation of nanoparticles via spray route. *Chemical Engineering Science* 58(3), 537-547.

Omar, E.A.M., Roos, Y.H., (2007). Glass transition and crystallization behaviour of freeze-dried lactose–salt mixtures. *LWT- Food Science and Technology* 40, 536-543.

Onwulata, C., Smith, P., Craig, J., Holsinger, V., (1994). Physical properties of encapsulated spray-dried milkfat. *Journal of Food Science* 59(2), 316-320.

Onwulata, C., Smith, P., Cooke, P., Holsinger, V., (1996). Particle structures of encapsulated milkfat powders. *LWT-Food Science and Technology* 29(1), 163-172.

Onwulata, C., Konstance, R., Holsinger, V., (1998). Properties of single-and double-encapsulated butteroil powders. *Journal of Food Science* 63(1), 100-103.

Osborn, H.T., Akoh, C.C., (2004). Effect of emulsifier type, droplet size, and oil concentration on lipid oxidation in structured lipid-based oil-in-water emulsions. *Food Chemistry* 84(3), 451-456.

Palzer, S., (2010). The relation between material properties and supra-molecular structure of water-soluble food solids. *Trends in Food Science & Technology* 21(1), 12-25.

Papadakis, S.E., King, C.J., (1988). Air temperature and humidity profiles in spray drying. 2. Experimental measurements. *Industrial & Engineering Chemistry Research* 27(11), 2116-2123.

Pawliszyn, J., (2000). Theory of solid-phase microextraction. *Journal of Chromatographic Science* 38, 270-278.

Pedersen, G.P., Fäldt, P., Bergensåthl, B., Kristensen, H.G., (1998). Solid state characterization of a dry emulsion: a potential drug delivery system. *International Journal of Pharmaceutics* 171(2), 257-270.

Peña-Ramos, E.A., Xiong, Y.L., Arteaga, G.E., (2004). Fractionation and characterisation for antioxidant activity of hydrolysed whey protein. *Journal of the Science of Food and Agriculture* 84(14), 1908-1918.

Peng, X., Xiong, Y.L., Kong, B., (2009). Antioxidant activity of peptide fractions from whey protein hydrolysates as measured by electron spin resonance. *Food Chemistry* 113(1), 196-201.

Perkins, M.L., D'Arcy, B.R., Lisle, A.T., Deeth, H.C., (2005). Solid phase microextraction of stale flavour volatiles from the headspace of UHT milk. *Journal of the Science of Food and Agriculture* 85(14), 2421-2428.

Pillai, D.S., Prabhasankar, P., Jena, B., Anandharamakrishnan, C., (2012). Microencapsulation of Garcinia cowa fruit extract and effect of its use on pasta process and quality. *International Journal of Food Properties* 15(3), 590-604.

Pinnamaneni, S., Das, N., Das, S., (2003). Comparison of oil-in-water emulsions manufactured by microfluidization and homogenization. *Die Pharmazie-An International Journal of Pharmaceutical Sciences* 58(8), 554-558.

Pisecky, J., (1997). *Handbook of milk powder manufacture*. Niro A/S, Copenhagen, Denmark.

Ponginebbi, L., Nawar, W.W., Chinachoti, P., (1999). Oxidation of linoleic acid in emulsions: Effect of substrate, emulsifier, and sugar concentration. *Journal of the American Oil Chemists' Society* 76(1), 131-138.

Potes, N., Kerry, J.P., Roos, Y.H., (2012). Additivity of water sorption, alpha-relaxations and crystallization inhibition in lactose–maltodextrin systems. *Carbohydrate Polymers* 89(4), 1050-1059.

Przybylski, R., Eskin, N.A.M., (1995). Methods to measure volatile compounds and the flavor significance of volatile compounds, In: Warner, K., Eskin, N.A.M. (Eds.), *Methods to assess quality and stability of oils and fat-containing foods*. AOCS Press, Champaign, IL, USA, pp. 107-133.

Przygonski, K., (2003). Analysis of volatile lipid oxidation products in infant formula by dynamic-headspace SPME/GC. *Prace Instytow i Laboratoriow Badawczych Przemyslu Spozywczego* 58, 86-94.

Qian, C., McClements, D.J., (2011). Formation of nanoemulsions stabilized by model food-grade emulsifiers using high pressure homogenization: Factors affecting particle size. *Food Hydrocolloids* 25(5), 1000-1008.

Quinn, J., (1965). The economics of spray drying. *Industrial & Engineering Chemistry* 57(1), 35-37.

Quintanilla-Carvajal, M.X., Camacho-Díaz, B.H., Meraz-Torres, L.S., Chanona-Pérez, J.J., Alamilla-Beltrán, L., Jimenéz-Aparicio, A., Gutiérrez-López, G.F., (2010). Nanoencapsulation: a new trend in food engineering processing. *Food Engineering Reviews* 2(1), 39-50.

Reid, D.S., Kerr, W., Hsu, J., (1994). The glass transition in the freezing process. *Journal of Food Engineering* 22(1-4), 483-494.

Reineccius, G.A., (1988). Spray drying of food flavors, In: Risch, S.J., Reineccius, G.A. (Eds.), *Flavor encapsulation*. American Chemical Society, Washington DC, USA, pp. 151-185.

Reineccius, G.A., (2001). Multiple-core encapsulation: The spray drying of food ingredients, In: Vilstrup, P. (Ed.), *Microencapsulation of food ingredients*. Leatherhead Publishing, Surrey, UK, pp. 151-185.

Rennie, P.R., Chen, X.D., Hargreaves, C., Mackereth, A., (1999). A study of the cohesion of dairy powders. *Journal of Food Engineering* 39(3), 277-284.

Risch, S.J., Reineccius, G.A., (1988). Spray-dried orange oil: Effect of emulsion size on flavor retention and shelf stability. *Flavor Encapsulation* 370, 67-77.

Robins, M.M., (2000). Emulsions - creaming phenomena. *Current Opinion in Colloid and Interface Science* 5, 265-272.

Robson, E.W., Dalgleish, D.G., (1987). Interfacial composition of sodium caseinate emulsions. *Journal of Food Science* 52(6), 1694-1698.

Roe, K.D., Labuza, T.P., (2005). Glass transition and crystallization of amorphous trehalose-sucrose mixtures. *International Journal of Food Properties* 8(3), 559-574.

Roetman, K., (1979). Crystalline lactose and the structure of spray-dried milk products as observed by scanning electron microscopy. *Netherlands Milk and Dairy Journal* 33, 1-11.

Romeu-Nadal, M., Castellote, A.I., López-Sabater, M.C., (2004). Headspace gas chromatographic method for determining volatile compounds in infant formulas. *Journal of Chromatography A* 1046(1–2), 235-239.

Roos, Y., Karel, M., (1990). Differential scanning calorimetry study of phase transitions affecting the quality of dehydrated materials. *Biotechnology Progress* 6(2), 159-163.

Roos, Y., (1993). Melting and glass transitions of low molecular weight carbohydrates. *Carbohydrate Research* 238, 39-48.

Roos, Y., Karel, M., Kokini, J., (1996a). Glass transitions in low moisture and frozen foods: effects on shelf life and quality. *Food Technology*.

Roos, Y.H., Karel, M., (1991a). Phase transitions of amorphous sucrose and frozen sucrose solutions. *Journal of Food Science* 56(1), 266-267.

Roos, Y.H., Karel, M., (1991b). Plasticizing effect of water on thermal behaviour and crystallization of amorphous food models. *Journal of Food Science* 56(1), 775-777.

Roos, Y.H., Karel, M., (1991c). Applying state diagrams to food processing and development. *Food Technology* 45(12), 66-68.

Roos, Y.H., Karel, M., (1991d). Water and molecular weight effects on glass transitions in amorphous carbohydrates and carbohydrate solutions. *Journal of Food Science* 56(6), 1676-1681.

Roos, Y.H., (1995). Characterization of Food Polymers Using State Diagrams. *Journal of Food Engineering* 24(3), 339-360.

Roos, Y.H., Karel, M., Kokini, J.L., (1996b). Glass transitions in low moisture ansd frozen foods: Effect on shelf lifeand quality. *Food Technology* 11, 95-108.

Roos, Y.H., (2007). Phase transitions and transformations in food systems, In: Heldman, D.R., Lund, D.B. (Eds.), *Handbook of food engineering*, 2nd ed. Taylor & Francis Group, FL, USA, pp. 287-352.

Roozen, J., Frankel, E., Kinsella, J., (1994). Enzymic and autoxidation of lipids in low fat foods: model of linoleic acid in emulsified hexadecane. *Food Chemistry* 50(1), 33-38.

Rosenberg, M., Kopelman, I.J., Talmon, Y., (1990). Factors affecting retention in spray-drying microencapsulation of volatile materials. *Journal of Agricultural and Food Chemistry* 38(5), 1288-1294.

Rosenberg, M., Young, S., (1993a). Whey proteins as microencapsulating agents. Microencapsulation of anhydrous milkfat: Structure evaluation. *Food Structure* 12(1), 31-41.

Rosenberg, M., Young, S.L., (1993b). Whey proteins as microencapsulating agents - Microencapsulation of anhydrous milkfat: structure evaluation. *Food Structure* 12(1), 31-41.

Rosenberg, M., Sheu, T.Y., (1996). Microencapsulation of volatiles by spray-drying in whey protein-based wall systems. *International Dairy Journal* 6, 273-284.

Rulkens, W., Thijssen, H., (1972). The retention of organic volatiles in spray-drying aqueous carbohydrate solutions. *International Journal of Food Science & Technology* 7(1), 95-105.

Saltmarch, M., Labuza, T., (1980). Influence of relative humidity on the physicochemical state of lactose in spray-dried sweet whey powders. *Journal of Food Science* 45, 1231-1237.

Sánchez, C.C., Patino, J.M.R., (2005). Interfacial, foaming and emulsifying characteristics of sodium caseinate as influenced by protein concentration in solution. *Food Hydrocolloids* 19(3), 407-416.

Sanguansri, P., Augustin, M.A., (2006). Nanoscale materials development - a food industry perspective. *Trends in Food Science & Technology* 17, 547-556.

Schenz, T.W., (1995). Glass transitions and product stability: an overview. *Food Hydrocolloids* 9(4), 307-315.

Schmidt, E.A., Law, D., Zhang, G.G.Z., (1999). Nucleation and crystallization kinetics of hydrated amorphous lactose above the glass transition temperature. *Journal of Pharmaceutical Sciences* 88(3), 291-296.

Schubert, H., (1993). Instantization of powdered food products. *International Journal of Chemical Engineering* 33, 28-45.

Schubert, H., Ax, K., Behrend, O., (2003). Product engineering of dispersed systems. *Trends in Food Science & Technology* 14(1), 9-16.

Schubert, H., Engel, R., (2004). Product and formulation engineering of emulsions. *Chemical Engineering Research and Design* 82(9), 1137-1143.

Schuck, P., (2002). Spray drying of dairy products: state of the art. *Le Lait* 82(4), 375-382.

Schuck, P., Méjean, S., Dolivet, A., Jeantet, R., (2005). Thermohygrometric sensor: a tool for optimizing the spray drying process. *Innovative Food Science and Emerging Technologies* 6, 45-50.

Shahidi, F., Han, X.Q., (1993). Encapsulation of food ingredients. *Critical Reviews in Food Science and Nutrition* 33(6), 501-547.

Shahidi, F., Pegg, R.B., (1994). Hexanal as an indicator of meat flavor deterioration. *Journal of Food Lipids* 1(3), 177-186.

Shahidi, F., Wanasundra, U.N., (2002). Methods for measuring oxidative rancidity in fats and oils, In: Akoh, C.C., Min, D.B. (Eds.), *Food Lipids: Chemistry, Nutrition and Biotechnology*. Marcel Decker Inc., New York, NY, USA, pp. 465-487.

Shamblin, S.L., Huang, E.Y., Zografi, G., (1996). The effects of co-lyophilized polymeric additives on the glass transition temperature and crystallization of amorphous sucrose. *Journal of Thermal Analysis and Calorimetry* 47(5), 1567-1579.

Sharma, A., Jana, A.H., Chavan, R.S., (2012). Functionality of milk powders and milk-based powders for end use applications - a review. *Comprehensive Reviews in Food Science & Food Safety* 11(5), 518-528.

Sharples, A., (1966). Overall kinetics of crystallization. In: Sharples, A. (Ed.), *Introduction to polymer crystallization*. Edward Arnold Ltd, London, UK, pp. 44-59.

Sheu, T.Y., Rosenberg, M., (1995). Microencapsulation by spray drying ethyl caprylate in whey protein and carbohydrate wall systems. *Journal of Food Science* 60(1), 98-103.

Shimada, K., Fujikawa, K., Yahara, K., Nakamura, T., (1992). Antioxidative properties of xanthan on the autoxidation of soybean oil in cyclodextrin emulsion. *Journal of Agricultural and Food Chemistry* 40(6), 945-948.

Shimada, Y., Roos, Y., Karel, M., (1991). Oxidation of methyl linoleate encapsulated in amorphous lactose-based food model. *Journal of Agricultural and Food Chemistry* 39(4), 637-641.

Shipe, W., Bassette, R., Deane, D., Dunkley, W., Hammond, E., Harper, W., Kleyn, D., Morgan, M., Nelson, J., Scanlan, R., (1978). Off flavors of milk: Nomenclature, standards, and bibliography. *Journal of Dairy Science* 61(7), 855-869.

Shiratsuchi, H., Shimoda, M., Imayoshi, K., Noda, K., Osajima, Y., (1994). Volatile flavor compounds in spray-dried skim milk powder. *Journal of Agricultural and Food Chemistry* 42(4), 984-988.

Sims, R.J., Fioriti, J.A., Trumbetas, J., (1979). Effect of sugars and sugar alcohols on autoxidation of safflower oil in emulsions. *Journal of the American Oil Chemists' Society* 56(8), 742-745.

Sims, R.J., (1994). Oxidation of fats in food products. *Inform* 5, 1020-1028.

Slade, L., Levine, H., (1991). Beyond water activity: recent advances based on an alternative approach to the assessment of food quality and safety. *Critical Reviews in Food Science and Nutrition* 30(2-3), 115-360.

Slade, L., Levine, H., Ievolella, J., Wang, M., (1993). The glassy state phenomenon in applications for the food industry: application of the food polymer science approach to structure–function relationships of sucrose in cookie and cracker systems. *Journal of the Science of Food and Agriculture* 63(2), 133-176.

Sliwinski, E.L., Lavrijsen, B.W.M., Vollenbroek, J.M., van der Stege, H.J., Van Boekel, M.A.J.S., Wouters, J.T.M., (2003). Effects of spray drying on physicochemical properties of milk protein-stabilised emulsions. *Colloids and Surfaces B: Biointerfaces* 31(1-4), 219-229.

Solans, C., Izquierdo, P., Nolla, J., Azemar, N., Garcia-Celma, M.J., (2005). Nano-emulsions. *Current Opinion in Colloid and Interface Science* 10, 102-110.

Soottitantawat, A., Yoshi, H., Furata, T., Ohkawara, M., Linko, P., (2003). Microencapsulation by spray-drying: Influence of emulsion size on the retention of volatile compounds. *Journal of Food Science* 68(7), 2256-2262.

Soottitantawat, A., Yoshii, H., Furuta, T., Ohgawara, M., Forssell, P., Partanen, R., Poutanen, K., Linko, P., (2004). Effect of water activity on the release characteristics and oxidative stability of *d*-limonene encapsulated by spray drying. *Journal of Agricultural and Food Chemistry* 52(5), 1269-1276.

Soottitantawat, A., Bigeard, F., Yoshii, H., Furuta, T., Ohkawara, M., Linko, P., (2005a). Influence of emulsion and powder size on the stability of encapsulated *d*-limonene by spray drying. *Innovative Food Science & Emerging Technologies* 6(1), 107-114.

Soottitantawat, A., Takayama, K., Okamura, K., Muranaka, D., Yoshii, H., Furuta, T., Ohkawara, M., Linko, P., (2005b). Microencapsulation of *L*-menthol by spray drying and its release characteristics. *Innovative Food Science & Emerging Technologies* 6(2), 163-170.

Soutari, N., Buanz, A.B.M., Gul, M.O., Tuleu, C., Gaisford, S., (2012). Quantifying crystallisation rates of amorphous pharmaceuticals with dynamic mechanical analysis (DMA). *International Journal of Pharmaceutics* 423, 335-340.

Sozer, N., Kokini, J.L., (2009). Nanotechnology and its applications in the food sector. *Trends in Biotechnology* 27(2), 82-89.

Stapelfeldt, H., Mortensen, G., Skibsted, L.H., (1997a). Early events in oxidation of whole milk powder detected by electron spin resonance spectrometry. Carry-over effects from butter used for instantization. *Milchwissenschaft* 52, 266-269.

Stapelfeldt, H., Nielsen, B.R., Skibsted, L.H., (1997b). Effect of heat treatment, water activity and storage temperature on the oxidative stability of whole milk powder. *International Dairy Journal* 7(5), 331-339.

Stokes, G.G., (1851). *On the effect of the internal friction of fluids on the motion of pendulums*. Pitt Press.

Sun, Y.E., Wang, W.D., Chen, H.W., Li, C., (2011). Autoxidation of unsaturated lipids in food emulsion. *Critical Reviews in Food Science and Nutrition* 51(5), 453-466.

Tadros, T., Izquierdo, P., Esquena, J., Solans, C., (2004). Formation and stability of nano-emulsions. *Advances in Colloid and Interface Science* 108-109, 303-318.

Taoukis, P.S., Labuza, T.P., Saguy, I.S., (1997). Kinetics of food deterioration and shelf-life prediction, In: Valentas, K.J., Rotstein, E., Singh, R.P. (Eds.), *Handbook of food engineering practice*. CRC Press, Boca Raton, FL, USA, pp. 419-460.

Tarladgis, B.G., Pearson, A., Jun, L., (1964). Chemistry of the 2-thiobarbituric acid test for determination of oxidative rancidity in foods. II.—formation of the tba-malonaldehyde complex without acid-heat treatment. *Journal of the Science of Food and Agriculture* 15(9), 602-607.

Taylor, M.J., Richardson, T., (1980). Antioxidant Activity of Skim Milk: Effect of Heat and Resultant Sulfhydryl Groups. *Journal of Dairy Science* 63(11), 1783-1795.

Thevenet, F., (1995). *Acacia gums: natural encapsulation agent for food ingredients*.

Thijssen, H., Rulkens, W., (1968). Retention of aromas in drying food liquids. *De Ingenieur* 80(47), 45-56.

Thomas, M.E.C., Scher, J., Desobry-Banon, S., Desobry, S., (2004a). Milk powders ageing: Effect on physical and functional properties. *Critical Reviews in Food Science and Nutrition* 44(5), 297-322.

Thomas, M.E.C., Scher, J., Desobry, S., (2004b). Lactose/β-Lactoglobulin Interaction During Storage of Model Whey Powders. *Journal of Dairy Science* 87(5), 1158-1166.

Tobin, M.C., (1974). Theory of phase transition kinetics with growth site impingement. I. Homogenous nucleation. *Journal of Polymer Science Part B: Polymer Physics* 12, 399-406.

Tong, L., Sasaki, S., McClements, D.J., Decker, E.A., (2000a). Antioxidant activity of whey in a salmon oil emulsion. *Journal of Food Science* 65(8), 1325-1329.

Tong, L.M., Sasaki, S., McClements, D.J., Decker, E.A., (2000b). Mechanisms of the antioxidant activity of a high molecular weight fraction of whey. *Journal of Agricultural and Food Chemistry* 48(5), 1473-1478.

Turchiuli, C., Fuchs, M., Bohin, M., Cuvelier, M.E., Ordonnaud, C., Peyrat-Maillard, M.N., Dumoulin, E., (2005). Oil encapsulation by spray drying and fluidised bed agglomeration. *Innovative Food Science and Emerging Technologies* 6(1), 29-35.

Tunick, M. H., Iandola, S. K., & Van Hekken, D. L. (2013). Comparison of SPME methods for determining volatile compounds in milk, cheese, and whey powder. *Foods, 2*,(4), 534-543.

Ulberth, F., Roubicek, D., (1995). Monitoring of oxidative deterioration of milk powder by headspace gas chromatography. *International Dairy Journal* 5(6), 523-531.

Urbanovici, E., Segal, E., (1990). New formal relationships to describe kinetics of crystasllisation. *Thermochimica Acta* 171, 87-94.

Van Aardt, M., Duncan, S., Marcy, J., Long, T., Hackney, C., (2001). Effectiveness of poly (ethylene terephthalate) and high-density polyethylene in protection of milk flavor. *Journal of Dairy Science* 84(6), 1341-1347.

van der Merwe, G.H., du Plessis, L.M., Taylor, J., (2004). Changes in chemical quality indices during long-term storage of palm-olein oil under heated storage and transport-type conditions. *Journal of the Science of Food and Agriculture* 84(1), 52-58.

van Ruth, S.M., Roozen, J.P., Posthumus, M.A., Janse, F.J.H.M., (1999). Volatile composition of sunflower oil-in-water emulsions during initial lipid oxidation: Influence of pH. *Journal of Agricultural and Food Chemistry* 47, 4365-4369.

van Ruth, S.M., Shaker, E.S., Morrissey, P.A., (2001). Influence of methanolic extracts of soybean seeds and soybean oil on lipid oxidation in linseed oil. *Food Chemistry* 75(2), 177-184.

Vega-Mercado, H., Marcela Gongora-Nieto, M., Barbosa-Cánovas, G.V., (2001). Advances in dehydration of foods. *Journal of Food Engineering* 49(4), 271-289.

Vega, C., Goff, H.D., Roos, Y.H., (2005a). Spray drying of high-sucrose dairy emulsions: Feasibility and physicochemical properties. *Journal of Food Science* 70(3), E244-E251.

Vega, C., Kim, E.H.J., Chen, X.D., Roos, Y.H., (2005b). Solid-state characterization of spray-dried ice cream mixes. *Colloids and Surfaces B: Biointerfaces* 45(2), 66-75.

Vega, C., Roos, Y.H., (2006). Spray-dried dairy and dairy-like emulsions - compositional considerations. *Journal of Dairy Science* 89(2), 383-401.

Vega, C., Goff, H.D., Roos, Y.H., (2007). Casein molecular assembly affects the properties of milk fat emulsions encapsulated in lactose or trehalose matrices. *International Dairy Journal* 17(6), 683-695.

Velikov, K.P., Pelan, E., (2008). Colloidal delivery systems for micronutrients and nutraceuticals. *Soft Matter* 4(10), 1964-1980.

Wang, L., Mutch, K.J., Eastoe, J., Heenan, R.K., Dong, J., (2008a). Nanoemulsions prepared by a two-step low-energy process. *Langmuir* 24(12), 6092-6099.

Wang, L., Tabor, R., Eastoe, J., Li, X., Heenan, R.K., Dong, J., (2009). Formation and stability of nanoemulsions with mixed ionic–nonionic surfactants. *Physical Chemistry Chemical Physics* 11(42), 9772-9778.

Wang, X., Jiang, Y., Wang, Y.W., Huang, M.-T., Ho, C.T., Huang, Q., (2008b). Enhancing anti-inflammation activity of curcumin through O/W nanoemulsions. *Food Chemistry* 108(2), 419-424.

Waraho, T., McClements, D.J., Decker, E.A., (2011). Mechanisms of lipid oxidation in food dispersions. *Trends in Food Science & Technology* 22(1), 3-13.

Weiss, J., Takhistov, P., McClements, D.J., (2006). Functional materials in food nanotechnology. *Journal of Food Science* 71(9), R107-R116.

White, G.W., Cakebread, S.H., (1966). The glassy state in certain sugar-containing food products. *Journal of Food Technology* 1(1), 73-82.

White, P.J., (1995). Conjugated diene, anisidine value, and carbonyl value analyses, In: Warner, K., Eskin, N.A.M. (Eds.), *Methods to assess the quality and stability of oils and fat-containing foods*. AOCS Press, Champaign, IL, USA, pp. 159-176.

Wilson, N., Shah, N., (2007). Microencapsulation of vitamins. *ASEAN Food Journal* 14(1), 1-14.

Wooster, T.J., Golding, M., Sanguansri, P., (2008). Impact of oil type on nanoemulsion formation and Ostwald ripening stability. *Langmuir* 24(22), 12758-12765.

Yamauchi, R., Aoki, Y., Sugiura, T., Kato, K., Ueno, Y., (1982). Effect of sugar and sugar analogs on autoxidation of methyl linoleate and safflower oil. *Agricultural and Biological Chemistry* 46, 2997-3002.

Yamauchi, R., Goto, Y., Kato, K., Ueno, Y., (1984). Pro-oxidant effect of dihyroxyacetone and reducing sugars on autoxidation of methyl linoleate in emulsions. *Agricultural and Biological Chemistry* 48, 843-848.

Yang, J., Grey, K., Doney, J., (2010). An improved kinetics approach to describe the physical stability of amorphous solid dispersions. *International Journal of Pharmaceutics* 384(1–2), 24-31.

Young, S.L., Sarda, X., Rosenberg, M., (1993a). Microencapsulating properties of whey proteins. 1. Microencapsulation of anhydrous milk fat. *Journal of Dairy Science* 76(10), 2868-2877.

Young, S.L., Sarda, X., Rosenberg, M., (1993b). Microencapsulating properties of whey proteins. 2. Combination of whey proteins with carbohydrates. *Journal of Dairy Science* 76(10), 2878-2885.

Yu, X., Schmidt, A.R., Bello-Perez, L.A., Schmidt, S.J., (2007). Determination of the bulk moisture diffusion coefficient for corn starch using an automated water sorption instrument. *Journal of Agricultural and Food Chemistry* 56(1), 50-58.

Zakarian, J.A., King, C.J., (1982). Volatiles loss in the nozzle zone during spray drying of emulsions. *Industrial & Engineering Chemistry Process Design and Development* 21(1), 107-113.

Zhou, Y., Roos, Y.H., (2011). Characterization of carbohydrate-protein matrices for nutrient delivery. *Journal of Food Science* 76(4), E368-E376.